Stochastic Long-Term Production Scheduling of the LabMag Iron Ore Deposit in Labrador, Canada

by

Michael Spleit

Department of Mining and Materials Engineering,

McGill University, Montréal

October, 2014

A thesis submitted to McGill University as partial fulfillment of the requirements of the degree of Master of Engineering

Dedication

I dedicate this work to Virginia Konchan. The most uncertainty is not found in the earth sciences or engineering, but rather in affairs of the heart. The uncertainty that can arise in love defies management and is never fully resolved. Instead, you must accept the unknown and simply do the best you can, blindly giving your utmost.

“I think it's much more interesting to live not knowing than to have answers which might be wrong. I have approximate answers and possible beliefs and different degrees of uncertainty about different things, but I am not absolutely sure of anything and there are many things I don't know anything about, such as whether it means anything to ask why we're here. I don't have to know an answer. I don't feel frightened not knowing things, by being lost in a mysterious universe without any purpose, which is the way it really is as far as I can tell.”

– Richard P. Feynman

“As far as the laws of mathematics refer to reality, they are not certain; and as far as they are certain, they do not refer to reality.”

– Albert Einstein

Acknowledgements

I would like to thank the people at New Millennium Iron Corp. who gave me the opportunity to learn and grow in the field of mining and who supported me with their wealth of knowledge and experience. Thiagarajan Balakrishnan, Chief Geologist, was very helpful explaining geological concepts and discussing them with me. Moulaye Melainine, Senior Vice President – Development, has been my supervisor at New Millennium Iron for the last 5 years, and has served as a role model to me in his diligence, ethics, and kindness. Robert Martin and Dean Journeaux, both of whom served as President & CEO of New Millennium at various points, were instrumental in my development in the field of mining and are role models to me in their shared vision of the development of the Millennium Iron Range. They gave me great freedom to explore and learn, approved the use of technical data and approved the company support of this Master's Degree. I thank Roussos Dimitrakopoulos for introducing me to stochastic mine planning and helping me to research and explore this field. Finally, the biggest thanks goes to Zeidane Moulaye Zeine for his technical assistance in putting together the models, charting results, his in-depth technical assistance, as well as his input to all the discussions we had while performing this study.

Contribution of Authors

The author of this thesis is the primary and sole author of both papers that as served the basis for this thesis. Professor Roussos G. Dimitrakopoulos was the supervisor of the author's Masters of Engineering program and participated in technical editing of both papers.

Abstract

In long-term production scheduling, which is of vital importance to a project's success and profitability, the goal is to determine a feasible extraction sequence that maximizes the discounted cash flows of a mine while also ensuring the target ore quantities and qualities are met. There is risk of the actual production deviating from what is planned due to geological variability, which is not considered by conventional mine designs and production schedules that are based on a single estimated ore body model. In order to address this issue, multiple simulations of an orebody can be created to represent its geological variability and allow for quantifying expected bounds, instead of single estimates, for grades, tonnages, and financial results. Beyond simply quantifying the geological uncertainty, a mine production schedule can be optimized while directly considering simulations in order to manage the geological risk.

In this study, a set of geological simulations of the LabMag iron ore deposit in Labrador, Canada is generated in order to quantify the geological variability in an existing mining schedule and assess the schedule's performance. The 'DBMAFSIM' algorithm is used to provide joint geostatistical simulation of spatially correlated variables of interest. First, a novel application of the method is used to jointly simulate the

thicknesses of seven lithological layers, and then four correlated grades within each lithology are jointly simulated. The variability in an existing production schedule, designed based on a single deterministic geological model, is then evaluated using the simulations. This evaluation quantifies the potential deviations from expected production target grades and tonnages as well as the associated financial impact of these deviations.

Subsequently, a production schedule optimization based on stochastic integer programming (SIP) is presented that aims to improve mine profitability while simultaneously managing the risk of production tonnage and quality deviations. In addition, the formulation has components for equipment and waste material management: the truck fleet requirements are minimized while ensuring that the number of required trucks is an increasing function to avoid unnecessary peaks; and the evolution of the pit is controlled so that space within the mined out pit is continuously provided to allow for tailings and waste rock to be replaced, thus minimizing the project's environmental footprint.

The results of the study demonstrate the need for stochastic mine planning in order to ensure production targets and financial expectations are met. The simulation methodology presented can be generalized to sedimentary deposits with correlated lithology thicknesses and/or multiple correlated qualities, and in the case of LabMag, the method yielded good

results in terms of the reproduction of data statistics. A set of ten simulations were created in order to quantify the uncertainty in grade and tonnage in an existing mine plan and significant variations were found within the first 10 periods, which have an impact on the project NPV. This motivated the development of an SIP formulation that produced a production schedule with an NPV 16.9% higher than that of the conventional schedule. The stochastic schedule reduces the required number of trucks by 15 (previous total of 35 trucks) to 20 total trucks and the required number of shovels by 1 to 5 shovels total. This has a corresponding impact of 23.7% reduction in capital costs, and 26.2% reduction in operating costs over the first ten years. The stochastic schedule also achieves the desired progressively deepening sequencing of the pit, which maintains a larger working area at any given time that permits the eventual disposal of dry tailings and waste inside the pit in order to reduce the environmental footprint.

Future work could consider more selectivity in the mining process in order to better capture the short-range variability of the deposit and to provide the optimizer with greater flexibility. In this study, the optimization was broken down into four sub-optimizations in order to have optimization problems that could be solved in a reasonable amount of time. A stronger problem formulation could allow for solving the initial problem in one pass,

finding a truly optimal result in a reasonable amount of time. An alternate approach to take could be to use a heuristic method such as simulated annealing, which would not find the optimal result, but could find a near-optimal result for the problem without the need for breaking the problem down into sub-problems. Finally, future work could consider semi-mobile crushers located within the pit instead of one fixed crusher, which would further reduce the truck haulage distances and number of trucks needed. The optimization formulation could also be built to determine the ideal crusher locations for each period.

Résumé

L'établissement du calendrier de production minière à long terme est d'importance vitale pour le succès et la rentabilité d'un projet. Son but est de déterminer une séquence d'extraction réalisable qui maximise les flux de trésorerie actualisés d'une mine tout en assurant les quantités et qualités visées de minerai. La production réelle risque de s'écarter des prévisions à cause de la variabilité géologique, qui n'est considérée ni dans les conceptions de mine ni dans les calendriers de production conventionnels car ils sont basés sur un modèle d'évaluation unique du corps minéralisé. Pour y remédier, de multiples simulations peuvent être créées plutôt qu'une évaluation unique pour représenter la variabilité géologique d'un corps minéralisé et permettre de mesurer les limites escomptées pour les teneurs, tonnages et résultats financiers. Au-delà de la simple mesure d'incertitude géologique, un calendrier de production minière peut être optimisé en tenant compte directement des simulations pour gérer le risque géologique.

Cette étude comporte un ensemble de simulations géologiques du gisement de minerai de fer LabMag au Labrador, Canada, générées afin de mesurer la variabilité géologique d'un calendrier de production minière existant et d'évaluer la valeur de celui-ci. L'algorithme « DBMAFSIM » est

utilisé en géostatistique pour simuler conjointement des variables qui sont spatialement corrélées. D'abord, la méthode est appliquée d'une nouvelle façon pour simuler conjointement les épaisseurs de sept couches lithologiques. Ensuite, quatre teneurs corrélées sont simulées conjointement dans chaque lithologie. La variabilité d'un calendrier existant de production conçu sur base d'un modèle géologique déterministe unique est ensuite évaluée en fonction des simulations. Cette évaluation mesure les écarts possibles avec les teneurs et tonnages initialement visés dans les prévisions de production, de même que l'impact financier associé à ces écarts.

Une optimisation du calendrier de production basée sur la programmation stochastique en nombres entiers (« SIP ») est ensuite présentée. Elle a pour but d'améliorer la rentabilité de la mine tout en gérant le risque d'écarts pour le tonnage et la qualité de production. De plus, la formulation contient des éléments de gestion d'équipements et de déchets miniers. Ainsi, les besoins de la flotte de camions sont réduits au minimum tout en maintenant une fonction croissante pour calculer le nombre de camions nécessaires et éviter les pics inutiles. De même, l'évolution de la mine à ciel ouvert est contrôlée afin que la mine épuisée procure toujours l'espace nécessaire pour replacer les résidus et stériles miniers, réduisant ainsi l'empreinte environnementale du projet.

Les résultats de l'étude démontrent le besoin de planification minière stochastique pour assurer l'atteinte des objectifs de production et des attentes financières. La méthode de simulation présentée peut être généralisée aux dépôts sédimentaires présentant des épaisseurs lithologiques corrélées et/ou des qualités corrélées multiples. Dans le cas de LabMag, la méthode a donné de bons résultats en termes de reproduction des données statistiques. Un ensemble de dix simulations a été créé afin de mesurer l'incertitude au niveau de la teneur et du tonnage dans un plan de mine existant. Comme des variations importantes ont été trouvées dans les dix premières périodes, qui ont un impact important sur la valeur actualisée nette du projet, une formulation SIP a été développée et a produit un calendrier de production avec une valeur actualisée nette de 16,9% supérieur à celle obtenue par le calendrier conventionnel. Le calendrier stochastique réduit de 15 unités le nombre requis de camions (le total précédent de 35 camions passe à 20) et réduit d'une unité le nombre requis de pelles (pour un total final de 5 pelles). L'impact correspondant est une réduction de 23,7% sur les dépenses en capital des équipements miniers, et une réduction de 26,2% sur les dépenses d'exploitation durant les dix premières années. Le calendrier stochastique permet aussi d'établir la séquence progressive souhaitée d'approfondissement de la mine, afin de maintenir en tout temps une zone

plus vaste de travail permettant l'élimination future des résidus du concentrateur et des stériles à l'intérieur de la mine à ciel ouvert, réduisant ainsi l'empreinte environnementale du projet.

Une considération future serait d'être plus sélectif dans le processus minier, en saisissant mieux la variabilité à courte portée du gisement et en offrant une plus grande flexibilité à l'optimiseur. Dans cette étude, l'optimisation a été décomposée en quatre sous-optimisations afin de pouvoir résoudre chacun des problèmes d'optimisation dans un délai raisonnable. Renforcer la formulation du problème permettrait de résoudre le problème initial en une seule opération et de trouver un résultat optimal dans un délai raisonnable. Une approche alternative pourrait être d'employer une méthode heuristique telle que le recuit simulé, qui ne trouverait pas le résultat optimal, mais pourrait trouver une solution presqu'optimale au problème sans devoir diviser le problème en sous-problèmes. Enfin, une autre considération future serait de remplacer le concasseur fixe situé hors de la fosse minière par des concasseurs semi-mobiles, ce qui réduirait encore les distances de transport par camion et le nombre requis de camions. La formulation d'optimisation pourrait aussi inclure la détermination de l'emplacement idéal du concasseur et les déplacements optimaux selon les coûts de déplacements et de camionnage.

Table of Contents

List of Tables

List of Figures

Chapter 1

Introduction and Literature Review

1.1. Stochastic Mine Planning

Stochastic mine planning seeks the most profitable configuration of a mining operation while considering uncertainty in the geology and/or any of the other scheduling inputs. The full-scale problem consists of global asset optimization, which integrates mining and processing of multiple deposits, multiple mined materials, stockpiles, blending options, and alternative processing streams to yield distinct products. Part of this problem is production scheduling, which determines the optimal feasible extraction sequence of a mineral resource. Production scheduling can be considered at varying levels of time resolution from life-of-mine (LOM) or long-term production scheduling down to daily scheduling. It is long-term production scheduling, which usually considers time periods on the order of years, that determines a project's cash flows and thus the project's value. The cash flows of a mining project depend heavily on the mine production schedule because the mined material determines the quantity and qualities of products available to be sold to the market in each period. In addition, the mining equipment capital and operating costs can vary significantly based on the sequence of extraction. Mining projects require

large capital investments, which are risky because they involve large, up-front expenditures on assets intended for many years of service and that will take a long time to pay for themselves. Iron ore projects in particular are heavily dependent upon capital-intensive infrastructure and four recent technical studies of magnetite iron ore projects in northern Canada have estimated capital expenditures ranging from $1.3 billion to $12.9 billion (Grandillo, et al. 2012, Bertrand, et al. 2012, SNC-Lavalin 2014, Boilard, et al. 2011). Vallée (2000) refers to a study by Harquail (1991), wherein a review of nearly 50 North American projects showed only 10% achieved their commercial aims with 38% failing within about one year. To make the high-stake decision to invest in such mining projects, the highest degree of profitability must be sought while also minimizing project risks. One of the key risks in a mining project is geological uncertainty because the understanding of the geology, spatial distribution, and variability of the ore qualities can only be inferred from limited data, which is not necessarily representative of the entire deposit. Since mine production scheduling depends on the underlying geological resource model for the forecasting of tonnages and material qualities, geological uncertainty implies a risk of deviations from the planned production schedule. However, by assessing and quantifying geological uncertainty, the minimum acceptable level of risk can be determined, the risk can be minimized, and the residual risk

can be managed (Dowd 1994, 1997). A method for capturing geological uncertainty is to create stochastic simulations (multiple equally-probable scenarios) of the resource model, where the term ‘stochastic’ means that the properties of the model are variable or uncertain (Birge and Louveaux 1997). Each simulation reproduces the input data and its spatial variability, but the local values throughout the model are varied randomly according to probability distributions that are inferred from the surrounding data. Simulations capture the full range of possible grades, whereas estimated models, although potentially locally accurate, exhibit smoothing of the values: estimated models are based on weighted averaging, so they generally underestimate high grades and overestimate low grades (David 1977, 1988). A set of such simulations allows for assessing and quantifying the uncertainty in a mine production schedule: a single schedule can be evaluated separately for each simulation, and the distribution of results provides probabilistic bounds for each property of the model (David 1977, Ravenscroft 1992, Dimitrakopoulos et al. 2002). Understanding the risk in the production schedule makes for a more informed investment decision, but ideally production scheduling methods take these simulations directly into account in order to mitigate the uncertainty and create a schedule whose expectations in terms of mined material have the highest probability of being met.

Stochastic production scheduling does precisely this, and studies have shown that stochastic production schedules not only have a higher chance of meeting production targets, but can produce a higher economic value than deterministic schedules (Dimitrakopoulos et al. 2002, Albor Consuegra and Dimitrakopoulos 2010, Leite and Dimitrakopoulos 2014, Godoy and Dimitrakopoulos 2011). Stochastic scheduling produces a higher economic value when scheduling the same material as a conventional schedule (i.e. same ultimate pit limit) because it is able to determine groups of mining blocks that, when mined together, have an upside potential in ore tonnage and quality. Conventional scheduling only considers a single orebody model, and so is unable to recognize upside potential or downside risk. When stochastic scheduling is used to determine the ultimate pit limit, an even higher economic value is found because a larger pit with more metal/mineral is typically established through more efficient blending. Stochastic scheduling thus also maximizes the utility of a resource and contributes to more sustainable development.

The stochastic mine schedule optimization methods developed herein are for a specific case-study site: the LabMag iron ore deposit in northern Labrador, Canada, which is controlled by New Millennium Iron. Iron ore occurs in two common types of mineral iron oxide: hematite and

magnetite. LabMag is composed of seven stratigraphic units of magnetite and is a taconite deposit, which is similar to banded iron formations (BIFs) and is the name given to magnetite in the Lake Super region. Whereas hematite typically has iron grades in excess of 50%, Taconite only has about 30% iron naturally, and contains a significant amount of host waste rock composed of quartz, chert, and carbonates. Taconite is very hard compared to hematite, and requires energy-intensive crushing to be ground very fine in order to liberate the iron. A benefit in grinding the ore very fine, however, is that there is better liberation of the iron and of the common impurities that are of concern for hematite (phosphorus, magnesium, alumina, organics, and silica), only silica is commonly of any significance for taconite. Magnetic separation is typically used to extract the iron particles from the waste, but any iron in the form of hematite is lost without additional beneficiation, which is typically not cost-effective for the quantity of hematite contained in taconite. Therefore, an important quality of taconite is the expected process plant magnetite weight recovery. This is commonly estimated in a laboratory setting using what is known as the Davis Tube test (Schulz 1964), which produces a clean concentrate of magnetic material that can then be analyzed for iron grade as well as silica. There are thus four highly correlated qualities of interest: the head iron grade (FeH), the Davis Tube weight recovery (DTWR), the Davis

Tube iron concentrate grade (FeC), and the Davis Tube concentrate silica grade (SiC).

The fine iron concentrate that is produced through beneficiation can be sold, but preferably it is pelletized because pellets receive a premium in price over concentrate. In fact, pellet plants can produce two types of pellets: blast furnace (BF) pellets and direct reduction (DR) pellets. DR pellets receive an additional premium because they must meet more stringent impurity tolerances. In crushing iron ore, excessive fines can be generated that are not in the required size range for pelletization and are then exported as concentrate, which is sold at a less attractive price. In order to meet the pellet grade specifications, the average silica grade must be kept beneath a certain level for each pellet type. The LabMag process flow sheet is designed to balance profitability and recovery, and is optimized for a specific DTWR. Within a tolerance range around this target DTWR, the plant can be adjusted on-the-fly, but larger deviations would result in a degraded plant efficiency.

Within only roughly 30% iron content, the majority of the mined material is waste (tailings) and must be managed. Tailings from the process plant typically contain some amount of water, and impoundments are necessary to contain them, which can be expensive. An alternative option is to remove the moisture, which then permits the tailings to be dry-stacked

within the mined-out pit. Preventive measures must be taken to avoid the tailings wall from caving and waste from sliding into working areas of the pit, but this risk is minimal with dry-stacking because the stratigraphic layers of the LabMag deposit are inclined at a shallow dip angle of only about six degrees, daylighting on the south-west side of the deposit. The shallow dip is also highly advantageous in terms of designing the ultimate pit because the bottom of the ore can serve as the pit floor and exit ramp, which results in a low waste/ore stripping ratio. However, fully loaded trucks operate at slower speeds when exiting the pit than on even ground, which means haulage cycle times are dependent on both distance and depth of the ore from the process plant.

Overlying the economic ore layers are two types of waste: a thin cover of overburden and a layer of Menihek shale (MS). The deepest portions of the orebody have the most overlying MS, but this occurs progressively moving away from the process plant location and on the side of the deposit near the process plant, there is no MS and the ore is often exposed at surface. The MS layer contains some amount of sulphur and has the potential for creating acid rock drainage when exposed to air and water. This environmental concern requires special management, and it would be preferable to avoid mining it during the start of operations if sufficient quantities of ore within desired quality target ranges can be

mined without mining this waste unit. Stochastic simulations of the geology can capture the uncertainty in the ore tonnages and qualities, and stochastic scheduling is necessary to create plans that can ensure that targets are likely to actually be met.

In simulating the LabMag deposit, a joint-simulation framework known as 'DBMAFSIM' (Boucher and Dimitrakopoulos 2012) is used to preserve the spatial correlations (Goovaerts 1997) between the thicknesses of each lithology and between the ore qualities. A set of simulations is generated and then used to quantify the uncertainty in an existing mine production schedule that was designed based on a single orebody estimate. This procedure highlighted periods in this existing schedule in which target tonnages and qualities would potentially fail to be met, which motivates the need for stochastic production scheduling methods in order to control the uncertainty. The production schedule derived in this thesis uses a type of mathematical programming called stochastic integer programming (SIP) to address geological uncertainty and increase the chance of meeting target production quantities while also seeking to maximize discounted cash flows. Further considerations are given to equipment and waste management. In terms of equipment, the formulation ensures a smooth and increasing truck haulage fleet and seeks to delay equipment purchases as much as possible by seeking greater truck productivity in

earlier periods, which is accounted for by haul cycle times that are specific for the depth and distance to the crusher of each block within the pit. In terms of waste management, the problematic Menihek shale layer is almost completely avoided while still meeting production targets and part of the scheduling formulation ensures that the mining of the pit evolves in such a way so as to continually create space in the pit in each period for the placement of dry-stacked tailings.

This chapter presents an overview of the current trends in stochastic mine planning and optimization. The incorporation of stochastic simulation into the mine planning process has evolved from risk analysis to direct incorporation within the design process, now referred to as stochastic mine planning. The benefits of existing stochastic mine planning methodologies are presented, along with their limitations and short-comings, leading up to the definition of the specific goals and objectives of this thesis.

1.2. Stochastic Production Scheduling

Stochastic production scheduling, which is the current state of the art, consists of techniques aimed at determining the ideal extraction sequence from the initial state of a deposit to the ultimate pit limit while considering geological uncertainty, and more recently demand uncertainty as well (Sabour and Dimitrakopoulos 2011, Asad and Dimitrakopoulos 2013). The

optimal extraction sequence should forecast the greatest profit while having the greatest probability that the mined material will meet production forecasts. The most recent research treats the geology with Monte-Carlo methods in order to quantify and manage the degree to which the actual mined material may vary from forecasts. Orebody models are typically discretized into mining 'blocks' to make them suitable for numerical evaluation and Monte-Carlo methods are used to generate multiple simulations in order to obtain a distribution of possible material types as well as a distribution of possible values for each material property that are possible for each block. Stochastic schedulers incorporate the joint local uncertainty in the values of mining blocks in order to derive a probabilistic assessment. Typical estimation (as opposed to simulation) methods consist of interpolation algorithms that smooth out local details of the spatial variation of the estimated attribute; extreme values are dampened and only middle-range values are preserved. Stochastic conditional simulation overcomes this problem, and provides a measure of the joint uncertainty about attribute values at several locations taken together (David 1988, Journel and Huijbregts 1978, Goovaerts 1997).

1.2.1. Early work

Ravenscroft (1992) first showed a probabilistic assessment of geological uncertainty in production scheduling that uses a set of stochastic simulations. Using his method, a production schedule is evaluated separately for each scenario, which provides a range of values for the quantities and qualities of mined material in each period. An example of this is shown in Fig. 1, which involves a schedule of 50 periods where each period is represented by a separate zone within a resource model. The schedule was evaluated with a single estimated (Kriged) model as well as a 100 times using alternative simulated models. To assess the probability of error in the value for each period, the 5 lowest and 5 highest values (5% on either end of the distribution) of the simulated values were discarded. The new outer bounds thus reflect a 90% confidence interval for the value of each period. The probability limits are plotted as a percentage difference from actual production and should enclose the zero difference line 90% of the time. It can be seen that this is generally true, meaning that the actual production falls within the expected bounds of the probabilistic forecast. The deviations of the dotted line, however, represent deviations of actual production from the estimated model, of which no indication is given by the estimated model alone. This methodology provides a more informed understanding of the production schedule, but

offers no way of incorporating ore variability into the production scheduling process.

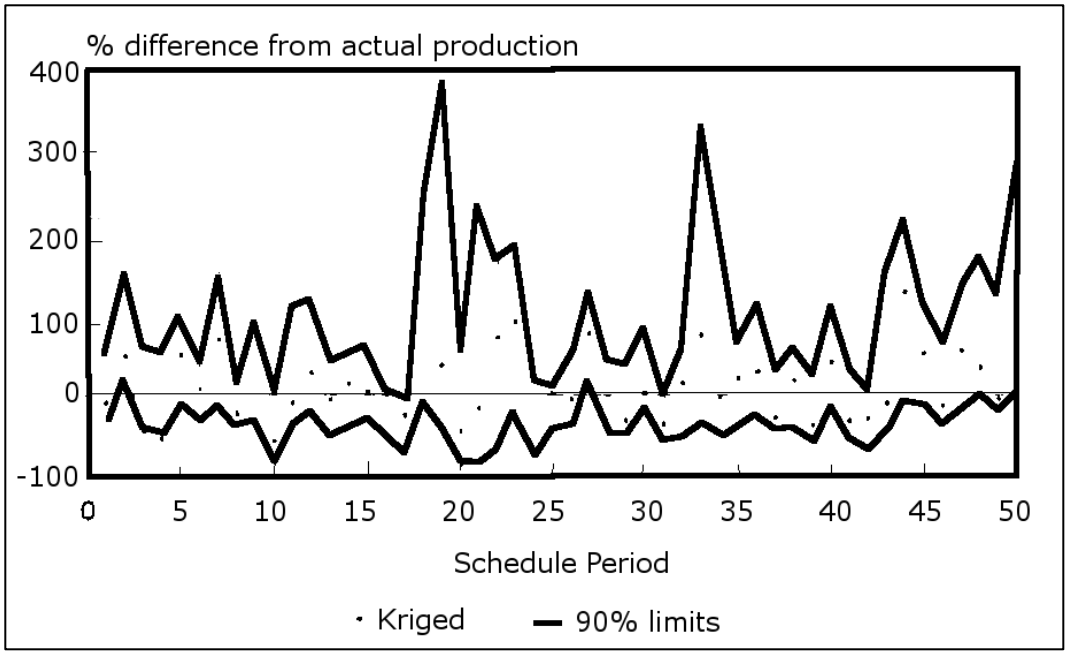

Fig. 1 Simulation Deviations from actual production grade, kriging estimate (dotted line) and 90% confidence limits (solid lines), after Ravenscroft (1992)

Using the same type of framework, Dimitrakopoulos et al. (2002) tested the performance of the conventionally “optimal” production schedule by evaluating the schedule using each of a set of 50 stochastic simulations. The study showed variability in the financial projections, i.e. a range of possible values rather than the single estimate obtained using a deterministic orebody model, and that there was a low probability of the single estimate being accurate. Using a low-grade gold deposit as a case

study, Fig. 2 and Fig. 3 show that the average mill feed tonnage and grade have a range of possible values by evaluating the mine plan using the 50 simulations. The annual mine production given by the “optimal” production schedule associated with each simulation differs, which creates a range of possible cash flows. Therefore, a different NPV is associated with each simulation (Fig. 4) and 80% of the outcomes are shown to cover a range of $AUS 5 million, which represents 20-25% of the single estimated NPV found using a single estimated orebody model. There was also a 95% probability of the project returning a lower NPV than that predicted using the estimated orebody model. This methodology has the ability to demonstrate the risk in a schedule, but is unable to manage it.

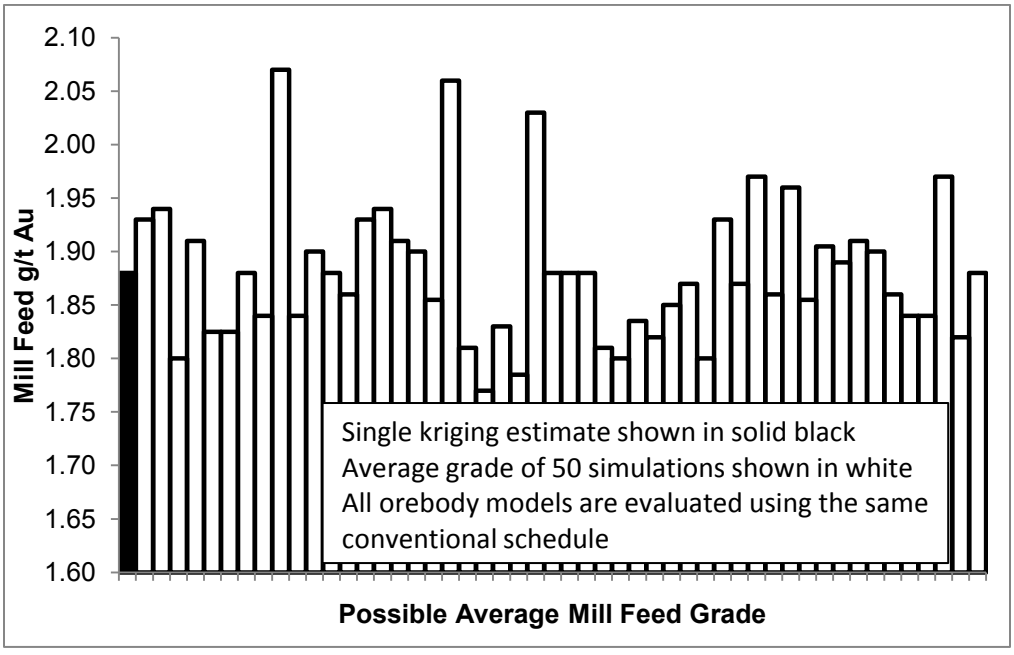

Fig. 2 Range of possible average mill feed grades (Dimitrakopoulos et al. 2002)

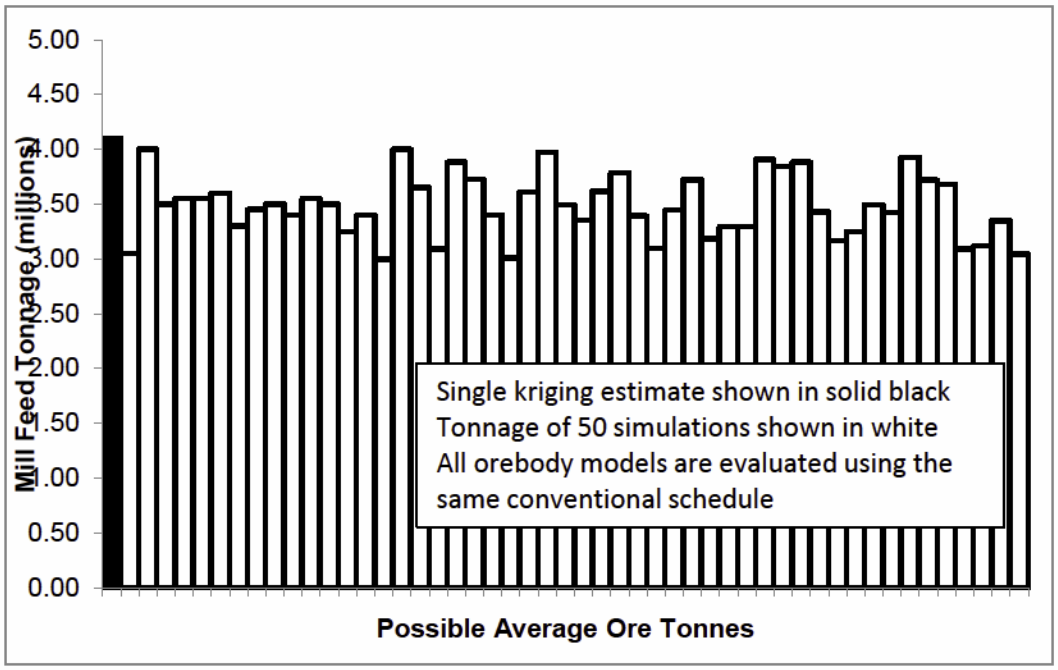

Fig. 3 Range of possible average ore tonnes (Dimitrakopoulos et al. 2002)

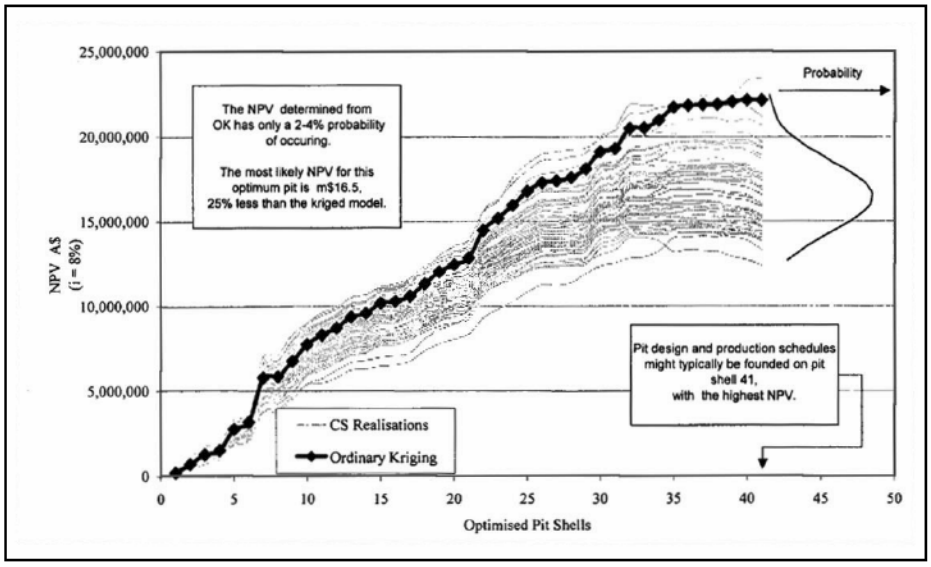

Fig. 4 NPV risk analysis showing the different responses using the conventionally optimal LOM schedule and testing its performance using equally probable models of the deposit to be mined (Dimitrakopoulos et al. 2002)

A framework for geological risk analysis is described by Godoy and Dimitrakopoulos (2011) that quantifies the impact of grade uncertainty to four different cases. The first case is an uncertainty analysis of conventionally optimal pit limit using the same concept as Dimitrakopoulos et al. (2002). The second case is an analysis of the impact to the definition of the ultimate pit limit when different equally probable orebody models are used in the conventional pit optimization process. This demonstrated that the conventional ultimate pit limit based on a single estimated orebody model is not actually optimal. The third case quantifies the impact of grade uncertainty to a given pushback similar to the procedure in the first case. The fourth case quantifies the impact of grade uncertainty to the incremental tonnage between two successive pushbacks. These methods allow a mine planner to have a better understanding of the risk in a schedule, but do not address how to create a schedule that can manage risk.

Dimitrakopoulos et al. (2007) introduces a more systematic approach to selecting an open pit mine design amongst a set by quantifying the upside potential and the downside risk for key project performance indicators, such as the periodical discounted cash flows and the amount of ore tonnes and metal production. The reference point that defines upside versus downside potential is the minimum acceptable return (MAR) on

investment, which usually differs from the expected value (or average or median value). Fig. 5 shows the range of possible DCF values for each of two pit designs for the same orebody with the MAR defining the difference between upside and downside potential. The upside potential is the expected value of simulations with an economic value greater than the MAR whereas the downside potential is the expected value of simulations with a value less than the MAR.

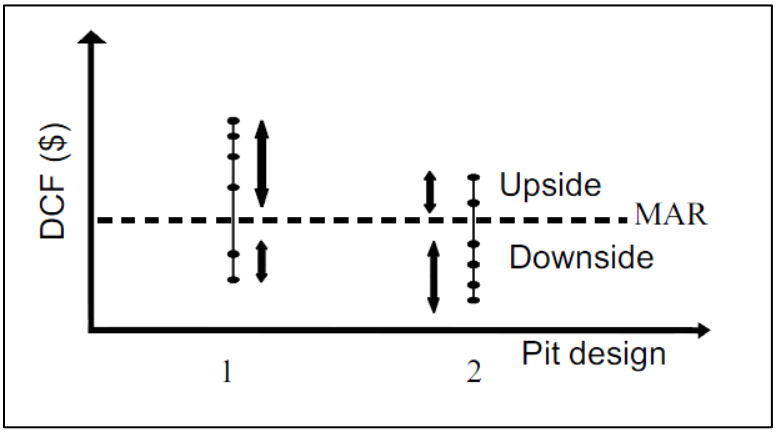

Fig. 5 Upside potential and downside risk for two pit designs for the same orebody (Dimitrakopoulos et al. 2007)

Although this approach can also be easily implemented using traditional and commercially available optimization tools, it is operationally tedious and does not find an optimal solution; it just finds the best solution in a set generated from nested pits for each orebody model.

The work of Sabour and Dimitrakopoulos (2011) is based on the maximum upside / minimum downside approach described above, but includes

stochastic models of prices and foreign exchange rates as well as a 'real options' approach that revises the ultimate pit limits if the continuing value of the project is less than zero. The 'real options' approach models the ability of a company to decide to stop mining if a project becomes unprofitable. Using a copper deposit as a case study, Sabour ranks a set of different mine designs using several different measures: 1) conventionally estimated NPV; 2) an indicator called "total rankings indictor" (TRI) that takes into account upside potential, downside risk, and statistics of the estimated values; 3) real options valuation (ROV) that provides the flexibility to revise the pit limits; and 4) an ROV indicator that takes into account upside potential, downside risk, statistics of the estimated values, and additionally includes ROV.

The results show that under the conditions of uncertainty, design values based on actual market data can be significantly different from those estimated at the planning time. Consequently, using the expected value to rank possible mine designs may result is sub-optimal decisions. The ranking that integrates the flexibility to revise the originally taken decisions regarding the ultimate pit limits have a more efficient selection process that more closely matched the ranking based on actual market data. Although providing for a better ranking system to select a design from a

set, this study is still based on only one model that is not guaranteed to be optimal.

Ramazan and Dimitrakopoulos (2004) use a conventional MIP approach applied to simulated orebody models to build a set of schedules based on a set of stochastic geological simulations where each schedule is based on one simulation. They then use a new MIP formulation to derive a schedule where the blocks have maximum combined probability of being mined in their selected periods. An additional term in the objective function is used to smooth out the schedule to ensure a practical excavation sequence with minimal equipment movement. Their formulation reduces the risk of deviations from production targets, but does not guarantee an optimal solution.

A multi-stage stochastic approach is presented by Godoy and Dimitrakopoulos (2004, 2011) that maximizes the expected NPV by first determining the optimal feasible annual mining rates while considering geological uncertainty, and then makes adjustments to minimize the risk of deviations from production targets. A schematic representation of their algorithm is shown in Fig. 6. The first step is to determine what Godoy calls the stable solution domain (SSD), which considers a set of equally probable orebody models S_1 to S_N (simulations) to determine the range of mining rates and stripping ratios that can be definitely be achieved despite

geological uncertainty. The SSD is the range of possible annual ore and waste tonnages that can be supported by all simulations, and is the intersection of the feasible domain for each separate simulation. A graph of the feasible domain for one orebody model is shown in Fig. 7, which shows the minimum and maximum cumulative waste tonnage that must be mined in order to mine any given cumulative ore tonnage.

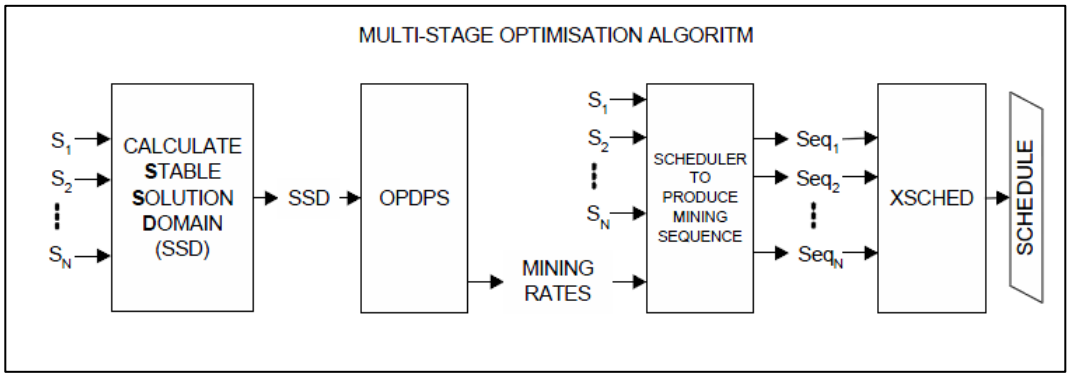

Fig. 6 Schematic representation of the multi-stage optimization algorithm presented by Godoy and Dimitrakopoulos (2004, 2011)

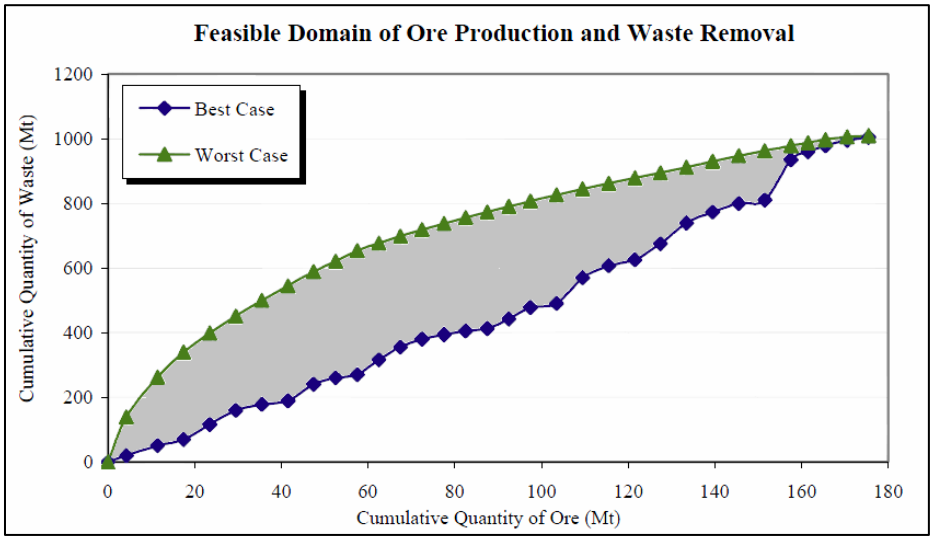

Fig. 7 Feasible domain of ore production and waste removal (Godoy 2003)

Next, Godoy uses a linear programming formulation (called OPDPS in Fig. 6, which stands for open pit design and production scheduling) that considers net revenue along with equipment purchasing and carrying costs to define the economically optimal mining rate that is feasible for all geological simulations (i.e. within the SSD). A conventional scheduling algorithm is then used to create a separate mining sequence for each geological simulation where the mining rate for each sequence is the previously defined optimal rate. The result is a set of solutions where the NPV of each solution has been maximized for the associated geological simulation, and each solution is also supposed to be likely to be feasible when considering geological uncertainty. However, although a mining rate and stripping ratio may be feasible for all the simulations, a different physical mining sequence may be needed for each simulation in order to actually achieve these results. This is due to local variations in the orebody, which has not been accounted for by the OPDPS stage. The production of a schedule that follows this optimal mining rate has uncertainty in the recovered metal, as shown in Fig. 8. This uncertainty in recovered metal creates uncertainty in the cash flows and the cumulative NPV of the project, which is shown in Fig. 9. The deviations on the bottom of the charts reflect the overestimations of traditional analysis that are based on a single deterministic orebody model. The expected NPV of the

OPDPS schedule is $492M, but could range anywhere between ~$450M to ~$540M.

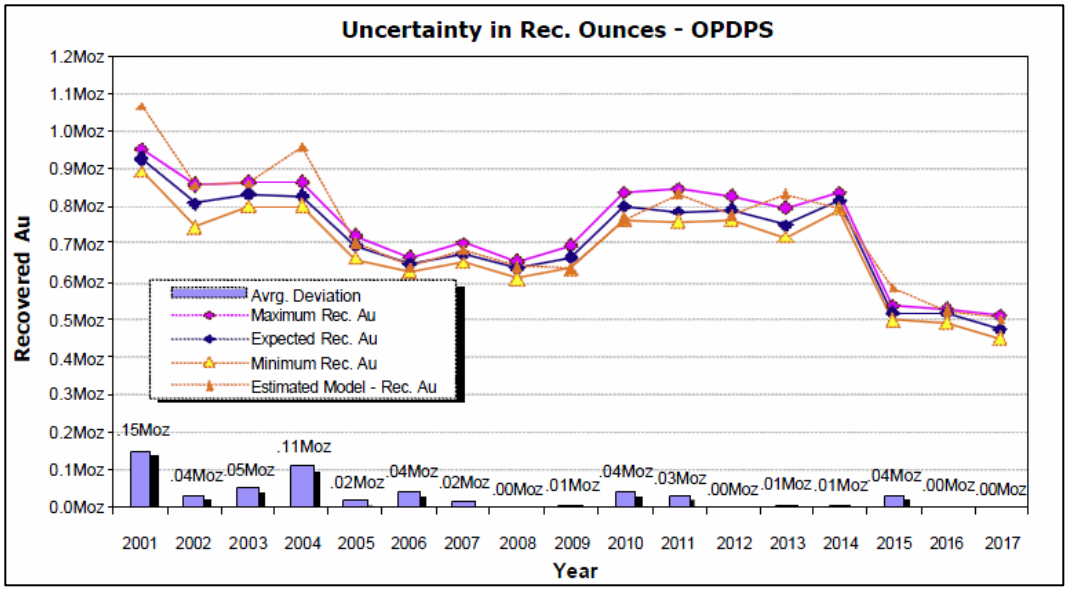

Fig. 8 Uncertainty in recovered metal in the OPDPS schedule (Godoy 2003)

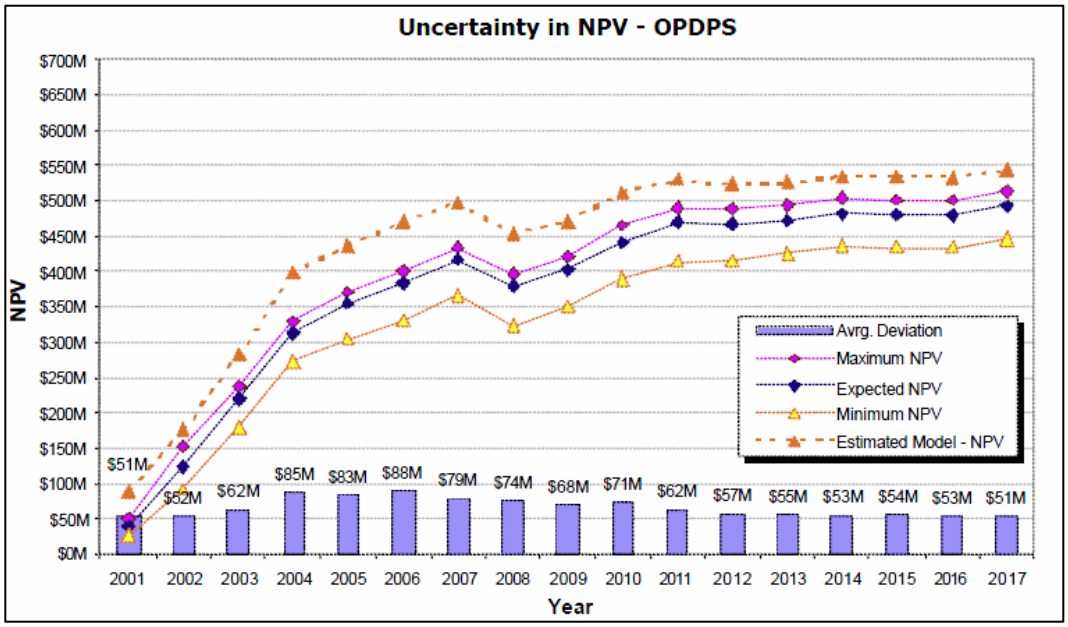

Fig. 9 Uncertainty in the cumulative NPV of the OPDPS schedule (Godoy 2003)

To directly consider the geological uncertainty in the scheduling process, Godoy (2003) uses a combinatorial optimization technique known as 'simulated annealing' to generate a final optimal schedule. In simulated annealing, a suboptimal configuration (i.e. an initial mine sequence) is continuously perturbed until it matches some pre-defined characteristics as coded into an objective function (Kirkpatrick et al. 1983). In this study, the objective function is a measure of the difference between the desired ore and waste production and those of a candidate mining sequence. Each perturbation is accepted or rejected based on whether it improves the value of the objective function. To avoid local minima, some undesirable perturbations are accepted based on a probability distribution (Metropolis, et al. 1953). The initial mining sequence is created such that blocks with maximum probability of belonging to a given period are frozen for that period. The probability of each block belonging to a given period is inferred from a set of conventionally optimized schedules based on the equally probable orebody models, where the mining rates and stripping ratios for each schedule are those determined by the OPDPS stage of the algorithm. Blocks whose schedule period varies across the different schedules are assigned to candidate periods according to their probability rank, and it is these remaining blocks that are randomly swapped between candidate periods in each perturbation. Godoy's implementation of

simulated annealing is called ‘XSCHED’, and a comparison of the uncertainty in recovered metal between the base case conventional schedule and the final risk-based optimized schedule using the algorithm in Fig. 6 is shown in Fig. 10. This figure shows that despite uncertainty in the recovered metal, the final risk-based schedule (XSCHED) has the same total recovered metal as the base schedule, but it consistently schedules greater amounts of recovered metal in earlier periods and so has a mine-life that is two years shorter. The conventional base schedule forecasts less annual recovered metal because it does not consider the stochastic simulations – it only considers a single deterministic orebody model with smoothed grades and thus cannot take advantage of potential high-grade areas of the deposit. The financial implications to capitalizing on grade uncertainty and waste deferral are shown for the optimal risk-based schedule in Fig. 11, which shows an expected NPV of $634M and risk profile range between $586M and $655M. This corresponds to an increase in expected NPV of 28.3% from that of the base schedule. Note that even the lower end of possible NPVs for the optimal risk-based schedule ($586M) is greater than the higher end of possible NPVs for the base schedule ($540M), demonstrating that robustness of the optimal risk-based schedule.

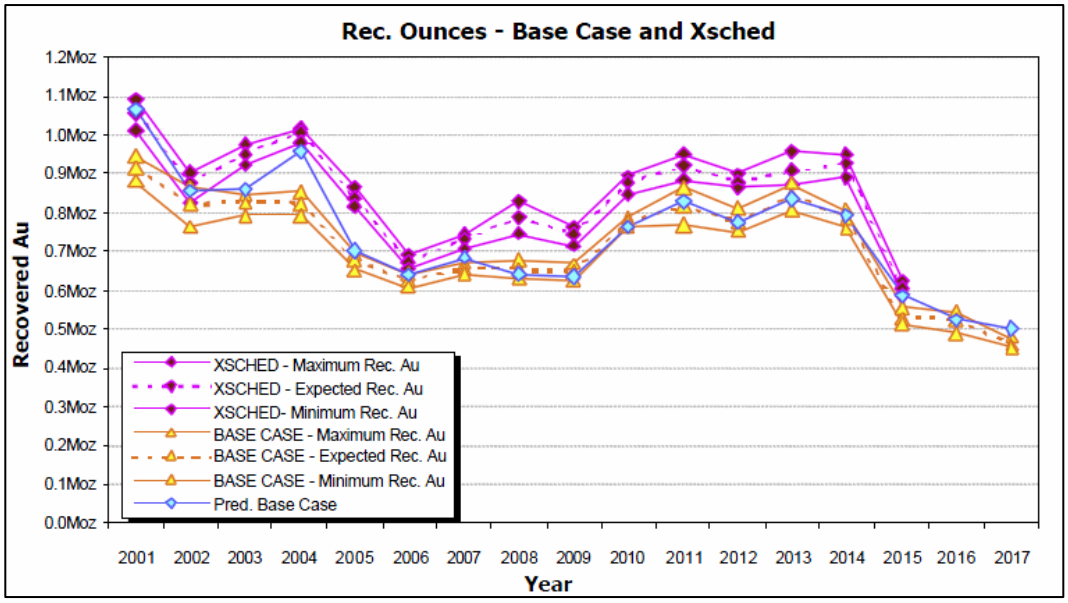

Fig. 10 Comparison of uncertainty in recovered metal between the base case and final risk-based optimized schedule (Godoy 2003)

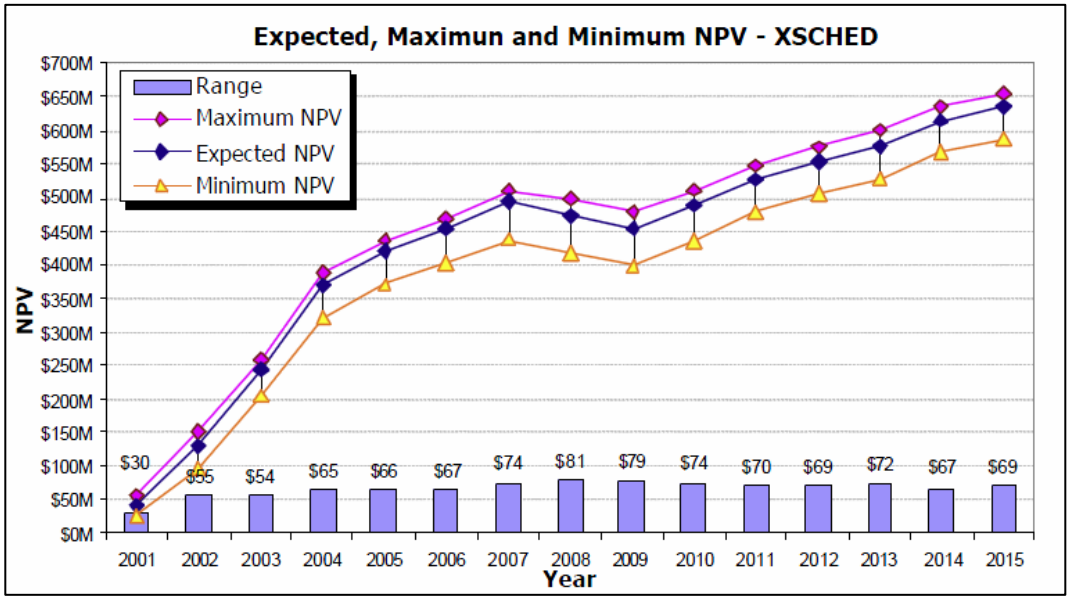

Fig. 11 Uncertainty in the cumulative NPV of the final risk-based optimized schedule (Godoy 2003)

Combinatorial optimization is dependent on the initial sequence and Godoy uses a randomly selected initial sequence from the generated set as input to the combinatorial optimization: a different initial sequence could potentially yield a better result. Another drawback of this procedure is that the optimal mining rate is defined prior to the final optimization, rather than being included in one holistic optimization.

Godoy's methodology was applied by Leite (2007) at a copper deposit, where an NPV 26% higher than that of the conventional schedule was found despite the relatively low grade variability of the deposit. The risk analysis of the stochastic schedule showed that it had low chances of significantly deviating from production targets, while the probability of the conventional schedule deviating from production targets was quite high. Besides noting the need for defining ultimate pit limits and optimizing pushbacks under uncertainty, Leite points out that further study of the impact of cut-off grade selection under uncertainty is needed.

An extension to Godoy's work by Albor Consuegra (2009) explores the sensitivity of the final result to several different aspects. As previously described, in the final combinatorial optimization step, blocks are swapped between candidate periods but Godoy freezes blocks with 100% probability of being in a given period. Albor Consuegra allows all blocks to be available for swapping but concludes that there is no benefit and that

freezing blocks is thus more efficient. Another parameter tested was the number of input schedules to the simulated annealing algorithm. For the copper deposit case study used, it was found that a set of ten schedules was needed in order to meet production targets but that more than ten had no added benefit. Furthermore, with ten schedules as input to the simulated annealing algorithm, it was found that the result was insensitive to the initial scheduled used. Albor Consuegra also found that selecting a different ultimate pit from the available pit shells and using simulated annealing to schedule found a result with an NPV 10% greater than that of the optimized schedule for conventional pit limits. This study was further confirmation that stochastic pit limits are larger than those of conventional pit limits, which means that stochastic scheduling can yield more metal and more value from the same orebody and thus offers a better utilization of natural resources.

Menabde et al. (2007) use an integer programming model similar to that of Caccetta and Hill (2003) but generalized to include stochastic simulations and variable cut-off grades. Their formulation has an objective function to maximize the expected NPV and allows a different cut-off grade from a discrete set to be selected for each mining period. As shown in Fig. 12, the schedule using a variable cut-off grade based on a single estimated orebody model produced an NPV of $(485 ± 40) million, an increase of

20% over the base case schedule with a marginal cut-off $(404 ± 31) million. The schedule using a variable cut-off grade that considers the full set of simulations through their formulation generated an NPV of $(505 ± 43) million, a further increase of 4.1%. Although the increase of 4.1% in NPV may be seen as unsubstantial, the authors note that the orebody model under study did not have very high variability. Their method clearly demonstrates the benefit of a variable cut-off grade based on stochastic simulation, but does not offer the ability to control variability in the production and so targets may fail to be met.

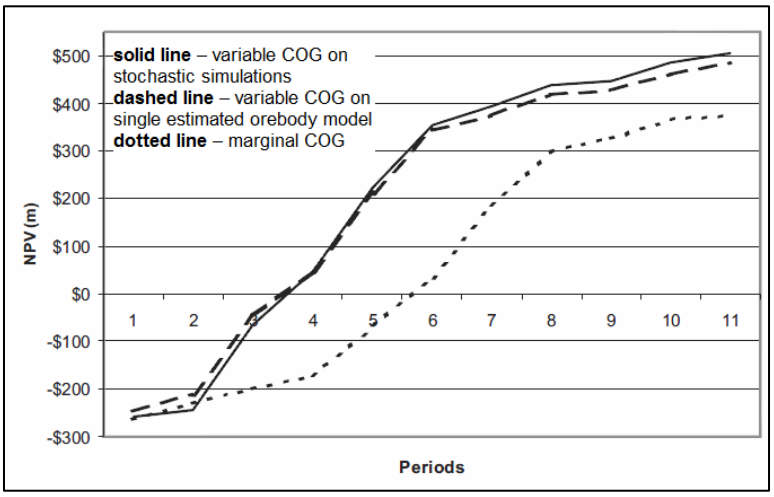

Fig. 12 Cumulative NPV for mining schedules with different cut-off grade strategies (Menabde et al. 2007)

A production scheduling formulation under conditions of orebody uncertainty is introduced by Dimitrakopoulos and Ramazan (2004). Their formulation uses a mathematical programming formulation (Linear Programming) to integrate orebody uncertainty in respect of grade, ore quality and quantity and risk quantification as well as equipment access and mobility and other typical operational requirements. The key part of the formulation evaluates the probability of the material in each period having the desired properties and penalizes deviations from 100% probability. They also introduce the concept of geological risk discounting (GRD), which uses a parameter akin to a financial discount rate to place more emphasis on meeting grade targets in earlier periods. In order to avoid disjunctive impractical mining, their formulation also checks what percent of blocks surrounding a given block are mined concurrently and penalizes deviations from 100%. Using this formulation and comparing the results to a schedule produced through conventional optimization that does not consider geological uncertainty, they showed that the stochastic optimization approach produced a schedule with 6% less risk of not meeting grade targets. The conventional schedule had a 2% higher total NPV, but it is important to note that the stochastic approach did not explicitly attempt to maximize the NPV and that given the risk of not meeting production targets, the higher NPV result is misleading. This

suggested that integration of orebody uncertainty in production schedule optimization formulations might have further benefit.

1.2.2. Stochastic Integer Programming

Stochastic integer programming (SIP) is a type of mathematical programming and modelling that considers multiple equally probable scenarios and generates the optimal result for a set of defined objectives within the feasible solution space bounded by a set of constraints. SIP is an extension of mixed integer programming (MIP) with uncertainty in one or more of the related coefficients (Escudero 1993). Different approaches to SIP formulations are discussed in Birge and Louveaux (1997); however, these approaches and other existing developments in the technical literature are not directly applicable to mining problems (Dimitrakopoulos and Ramazan 2008).

Ramazan and Dimitrakopoulos (2007) introduce a stochastic integer programming (SIP) formulation that directly maximizes the NPV while minimizing deviations from production targets by penalizing deviations within the objective function. Penalizing the deviations rather than setting hard constraints is an important concept because when considering many different goals and constraints, setting absolute constraints can make a problem infeasible and it prohibits the scheduler from using blending to manage risk, which is a major source of value in SIP models. The relative

value of the penalties determines their priority, whose selection is a management decision in the absence of actual dollar values (ex. impurity penalties in sales agreements). Empirical testing for specific problems can be used to determine appropriate penalties, and it is the relative magnitude of the costs for deviations rather than their precise value. The scheduling method developed here allows for a management decision of defining a risk profile based on the existing uncertainty quantified by simulated orebody models. The decision-maker has the option of minimizing the risk in each of the production periods, or tolerating some risk in some or all periods. In the traditional scheduling model, geological risk is randomly distributed over the periods and can be significantly large. The new SIP model allows the selection of the best mine design based on the resultant NPV and the risk profile defined.

In Dimitrakopoulos and Ramazan (2008), the previous stochastic framework was tested in two applications, demonstrating the value of the stochastic solution: a gold deposit had a 10% higher NPV than conventional schedule optimization and a copper deposit had a 25% higher NPV, both with greater chance of meeting production expectations than conventional scheduling. Also discussed are the concepts of Expected Value of Perfect Information (EVPI) and the Value of Stochastic Programming (VSP), that provide respectively the maximum economic

value a decision maker should be willing to pay for complete and accurate information about the deposit, and the difference between the value of the stochastic solution and the expected value (under uncertainty) of the conventional solution.

Ramazan and Dimitrakopoulos (2013) formalize their previous work and provide the complete formulation (providing full details of the objective function and all constraints) of a full two-stage SIP framework that maximizes the NPV of a production schedule while minimizing the risk of not meeting production targets. The formulation also provides for stockpiling and stockpile retrieval to further aid in the blending of material to meet production targets, which is a common employed mining practice. The results clearly indicate that the SIP model is a powerful tool for controlling the distribution of risk between production periods and is able to control both the magnitude and probability of the risk within individual production periods. The SIP model also generates a schedule with greater expected economic value by delaying risk to later production years, ensuring that production targets are met in the earlier years that most affect the NPV. This model serves as the basis of several other studies that are discussed next.

Leite and Dimitrakopoulos (2014) use the SIP framework in an application at a copper deposit that yields an NPV 29% higher than that of a

conventional scheduler. In addition, the stochastic schedule forecasts a shorter mine life (seven years vs. eight years for the conventional schedule) because the conventional schedule based on a single orebody model overestimates the amount of ore above the 0.3% Cu cut-off that is applied.

Albor Consuegra and Dimitrakopoulos (2010) use the SIP framework to examine the selection of pushback designs (mining phases). Pushbacks are intermediate pit configurations designed to guide the sequence of extraction up to the point where the ultimate pit limits are reached. Each pushback may consist of several actual mining periods and a mining period could extend across two pushbacks. The conventional method of designing pushbacks is based on grouping nested pits, a process that does not consider geological uncertainty and thus the pushbacks may have risk of not meeting production targets. Albor Consuegra and Dimitrakopoulos select a set of pushback sequences where each sequence has a different total number of pushbacks and each sequence has the maximum NPV for that number of pushbacks. An SIP framework is then used to create a schedule based on each pushback sequence and then a geological risk analysis is performed to evaluate which sequence has the highest NPV but also meets the production targets. Conceptually, this is a convoluted approach with many steps and a better approach to

pushback design under uncertainty is to simply use an SIP framework in two stages: once for scheduling pushbacks, and once for scheduling the periods following the pushback sequence.

Benndorf and Dimitrakopoulos (2013) use an SIP formulation to create a long-term production schedule for a hematite iron ore deposit. The case study deposit involves geological uncertainty with multiple correlated elements: iron, phosphorus, silica, alumina, and loss on ignition. Although the financial risk associated with the schedules is not presented, the results demonstrated the ability of the stochastic approach to jointly control the risk of multiple quality-defining elements deviating from targets as well as control the risk of ore tonnage production deviations.

In cases where production scheduling requires scheduling hundreds of thousands or more blocks, there are a large number of integer variables in the SIP model, which can translate to computational issues for conventional solvers like CPLEX (IBM 2009). In such cases, the production schedule optimization solve time can be impractical, and so some research has gone into meta-heuristic methods such as Tabu Search and Variable Neighbourhood Search to efficiently generate strong solutions in reasonable computation times (Lamghari and Dimitrakopoulos 2012, 2014).

The SIP methods discussed thus far are all long-term planning approaches to production scheduling that are based on geological models created using exploration data only. Should a mine go into production, new high-density data becomes available and would ideally be incorporated into the existing models so that stochastic production scheduling could be based on the best information available. Jewbali (2006) and Dimitrakopoulos and Jewbali (2013) present a methodology for inferring better short-scale spatial statistics from initial production grade-control data in order to simulate possible future grade-control data. The simulated grade-control data is used to update the existing geological models using the method of conditional simulation by successive residuals introduced by Vargas-Guzman and Dimitrakopoulos (2002). Vargas-Guzman's setup is not computationally possible, however, which Jewbali and Dimitrakopoulos address using a column and row decomposition of the correlation matrix. Jewbali applies an SIP framework at the Sunrise Dam gold deposit in Western Australia to create production schedules based on the original geological models (that are based only on exploration data) and the updated models (that are based on exploration data as well as grade-control data). The approach was shown to create a schedule that more closely matched the mine's actual reconciliation data,

even though the majority of grade-control data used was only simulated based on some initial production data.

Boland et al. (2008) propose a multistage optimization model that incorporates stochastic geological simulations and in which decisions made in one period can depend on information obtained from the mining in earlier periods. Processing decisions are made assuming full knowledge of the mined material, which creates a scenario-based solution that cannot be used for long-term planning prior to mining. Applying this framework to globally optimize a mine complex is complicated because the optimized destination policy is based on linear assumptions that imply partial blocks can be sent to a given destination, which is not practical since after extraction periods of blocks are determined, it is very hard to change the extraction sequence because of slopes, roadways and equipment movement.

1.2.3. Global optimization of mining assets

With the advances in mine production scheduling, a larger problem that is now being tackled is the strategic optimization of entire mining complexes. This means considering not just mining and production scheduling, but all the activities of a mining operation, which include blending, different processing streams, transportation, and product creation and sales. In optimization of an entire mining complex, processing path decisions are an

important aspect. For a given processing path, there may even be multiple alternative operational configurations (fine and coarse grinding for example). If a process plant is used for more fine grinding, energy consumption is typically much higher, which results in higher processing costs and longer process times. For more coarse grinding, energy consumption is typically less, which results in lower processing costs and shorter process times, but the weight recovery suffers. When in different operating modes, the tolerable amount of various impurities could be different: more coarse grinding of an iron ore for instance may not be able to liberate as much iron from the host silica. Traditionally, the process plant is optimized separately from the mining, but studies have shown that there can be significant benefit from globally optimization that considers both jointly.

In the late 1990s, Newmont Mining Corporation identified a need to co-ordinate mine planning efforts between multiple mines, stockpiles, and processing facilities (Hoerger et al. 1999). Their operation in northern Nevada identified more than 90 metallurgical ore types and has over 60 defined gold-recovery process options. Since costs and processing options can be shared across multiple sites, a holistic optimization is able to determine a better plan for their operation than multiple and separate site optimizations. They develop an MIP model to maximize the NPV by

selecting the optimal flow of materials from mine sources to plant processes and stockpiles, and from stockpiles to plant processes. Their optimization process lead to decisions that increased the company's overall profitability and also helped eliminate promising scenarios that were, in fact, unattractive. As an example, their optimization found that treating ore from the high-grade Deep Star mine at the Twin Creeks mine autoclave (a processing technique that uses pressure oxidation to liberate metal) rather than the original destination at the Carlin mine roaster (a processing technique that burns off impurities). Although this decision incurred a higher transportation cost due to an additional distance of 160 km, the cost was offset by an increase in recovery at the autoclave and there was a net benefit. An optimization of the Deep Star mine and nearby processing options alone would not have identified this option.

A practical implementation of an MIP framework was developed as an "intuitive and flexible" software tool called "Blasor" by BHP Billiton (Menabde et al. 2007). The complexities of optimization frameworks usually require a great deal of specialized knowledge, and so packaged planning tools like Blasor are important for mine planners to be able to perform pit development optimizations without assistance. This was also one of the first packaged tools capable of optimizing the life-of-mine development plan, including ultimate pit and mining phase designs, for

blended-ore multi-pit operations. This is proprietary software, however, so full details of the framework are not disclosed.

G. Whittle (2010) discusses the typical characteristics of a globally optimized mine plan in detail and how to model these characteristics. Due to the large number of aspects to consider, Whittle points out that solving for optimized solutions often exceeds the capabilities of readily available mining tools. To address this issue, he proposes that mine production sequencing use material aggregation techniques. This reduces the problem size significantly, but also restricts the ability of the optimizer to take advantage of material and risk blending benefits, which are of extreme importance especially when considering geological uncertainty. The methods Whittle uses to solve his problem formulations are heuristic in nature: they search for good solutions but cannot guarantee a globally optimal solution.

J. Whittle (2010) goes into more detail on the development and performance of the optimization algorithms used by G. Whittle. He specifically cites the problem of local maxima, which often arises with heuristic methods because they typically make small adjustments to each variable and stop when no further improvements can be found. Although the solution found might be the best for the current range the variables are

in, if a large change is made to one or more of the variables, an entirely different optimal solution could be found, possibly higher than the first.

Goodfellow and Dimitrakopoulos (2014) propose a two-stage stochastic mining complex optimization model that can accommodate non-linear aspects of the supply chain and also does not require simplifying assumptions to generate high-quality solutions. Their model creates destination policies that are robust with respect to geological uncertainty, avoids using a-priori cut-off grade policies, and addresses blending, stockpiling and multiple processing streams.

Montiel and Dimitrakopoulos (2014) also addresses mining complex optimization with multiple of each of the following: pits, material types, stockpiles, process destinations, process operating configurations, transportation systems, and final products. This is shown diagrammatically

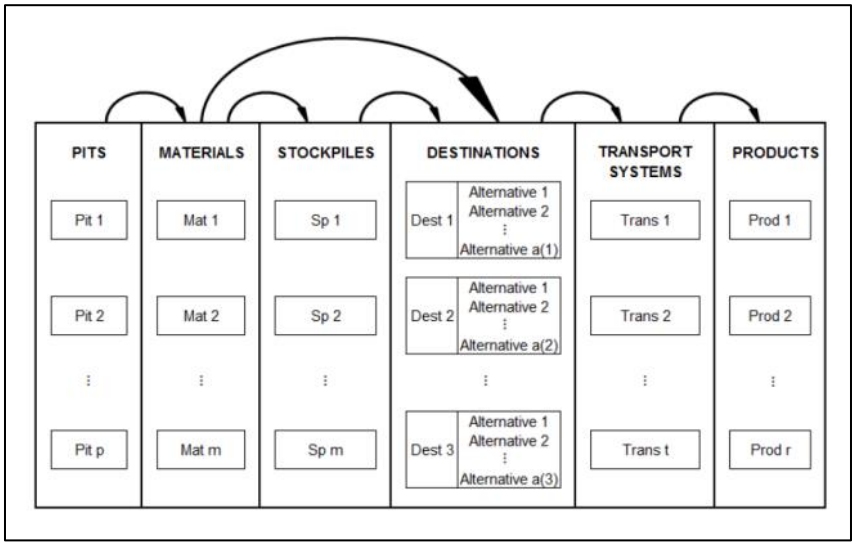

Fig. 13 Flexibility within a mining complex (Montiel 2014)

in Fig. 13. In order to optimize this large number of variables, a heuristic algorithm based on simulated annealing is used. An initial scheduling solution is fed into a three-stage hierarchy of perturbation cycles. In the outermost cycle, perturbations occur on the block scale, modifying the periods and destinations of each block. In the second level, perturbations to the operational alternatives at each given destination are made. In the third level, perturbations are made to the proportion of output material transported using the available transportation systems. Since changes to any activity within the mining complex affects the others as well, the algorithm cycles through the three levels of perturbations iteratively within a predetermined computational time or until a desired quality of solution is obtained.

Optimization of entire mining complexes demonstrates value over separate individual optimizations that when combined do not make for a globally optimal solution. Research continues to focus on methods to efficiently model and solve the full-scale problems faced by mining operations in order to generate greater profitability while also reducing risk.

1.2.4. Iron ore case studies

This thesis addresses production schedule optimization at an iron ore mine, and so the existing literature specifically addressing applications at

iron ore deposits is now briefly reviewed. The majority of production scheduling methods discussed up until now are general in that they can be adapted for any type of open pit mine, but it is worth noting the few iron ore case studies exist. This is probably primarily due to the fact that the iron ore market is dominated by only a few very large companies: 75% of seaborne shipments are controlled by Vale of Brazil, Rio Tinto, and BHP Billiton (Kakela 2014). The existing research focuses on two specific mines: BHP Billiton's Yandi mine in Western Australia, and the Kiruna mine in Sweden controlled by LKAB, a smaller producer in terms of total tonnes of delivered iron ore, but a company that is remaining competitive by careful management of its resources through implementation of the more recent approaches to mine planning.

Stone et al. (2004) use the Blasor software tool described in Section 1.2.c. in an application at the Yandi iron ore deposit to ensure that all market tonnage, grade and impurity constraints are observed while maximizing the discounted cash flows generated by the schedule. However, this tool uses block aggregations that can lead to sub-optimal design and there is also significant risk of not meeting production targets during actual production, as demonstrated by Benndorf and Dimitrakopoulos (2013), who studies the same deposit but while considering geological uncertainty.

Benndorf applies an SIP model with an objective function that also seeks to maximize the discounted economic value, but also minimizes deviations from production targets in terms of ore tonnage and quality as well as minimizing the costs of non-smooth mining. This can be clearly seen in Fig. 14, which shows the risk profiles for two impurity grades (silica and alumina) for the stochastic schedule and for the E-type schedule (a non-risk-based conventional schedule that is based on a single estimated orebody model). The graphs show the uncertainty in the grades for each period through the distribution of possible values that could be obtained by each schedule. The solid horizontal lines indicate the target tolerance limits. It is evident that the E-type based schedule is not able to account for geological uncertainty. Although the mean values of the element grades produced per period are inside the production targets, there are considerable deviations from upper and lower production limits for both grades. In the stochastic schedule silica deviates just slightly in periods two and five with a probability of 5% and 20%, respectively. The E-type schedule shows silica deviations from targets in every period with an average probability of 30%. The probabilities of deviating from upper and lower limits are almost twice high for the E-type schedule compared to the stochastic based schedule, especially for alumina. The stochastic

schedule shows a higher probability of meeting production targets, which diminishes project risk and can increase project value.

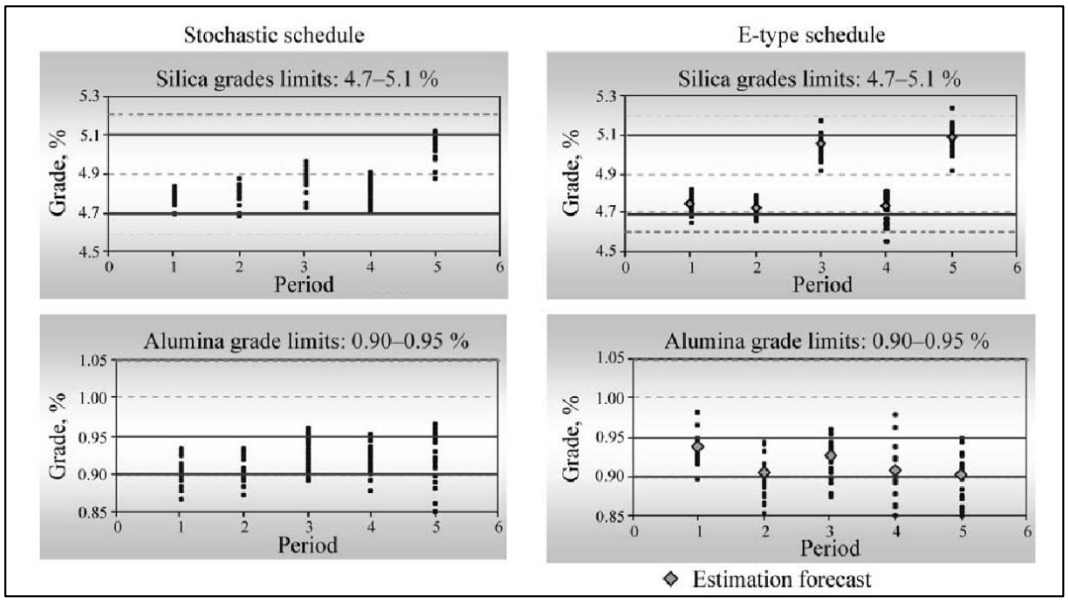

Fig. 14 Risk profiles for impurity grades (silica and alumina) for a stochastic schedule (left) and a conventional non-risk-based schedule (right) (Benndorf and Dimitrakopoulos 2013)

The majority of production schedule optimizations do not explicitly model waste handling. Typically, formulations decide what destination to which to send waste material, where a ‘destination’ is usually a waste dump of stacked material. They do not usually specify the exact locations within the dump to place the material, as this is often not of importance. However, there are operations where the space available outside of the pits for waste rock dumping may be very limited. In such cases it eventually becomes necessary to dump waste back into the pit into the voids created

by the extractions. This may also be required at some sites due to environmental concerns. The standard version of Blasor does not explicitly model waste handling, but a specialized version of Blasor called Blasor-InPitDumping (BlasorIPD) was developed for this reason (Zuckerberg, et al. 2007). In BlasorIPD, a space can only be classified as available for dumping if all blocks within a user defined radius have already been cleared, and if additionally all spaces within the ore body that lie below the dumping location have been refilled such that maximum pit slope angles are respected. Additionally, a space cannot be made available for dumping if that space sits atop material classified as ore that has not yet been cleared. An alternative implementation could allow dumping to take place on top of ore, thereby sterilizing that ore. BlasorIPD uses material aggregation to ensure problem tractability and the authors allude to other relaxations to the problem that they make to reduce the problem size, but do not go into details.

Despite the proven risk to mine plans and financial forecasts, there are other recent examples of iron ore operations that use deterministic MIP frameworks for production scheduling of an underground iron ore mining operation at the Kiruna mine in Sweden (Kuchta et al. 2003, Newman and Kuchta 2007). They design a heuristic based on solving a smaller, more tractable model in which periods are aggregated; they then solve the

original model using information gained from the aggregated model. By computing a bound on the worst-case performance of this heuristic, they demonstrate empirically that this procedure produces good-quality solutions while substantially reducing computation time.

These iron ore studies demonstrate that recent production schedule optimization of iron ore mines are still mostly using deterministic approaches that do not incorporate geological uncertainty and thus mine production could have significant risk of deviation from targets and significant financial risk. With respect to iron ore mining, only the work by Benndorf (2013) is based on stochastic mine production scheduling, which demonstrates that there is a clear need for more case studies to demonstrate the benefits of stochastic production scheduling methods and that such methods can be practically implemented.

1.3. Stochastic Simulation

Incorporation of geological uncertainty via simulated orebody models in stochastic mine planning and optimization requires the generation of multiple realizations of the orebody. A common technique for creating multiple realizations is through geostatistical simulation. Geostatistics is a branch of statistics that can be used to predict probability distributions of the spatial datasets acquired by mining operations.

Two of the most commonly used forms of geostatistical simulation for deposits are sequential Gaussian simulation (SGS) for continuous variables and sequential indicator simulation (SIS) for continuous variables through a set of cut-offs as well as for categorical variables (Goovaerts 1997). These methods require computation of the inverse of a covariance matrix, which can be very computationally intensive. As an example, generating 50 simulations of an orebody model discretized by 100 million nodes would require 135×10^{12} floating point operations (135 Tera Flops). Memory usage is an additional consideration. Using the same example, if the simulated values are stored as double precision floating point numbers (8 Bytes) and spatial coordinates as single precision floating point numbers (4 Bytes), then the total memory allocation required to store the simulation grid would be approximately 2 Giga Bytes.

Implementations of SGS were developed that are highly computationally efficient and can manage the limitations of finite memory. The generalized sequential Gaussian simulation, or GSGS is a general form of SGS that replaces the node-by node sequential process in SGS with a group of nodes and the simulation is carried out for groups of nodes simultaneously (Dimitrakopoulos and Luo 2004). Fig. 15 shows four nodes to be simulated (numbered in white) along with surrounding data (in black). A hatched circle around each node to be simulated represents the neighborhood

from which data is considered for informing the simulation process. For nodes that are close to one another, the neighborhoods overlap. By using one common neighborhood for a set of close nodes rather than separate neighborhoods, a more computationally efficient algorithm can be derived.

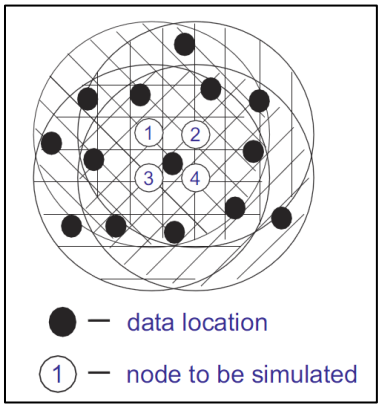

Fig. 15 Shared neighborhoods of group-nodes (Dimitrakopoulos and Luo 2004)

There is a trade-off between computational efficiency and accuracy that depends on the size of the neighborhood used. In order to measure this trade-off, Dimitrakopoulos and Luo introduce the screen-effect approximation loss (SEA loss) defined as the mean-square difference between the simulated value conditioned on the neighborhood and the simulated value conditioned on the complete data set. This measure can be used to determine a neighborhood size with an acceptable trade-off, although the study suggests that in most situations, a relatively small neighborhood can be used without significant loss of accuracy. A drawback of this algorithm (and traditional SGS) is that a change of

support is needed to change the point-support scale simulations to the block-support scale needed for mine planning.

A further improvement to the algorithm was the direct block support simulation method (Godoy 2002). The algorithm simulates point values within each block using the GSGS concept, then calculates the block average of the point values before discarding them. The algorithm uses a joint-simulation integrating points and blocks, which sees a reduction in calculations needed as well as a significant reduction in the amount of data stored in memory. Additionally, no change of support is needed at the end of simulation. In a comparison study between GSGS (with a group configuration of 2x2x2 nodes and a neighborhood size of 45) and DBSIM (Benndorf and Dimitrakopoulos 2007), DBSIM took 7% less time than GSGS to run, and only required 1% of the memory requirements of GSGS.

Variants of SGS can only be used to simulate one variable at a time, which is problematic for simulating multi-element deposits that have correlations between the elements. Individual simulation of each element would not result in the correlations being preserved in the simulations and so in such cases, a method for joint multi-element simulation is required.

One approach to joint multi-element approach is to use a procedure known as max/min autocorrelation factors (MAF) (Switzer and Green

1984), (Desbarats and Dimitrakopoulos 2000) to transform a set of correlated variables into uncorrelated factors, which can then be independently simulated. The MAF technique allows for transforming the factors back to the original data space with the original data correlations preserved. An algorithm was developed by Boucher and Dimitrakopoulos (2009) that combined MAF with the direct block approach to create the DBMAFSIM algorithm for an efficient joint simulation framework. They use this procedure to simulate the grades of the Yandi iron ore deposit in Western Australia (Boucher and Dimitrakopoulos 2012) demonstrating the method is practical and able to reproduce the spatial correlations between multiple elements.

Although structural aspects of geological modeling are often treated as categorical (i.e. a discrete set of different lithologies), Eggins (2006) demonstrated a technique that represents a set of lithologies in a stratiform deposit as discontinuous geological layer thicknesses. The layer thicknesses are treated as correlated variables and the MAF technique is used to simulate them throughout a deposit. In the case of a stratiform deposit with multiple correlated variables whose distributions are approximately normal, the DBMAFSIM algorithm is the most efficient existing method of stochastically simulating both structural and quality elements such that correlations are preserved.

Although unable to account for multiple correlated variables, a number of multi-point and higher-order stochastic simulation frameworks have been developed in the last two decades in order to account for higher order spatial relations and connectivity. This is because past conventional practice for stochastic simulation of spatial random fields is only based on the first two orders of statistics (histograms and variograms) (David 1988, Goovaerts 1997, Chiles and Delfiner 1999), which is limited in that such two-point methods are unable to characterize curvilinear features and complex geometries that are common in geological environments. An example of this is shown in Fig. 16 where three patterns that are completely different all result in essentially the same variogram.

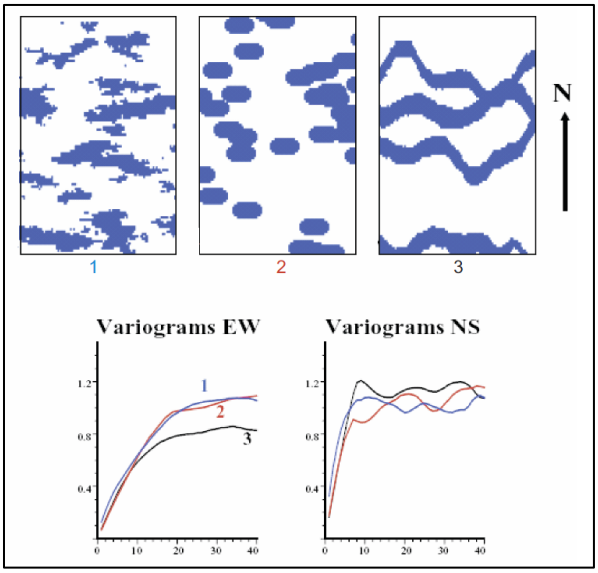

Fig. 16 Vastly different patterns resulting in the same variogram (after Journel 2007)

Multiple-point statistics consider the joint neighborhood of any number of *n* points. A template of any size *n* can be used along with different shapes to capture data events surrounding a central value (see Fig. 17). Whereas

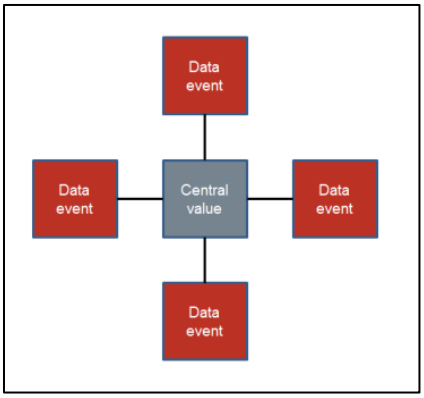

Fig. 17 A 4-point data event template around a central value (after Osterholt and Dimitrakopoulos 2007)

variograms can only consider 2-point statistics in one direction in 2D, multiple-point templates can be built in 3D.

Guardiano and Srivastava (1993) first introduced the concept of multiple-point statistics. Their algorithm depends on a training image from which they infer the probability of a given data configuration occurring and then simulate values based on the conditional probability of the data configuration around the point to be simulated. An extension of their work is presented by Strebelle (2002) as the *snesim* (single normal equation simulation) algorithm, which is much more efficient because it builds a search tree of the different data events in the training image. The *snesim*

algorithm requires an exact match of the conditioning data event by the training image, so if no such pattern is found, the conditioning data is reduced by dropping the furthest data event. This is an intensive approach requiring a training image that is large and rich enough to contain the majority of possible conditioning data events that could be found during simulation. To take advantage of more recent computer hardware such as multiple-processor computers, multiple-core processing units and graphics processing units (GPU), Huang et al. (2013) develop a parallel implementation of *snesim* that runs more efficiently. Strebelle and Cavelius (2014)propose several improvements to the *snesim* algorithm that further increase speed and reduce memory requirements. However, for large three-dimensional problems with numerous facies, large templates may not be possible due to memory limitations. An alternative algorithm called *impala* is proposed by Straubhaar et al. (2011) that uses a list instead of a tree to store the statistics inferred from the training image. This approach allows for a significant reduction in memory requirements and the algorithm can also be easily parallelized. Both *snesim* and *impala* use a multiple-grid approach (Tran 1994) to capture features at different scales.

Another approach to multiple-point simulation is to simulate patterns directly rather than points within patterns using statistics. However, these

methods are based on heuristic arguments rather than any formal theory and so it is difficult to verify performance other than through visual checks. Arpat and Caers (2007) select the pattern from a pattern database in two steps by distinguishing the hard data from the previous simulated nodes. An algorithm called *filtersim* (Zhang et al. 2006, Wu et al. 2008) uses weighted distances to give more importance to previously simulated nodes. This algorithm trades the exact data event reproduction for an approximate reproduction, which has the benefit of not needing to drop data and having a loss of conditioning information. Tahmasebi et al. (2012, 2014) use a raster simulation path rather than using a multiple grid approach. Their algorithm uses a cross-covariance function to express the similarity of patterns, and deals with the hard data by splitting the pattern into smaller regions. Several recent methods look to reduce the dimensionality of the pattern classification problem. Honarkhah and Caers (2010) introduced a distance-based method for efficiently classifying the pattern database and kernel space mapping to reduce the dimensionality. Chatterjee et al. (2012) classify the pattern database using wavelet approximate sub-band coefficients of each pattern to reduce the dimensionality yet still capture most of the pattern variability. They then use k-means clustering for classification of the pattern database. Mustapha et al. (2014) build cumulative distribution functions of the one-

dimensional patterns that are then used to classify the patterns. During the simulation process, a conditioning data event is compared to the class prototype, and a pattern is randomly drawn from the best matched class.

Mustapha and Dimitrakopoulos (2009), Dimitrakopoulos et al. (2010), and Mustapha et al. (2011) introduce the concept of spatial cumulants to model and simulate continuous variables, where spatial cumulants are simply combinations of lower- or equal-order spatial moments. A moment is quantitative measure of the shape of a set of points, where the first raw moment is the mean, the second central moment is the variance, the first two commonly known higher-order standardized moments are skewness and kurtosis, and any number of higher order moments can be computed. Mustapha and Dimitrakopoulos (2010, 2011) propose a high-order sequential simulation algorithm called *hosim* for continuous variables, which has been shown to accurately reproduce many orders of spatial statistics on sparse data sets. Methods using cumulants are different from the previously mentioned multiple-point geostatistics algorithms because they attempt to quantify spatial interactions using maps of high-order statistics that are able to characterize non-linear and non-Gaussian stationary and ergodic spatial random fields.

Despite the advantages of these more recent developments in reservoir modeling, computational efficiency remains a problem for large full-field

simulations and another limitation of all the previously mentioned simulation techniques is that none of them is able to jointly simulate multiple correlated variables. However, as discussed, techniques exist based on older two-point statistical methods for efficiently jointly simulating multiple correlated variables.

1.4. Goals and Objectives of this thesis

The aim of this study is to document how geological risk can be quantified and to apply a stochastic mine planning framework at the LabMag open pit iron ore deposit in order to document improved profitability as well as reduced risk of not meeting production targets.

The specific goals of this thesis are as follows:

1. Review the technical literature related to stochastic geological modeling and stochastic mine production scheduling.
2. Model the LabMag deposit using stochastic joint simulation of multiple attributes and evaluate the effects of geological variability on an existing mine production schedule.
3. Create a stochastic long-term mine production schedule framework and apply it at the LabMag open pit iron ore deposit with the aim of demonstrating an increased value of stochastic production scheduling over deterministic production scheduling.

4. Draw conclusions from the study and make recommendations for future work.

1.5. Thesis Outline

This thesis is organized according to the following chapters:

Chapter 1: The technical literature related to the topics in this thesis is reviewed. The goals and objectives of this thesis are stated.

Chapter 2: The stochastic joint simulation of the multi-element LabMag deposit using the DBMAFSIM algorithm is presented and the effects of geological variability on an existing production schedule are evaluated based on these simulations.

Chapter 3: A SIP formulation for the stochastic optimization of a multi-element life-of-mine production schedule is used to stochastically optimize the LabMag deposit in order to minimize risk of deviation from production targets and to maximize the mine's expected discounted cash flows.

Chapter 4: Conclusions are made based on this study and recommendations are provided for further work.

Chapter 2

Modelling Geological Variability in the LabMag Iron Ore Deposit and Effects on the Long-Term Production Schedule

2.1. Introduction

Mining projects require very large financial investments and having reliable data is critical to making decisions that will lead to economic success (Dowd 1994, 1997, Vallée 2000). One of the main sources of risk in a mining project is the modeling of the orebody because the primary data used for modeling is usually sparse (usually consisting primarily of expensive sub-surface drilling) and there is inherent uncertainty in any estimation method used.

Conventional approaches to orebody modeling and mine planning are based on a deterministic orebody model and result in single, often biased, forecasts (Dowd 1994, David 1977, Dimitrakopoulos et al. 2002). A deterministic geological model assumes fixed lithological boundaries and has a single estimated set of qualities such as mineral grades, but does not provide for measurement of the associated variability of those properties. Subsequent work in mine design and production scheduling typically assumes that the deterministic model is 100% accurate and is optimized on that basis. However, given the inherent in situ variability in the resource model, variability in the materials being scheduled to be

mined in the long-term plan (and thus in financial forecasts) can also be expected.

Geological variability is evaluated using stochastic conditional simulation, a Monte Carlo-type simulation approach used to model variability in spatially distributed attributes such as pertinent characteristics of mineral deposits. The concept behind stochastic simulation is to generate equally probable representations of the *in-situ* orebody variability in both grade and material types. All realizations of the orebody are equally probable and reproduce the available data, their distribution and spatial continuity. A collection of conditionally simulated deposits captures the variability of the orebody and attributes of interest (David 1988, Goovaerts 1997). The computationally efficient method used here is a direct block support simulation method that discards point values as block values are calculated, and performs a joint simulation. The algorithm provides the means to simulate several hundreds of points per second (Godoy 2002).

Ore mineralizations frequently contain more than one quality of interest that are spatially related. As a result, they require the use of joint geostatistical simulation techniques that generate models conserving this correlation. In order to jointly simulate multiple variables, an effective technique is to de-correlate the variables. De-correlated variables can be independently simulated and then back-transformed in order to preserve

the correlations between the original variables. Decorrelation of geological attributes was first introduced by David (1988) using principal component analysis (PCA) at a Uranium deposit. This approach is limited in that it ignores cross-correlations at distances other than zero, which typically exist in mineral deposits. A decorrelation procedure called minimum/maximum autocorrelation factors (MAF) was introduced by Switzer and Green (1984) for the processing of multi-spectral remote sensing imagery and later applied in a geostatistical context by Desbarats and Dimitrakopoulos (2000). The MAF approach is based on PCA, but spatially decorrelates the variables involved to non-correlated factors. The independent MAF factors are individually simulated and then back-transformed to conditional simulations of the correlated deposit attributes. These simulations reproduce the cross-correlations of the original variables. The MAF approach is applied by Dimitrakopoulos and Fonseca (2003) at an oxide copper deposit located in northern Brazil. They show the successful reproduction of the original data spatial characteristics in stochastic simulations of the deposit and show the uncertainty in the grade-tonnage curves. Eggins (2006) applies the MAF approach to a silver/lead/zinc stratiform deposit located in northern Australia. Besides addressing the issue of simulating multiple correlated elements, his approach also addresses two further complications: folding in some areas

of the deposit, and missing data (the MAF transformation requires all variables at each location to be populated). An extension by Boucher and Dimitrakopoulos (2009) combined MAF with the direct block approach to create an efficient joint simulation framework. They use this procedure to simulate the grades of the Yandi iron ore deposit in Western Australia (Boucher and Dimitrakopoulos 2012), without treating different lithological domains separately as in the present study. In iron ore deposits, geological domains may include weathering, ore and contaminant envelopes, and domains could also be required for other physical properties such as density, hardness, and lump-fines yield. The variability in possible boundary locations translates to variability in ore volumes/tonnages and can lead to inconsistencies between mine planning and realized production. Besides allowing for quantification of uncertainty in existing mine production schedules, geological simulations can serve as input to stochastic mine planning in order to significantly improve the NPV and to reduce the risk of not meeting production targets, as was done for the Yandi iron ore deposit (Benndorf and Dimitrakopoulos 2013).

This paper presents a full-field application of a MAF procedure that simulates directly at the block-support scale. Firstly, multiple conformable lithological surfaces are jointly simulated based on thickness. Secondly, multiple ore qualities are jointly simulated within each controlling lithology.

The application of block simulation with MAF to surfaces successfully reproduces the inter-dependence between the thicknesses of the various lithologies, which is an issue that is often ignored.

The application is at the LabMag deposit controlled by New Millennium Iron Corp., located in a 210 kilometer belt of taconite in northern Québec and Labrador (see Fig. 18). The iron formation in the MIR (Millennium Iron Range) is of the Lake Superior type, which consists of banded sedimentary

Fig. 18 Location of the Millennium Iron Range and the LabMag deposit

rocks composed principally of iron oxides, magnetite, and hematite within quartz/chert-rich rocks with variable amounts of silicate and carbonate lithofacies. Taconite is the name given to a particular type of sedimentary iron formation whose iron content is commonly present as finely dispersed magnetite (generally 25-30%).

To liberate the iron in taconite, which is a hard rock, requires very fine crushing. Magnetic separation can then be used to separate the ore from the waste. The Davis Tube test is a method for measuring the quantity of magnetic iron recoverable from an ore. Traditional chemical analysis shows total iron content, whether magnetic or non-magnetic. However, since the typical processing of taconite uses magnetic separation, the non-magnetic iron is lost. The Davis Tube test thus gives a good approximation of the expected recovery by weight, although there is usually also some additional loss in the real plant. Clean concentrate of magnetic material can then be analyzed for iron grade as well as the primary impurity, silica.

The two overlying waste-types for the LabMag deposit are overburden (OB) and Menihek Shale (MS). The OB covers the entire deposit but is minimal (the underlying rock is commonly exposed at surface). The MS layer is present on the north-east side of the deposit, overlying the iron layers and dipping parallel to them. A typical cross-section of the LabMag deposit is shown in Fig. 19.

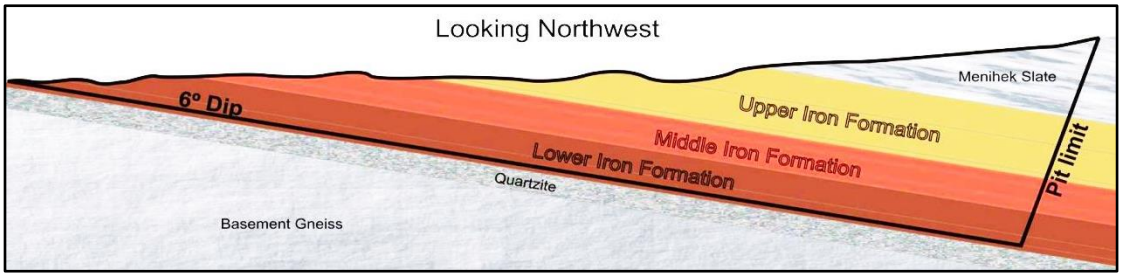

Fig. 19 LabMag typical cross-section

In the next sections, firstly the MAF-based block simulation algorithm is reviewed. Then an application at LabMag consisting of two parts is presented. In the first part, the lithological units of the deposit are jointly simulated based on layer thickness; and in the second part, the four metallurgical qualities of interest in this deposit are jointly simulated:

- Head iron grade of the material fed into the Davis Tube process (FeH)
- Davis Tube Weight Recovery (DTWR)
- Concentrate iron grade from the Davis Tube process (FeC)
- Concentrate silica grade form the Davis Tube process (SiC)

Then the quantification of an existing mining schedule follows using the full-field simulations in order to quantify the geological and financial risk. Finally, conclusions and recommendations from this study follow and are discussed.

2.2. Joint Simulation at Block Support-Scale Revisited

2.2.1. Min/Max Autocorrelation Factors at point support

The Min/Max Autocorrelation Factors (MAF) procedure is to transform a multivariate observation vector, such as metal grades or thicknesses in geological layers, to a new set of variables that are linear combinations of the original vector. These linear combinations are specifically chosen so as to be orthogonal, and to exhibit increasing spatial correlation. Consider

the stationary vector random function (RF) $\boldsymbol{Z}(u) = \{Z^1(u), \dots, Z^K(u)\}$ transformed into its Gaussian equivalent

$$\mathbf{Y}(u) = \{\phi_1(Z^1(u)), \dots, \phi_K(Z^K(u))\}. \quad (1)$$

The MAF are then defined as a new vector RF $\boldsymbol{M}(u) = \{M^1(u), \dots, M^K(u)\}$, where the K RFs are independent and obtained from the multi-Gaussian vector RF $\mathbf{Y}(u)$ using the co-efficients $\mathbf{A}$ such that

$$\mathbf{M}(u) = \mathbf{A}^T\mathbf{Y}(u) \quad (2)$$

The matrix of coefficients $\mathbf{A}$ that are used to orthogonalize $\mathbf{Y}(u)$ is generated from

$$2\boldsymbol{\Gamma_Y}(h)\boldsymbol{B}^{-1} = \boldsymbol{A}^T\boldsymbol{\Lambda}\boldsymbol{A} \quad (3)$$

with

$$\mathbf{B} = \mathrm{cov}[\mathbf{Y}(u), \mathbf{Y}(u)] \quad (4)$$

$$2\boldsymbol{\Gamma}_Y(h) = cov[\mathbf{Y}(u) - \mathbf{Y}(u+h), \mathbf{Y}(u) - \mathbf{Y}(u+h)] \quad (5)$$

where $\mathbf{B}$ is the variance/covariance matrix of $\mathbf{Y}(u)$, and $\boldsymbol{\Gamma}_Y(h)$ is the variogram matrix at lag h. This derivation of $\mathbf{A}$ is equivalent to performing two successive principle component (PCA) decompositions (Desbarats and Dimitrakopoulos 2000).

2.2.2. Direct block simulation with MAF

The point values (see A, Fig. 20) within a search neighborhood are used to simultaneously simulate the points in each block using an LU algorithm (see B, Fig. 20).

Consider a block at location v discretized with a vector of N points of the k^{th} MAF service variable

$\boldsymbol{m}_s^k = \{m^k(u_1), \ldots, m^k(u_N)\}$ with $u_i \subset v$, $i=1$ to K and with a neighborhood made of MAF factors and previously simulated blocks $\boldsymbol{m}_d^K$.

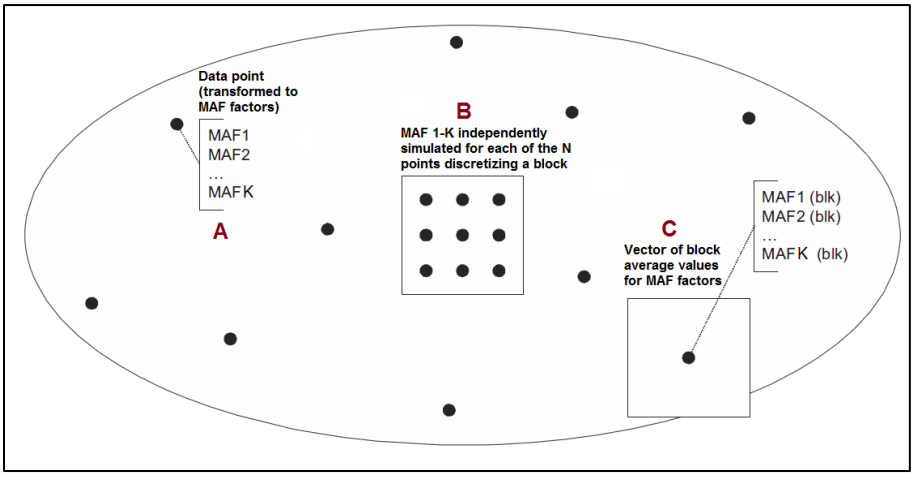

Fig. 20 Search neighbourhood for the multivariate direct block simulation, after (Boucher and Dimitrakopoulos 2009)

then

$$\mathbf{m}_s^k = \mathbf{C}_{sd}^k \mathbf{C}_d^{k\,-1} \mathbf{m}_d^k + \mathbf{L}_s^k \mathbf{w}_s \qquad (6)$$

where $\mathbf{C}_d$ is the covariance matrix of the conditioning data comprised of the drill-hole data and the previously simulated blocks; $\mathbf{C}_{sd}^k$ is the matrix of

point and point-to-block covariance between the discretizing points and the known values (drill holes and previously simulated blocks); and $\mathbf{L}_s^k, \mathbf{w}_s$are vectors determined by a Cholesky decomposition (Boucher and Dimitrakopoulos 2012).

The simulated point values within a block are averaged to find the MAF at the block-support scale (see C, Fig. 20). Once block-scale MAF values are calculated, they are introduced to the data set used for the simulation process rather than the discretized points. The final block values in the original data space are obtained by back-transforming the point support data and averaging them for each MAF k=1 to K using Eq. (7).

$$\mathbf{z}_s^k = \frac{1}{N}\sum_{N}(\phi^{-1}(\mathbf{A}^{-T}\mathbf{m}_s^k)) \tag{7}$$

where **A** is the matrix of MAF coefficients derived previously. This allows extending the direct block simulation (Godoy 2002) to the joint direct block simulation outlined in (Boucher and Dimitrakopoulos 2009).

2.2.3. DBMAFSIM algorithm

The DBMAFSIM algorithm proceeds as follows:

2. The data is transformed to normal scores.
3. The normal scores are transformed to MAF factors as previously described, which is the data set used during simulation.

4. The N groups of points for each block are sequentially simulated with the LU decomposition method. Independent simulations are carried out for each MAF factor.
5. The group points for each MAF factor are averaged to obtain block-support values. These block values are introduced to the data set created in step 2 and used for further conditioning.
6. The simulated variables are back-transformed from MAF-space to normal scores.
7. The normal scores are back-transformed to the original data space.
8. The simulated data points are re-blocked to a final block support model.
9. Steps 3-8 are repeated in order to produce each additional simulation.

An important step in addition to the above process is a validation of the final results, which consists of visual inspection, and comparison for the reproduction of the histograms, variograms and cross-variograms between the data and the simulations.

2.3. Two-stage Joint Simulation of the LabMag Deposit

2.3.1. Study area and data

The data set (Fig. 21) consists of the diamond drilling logs for 271 drill holes, drilled in four main campaigns. Each drillhole log consists of a set of

intervals coded by lithology and with the associated lab-determined qualities. The average drilling spacing is 370 m, which is large but common for taconite orebodies due to low variability over this distance.

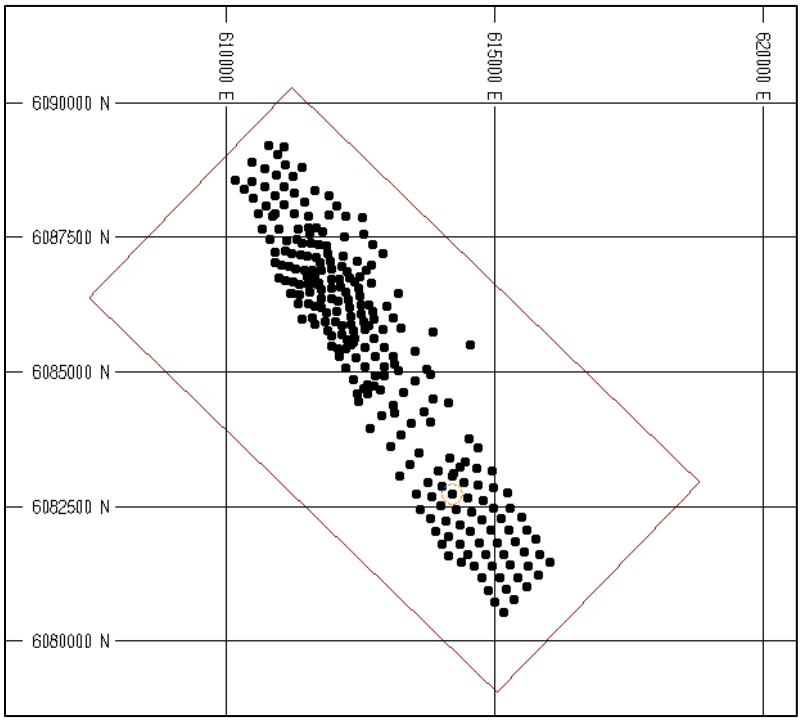

Fig. 21 LabMag drilling and study zone

Physical and chemical properties of ore are often controlled by the geology, and so modeling the spatial distribution of the deposit lithologies is critical to modeling the deposit (King, et al. 1986, David 1988, Sinclair and Blackwell 2002). The LabMag iron formation can be divided into three main members, as shown in Fig. 19: upper, middle, and lower. The iron formation dips more steeply to the east-northeast under the Menihek Shale formation. Overburden is slight over the deposit zone, with many

visible outcroppings. The entire iron formation rests on an Archean basement of granite gneiss.

Table 1 Lithological codes used in LabMag

Strata	Lithology	Code	Iron Formation
1	Overburden	OB	n/a
2	Menihek Shale	MS	n/a
3	Lean Chert	LC	Upper
4	Jasper Upper Iron Formation	JUIF	
5	Green Chert	GC	
6	Upper Red Cherty	URC	Middle
7	Pink-Grey Cherty	PGC	
8	Lower Red Cherty	LRC	
9	Lower Red-Green Cherty	LRGC	
10	Lower Iron Formation	LIF	Lower

The iron formation is approximately 120 m thick and all the sub-member units show variation in thickness as observed from drilling. The economic units are shown in Table 1 as strata 3 to 9, and are identified on the basis of chert colour and oxide texture. The LRGC units, and to some extent the JUIF units, show the most pronounced thickness variation. However, the total thickness of the iron formation remains relatively constant in the drilled area. The iron formation plunges slightly along the strike at approximately 1.4 degrees. Folds, where present, are broad monoclonal flexures with low amplitude and shallow dipping limbs (Geostat Systems International Inc. 2007).

The simulation approach is to treat the discontinuous layer thicknesses as correlated variables and use the MAF approach discussed earlier to simulate the layer thicknesses throughout the deposit. This method has been shown to be valid for stratiform deposits (Eggins 2006).

Table 2 and Table 3 show the Pearson's an Spearman's correlations between layer thicknesses respectively, with the absolute values greater than 0.3 highlighted in blue. Spearman's correlation is a rank correlation, which is important because the normal score transformation is a rank transformation and thus tends to only preserve the rank correlation. This has an impact when the two correlations differ significantly, which is not the case here. The relatively strong correlations between layers rationalizes the need for MAF in order to preserve those correlations within the simulations. Most of the correlations with $|R|>0.3$ are negative and between two successive layers, which is intuitive because if a marginal composite is added to one layer then it is likely removed from the next layer.

In terms of the metallurgical properties, spatial continuity is established based on analysis from 6m drilling composites because that is the length of the majority of drilling sample intervals. Since most of the lithological units are not sufficiently thick, there is insufficient data for individual variogram analysis. Therefore, it is more appropriate to analyze the spatial

Table 2 Pearson's correlation coefficients matrix for layer thickness

	LC	JUIF	GC	URC	PGC	LRC	LRGC	LIF
LC	1.00	-0.33	0.11	-0.02	-0.05	0.00	-0.08	0.12
JUIF	-0.33	1.00	-0.13	0.24	-0.33	-0.03	0.11	-0.16
GC	0.11	-0.13	1.00	-0.20	0.18	0.07	-0.21	0.17
URC	-0.02	0.24	-0.20	1.00	-0.35	-0.04	-0.02	-0.09
PGC	-0.05	-0.33	0.18	-0.35	1.00	0.03	-0.47	0.35
LRC	0.00	-0.03	0.07	-0.04	0.03	1.00	-0.49	-0.02
LRGC	-0.08	0.11	-0.21	-0.02	-0.47	-0.49	1.00	-0.57
LIF	0.12	-0.16	0.17	-0.09	0.35	-0.02	-0.57	1.00

Table 3 Spearman's correlation coefficients matrix for layer thickness

	LC	JUIF	GC	URC	PGC	LRC	LRGC	LIF
LC	1.00	-0.25	0.05	-0.01	-0.05	0.00	-0.08	0.13
JUIF	-0.254	1.00	-0.17	0.28	-0.31	-0.01	0.10	-0.17
GC	0.046	-0.17	1.00	-0.25	0.17	0.11	-0.18	0.11
URC	-0.012	0.28	-0.25	1.00	-0.39	0.00	-0.01	-0.14
PGC	-0.051	-0.31	0.17	-0.39	1.00	0.07	-0.49	0.38
LRC	0.001	-0.01	0.11	0.00	0.07	1.00	-0.51	0.02
LRGC	-0.085	0.10	-0.18	-0.01	-0.49	-0.51	1.00	-0.58
LIF	0.133	-0.17	0.11	-0.14	0.38	0.02	-0.58	1.00

continuity using a model based on one structure. Since the variograms that need to be modeled for MAF are based on the MAF factors, one MAF transformation is established based on compositing that ignores lithology and then applied to the data set for each individual lithology. The

variograms modeled are then used for each lithology, but only the composites belonging to each respective lithology are used.

The standard MAF procedure is carried out for each of the 7 economic iron units (LC, JUIF, GC, URC, PGC, LRC, LRGC). The data is composited, this time considering lithology in order to keep the samples from each domain separate.

The Pearson's and Spearman's correlations between variables for the LC layer are shown in Table 4 and Table 5 respectively, with the absolute values greater than 0.3 highlighted in blue. The relatively strong correlations between variables rationalizes the need for MAF in order to preserve those correlations within the simulations.

Table 4 Pearson's correlation coefficient matrix for LC qualities

	FeH	DTWR	FeC	SiC
FeH	1.00	0.553	0.426	-0.423
DTWR	0.553	1.00	0.606	-0.484
FeC	0.426	0.606	1.00	-0.852
SiC	-0.423	-0.484	-0.852	1.00

Table 5 Spearman's correlation coefficient matrix for LC qualities

	FeH	DTWR	FeC	SiC
FeH		0.517	0.192	-0.117
DTWR	0.517		0.380	-0.278
FeC	0.192	0.380		-0.892
SiC	-0.117	-0.278	-0.892	

2.3.2. MAF transformation

Separate MAF transformations are required for each of the two stages of simulation. In the first simulation stage, the lithological layer thicknesses are simulated; in the second stage, the metallurgical properties are simulated.

The MAF transformation requires all variables at each location to be populated. This is an issue for the MAF transformation of layer thickness variables for LabMag because shallow holes do not intersect all layers and due to the dip of the deposit and the erosion at surface, drillholes located further west-southwest intersect fewer of the layers. In these two cases, missing layers are referred to ‘externally missing’. In addition, if a middle layer like LRC is not observed in the drilling sequence, it is referred to as ‘internally missing’. Missing internal intervals are populated by simply setting the top elevation to that of the underlying layer. Missing external intervals are populated by fitting planes to each layer using linear least squares, calculating statistics of the deviations of the drillhole layer intercepts from these planes, and randomly sampling a deviation value using these statistics. Adjustments are made to clip values that would result in overlapping surfaces. The thicknesses of all layers can then be calculated at each drilling location using the fitted planes and the deviation values.

To validate this process, the histograms for the augmented data set that includes the simulated missing intervals is compared to that of the initial drilling data set. An example is shown in Fig. 22, showing the range of values, mean, and standard deviation of the two data sets are all consistent. For the rest of this study, the data set will refer to the augmented data set.

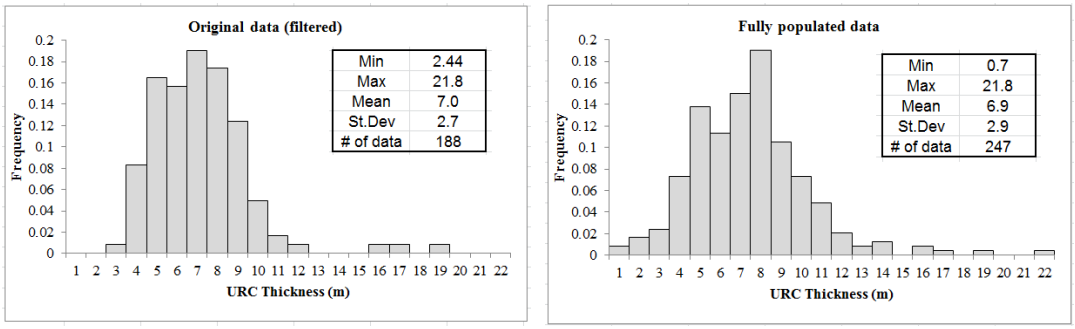

Fig. 22 Histogram comparison between original data and augmented data set with simulated missing intervals

The transformation matrix **A** from Eq. (2) must be determined twice: once for the layer thicknesses and once for the metallurgical properties. The MAF factors in Table 6 are used to transform the eight layer thicknesses into min/max autocorrelation factors for the first stage of simulation. The MAF factors in Table 7 are used to transform the four metallurgical properties into min/max autocorrelation factors for the second stage of simulation.

MAF are calculated by multiplying the vector of original data by the vector of MAF loadings, which are the rows of the transformation matrix. Fig. 23 shows a few cross-variogram examples between MAF factors in this study, demonstrating the variable decorrelation.

Table 6 MAF factors for lithology thickness variables

	LC	JUIF	GC	URC	PGC	LRC	LRGC	LIF
MAF1	0.158	0.395	-0.013	-0.010	-0.176	0.139	-0.357	0.358
MAF2	0.560	0.329	0.077	-0.148	0.409	-0.041	0.225	-0.178
MAF3	-0.312	-0.010	-0.160	-0.794	0.200	0.022	0.088	-0.110
MAF4	-0.131	0.076	0.464	-0.207	-0.052	-0.768	0.273	0.065
MAF5	-0.169	0.030	0.759	-0.187	0.107	0.606	-0.272	-0.136
MAF6	0.447	0.034	0.127	-0.010	-0.650	0.020	0.639	-0.098
MAF7	0.563	-0.760	0.353	-0.392	0.272	0.089	-0.467	0.208
MAF8	0.045	0.388	-0.188	0.340	-0.501	0.114	0.196	-0.867

Table 7 MAF factors for metallurgical property variables

	FeH	DTWR	FeC	SiC
MAF1	0.416	0.942	-0.418	0.331
MAF2	0.702	-0.931	0.014	-0.085
MAF3	0.147	0.478	1.353	-0.501
MAF4	-0.094	0.252	1.422	0.520

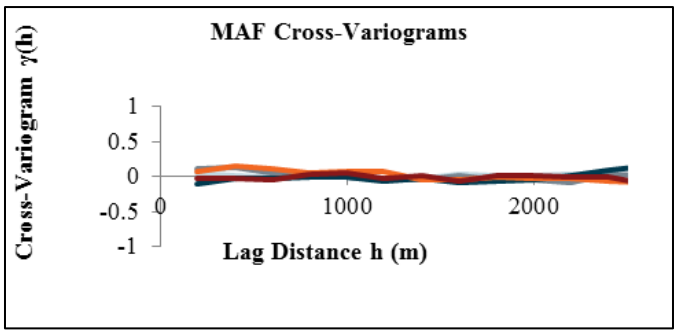

Fig. 23 Selected cross-variograms of MAF factors for thickness variables showing decorrelation

2.3.3. Joint simulation

Within each of the two stages, variography on each MAF is performed. Model variograms are fitted to the experimental variograms of each of the MAF. MAF variograms are then used in the simulation of each factor and can be used in the validation of the MAF simulation results. For brevity, the MAF simulation variography validation is omitted and only the final back-transformed simulation variography is validated against the data variography.

To simulate the lithology thicknesses, the study zone of 46,216 blocks (25 m by 50 m discretized by 5x10 points per block) is separately simulated using the DBMAFSIM algorithm 10 times for each of the eight MAF variables. For comparison, at the point-support scale this corresponds to 1,155,400 points per realization. Albor Consuegra and Dimitrakopoulos (2009) show that for the given example, the results converge when the

number of orebody simulations is increased past 10-15. This is an indicator that 10 orebody simulations are sufficient for schedule optimization because they capture near the full range of geological uncertainty.

Once the MAF are all simulated, they are transformed back to simulated normal score variables by multiplying a column vector of simulated MAF at each grid point with the corresponding inverse matrix of the MAF loadings. Then, the normal score layer thicknesses are back-transformed to the data space to produce eight lithology thicknesses: LC, JUIF, GC, URC, PGC, LRC, LRGC, and LIF. In (Eggins 2006), the bottom contact is a fully surveyed surface that can act as a reference, but for LabMag, no reference surface exists. Therefore, an artificial LIF surface serves as the reference surface, which is a 2D plane derived from the average of the planar fits to each layer surface, lowered by an arbitrary 50m in elevation. The real bottom LIF contact cannot be used because LIF continues at depth. The arbitrary choice of 50m beneath the LRGC-LIF surface ensures the simulated LRGC-LIF contact will not intersect the reference surface.

The thicknesses of the waste layers are not correlated with those of the ore layers, so these layers are constructed separately. The MS layer is created by intersecting the topographic surface with the LC contact and the OB surface is generated with a SGS simulation.

To simulate the metallurgical properties, the DBMAFSIM algorithm is used to jointly simulate the MAF factors of the four qualities for blocks 100 m by 100 m x 15 m, discretized by 3x3x3 points/block. The modeled area of the deposit is 55 by 106 by 26 blocks along the strike, dip, and vertically with a total of 151,580 blocks.

2.3.4. Results and validation

In addition to visual inspection, the simulations are subsequently validated by: histogram comparisons between data and simulated point-support values; variogram and cross-variogram validation between data and simulated point-support values.

In the first stage, the deposit is modeled as a discretized 2D grid of thicknesses. The DBMAFSIM algorithm is used to jointly simulate the layer thicknesses for blocks 25 m by 50 m, discretized by 5 x 5 points per block.

The histograms of the source data are compared to the simulation histograms. The histogram reproduction in the simulations is reasonable, and a typical example is shown in Fig. 24 for the JUIF layer thickness. Although the simulation mean in Fig. 24 is 11% higher than the data mean, this can be explained by the dominance of data higher than the mean on the eastern edge of the deposit that are used to simulate the lower right portion of the study zone shown in Fig.21. For the complete set of histograms, refer to Appendix A.

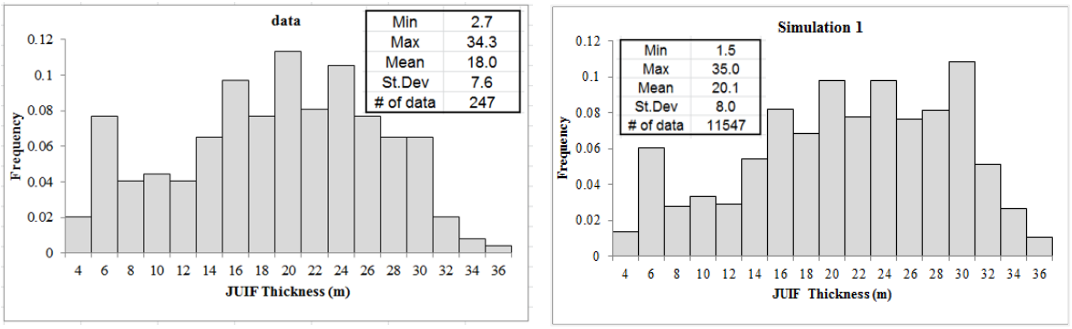

Fig. 24 Histogram comparison between the data set and a simulation

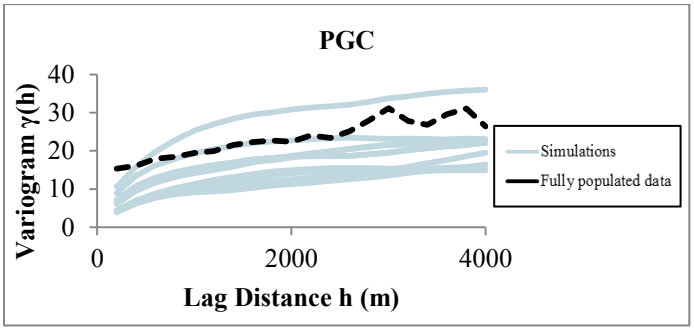

Fig. 25 PGC thickness variogram reproduction

The reproduction of variograms is also reasonable, and an example is shown in as shown in Fig. 25. Although the nugget effect of simulated thicknesses is roughly half that of the nugget effect of sampled thicknesses, this was a modeling decision due to the limited data available at lags less than 150m due to the drillhole spacing. The complete set of variograms can be found in Appendix B. The azimuth of the variograms shown is the direction of major continuity of approximately 315 degrees, which is roughly along the strike. A tolerance of 45 degrees was used for the data and 5 degrees for the simulations. A lag separation of 200m with a tolerance of 100m yielded the best results. Two selected cross-

variograms are shown in Fig. 26 and Fig. 27 for LC-JUIF and LGC-LRGC. The correlations between these variables in the drilling data were -0.57 and -0.53 respectively. Overall, the simulations reproduce spatial features of the original data.

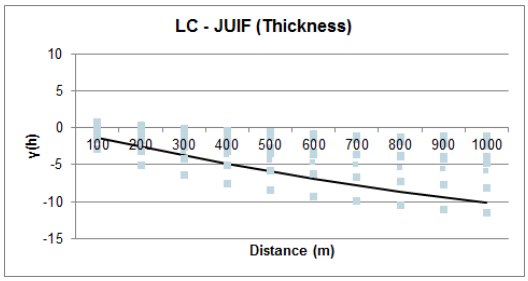

Fig. 26 LC-JUIF thickness cross-variogram

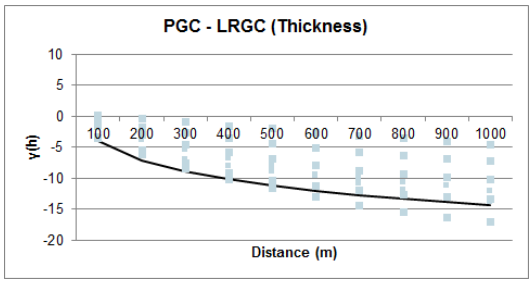

Fig. 27 PGC-LRGC thickness cross-variogram

An oblique view of a full manually constructed model of 3D solids is shown in comparison to a stochastically generated model in Fig. 28. Note the unlikely overly smoothed boundaries.

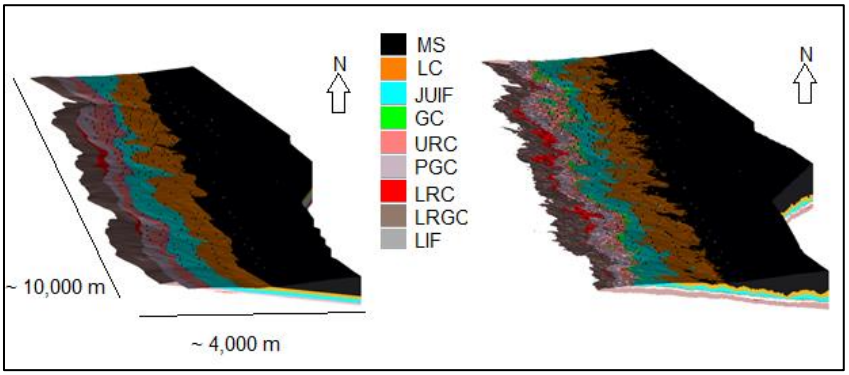

Fig. 28 Manual lithological model (left) vs. simulation (right)

In Fig. 29, a typical cross-section is shown through the manually constructed geological model. Note the smooth straight lines that connect

the lithological contacts between drill holes. An example of a simulation in cross-section is shown in Fig. 30 in comparison and shows two of the ten simulations. Each simulation features different variations in the areas between drill holes, but precisely meets the contacts at the drilling locations. In this manner, the simulations account for possible variations in the surface contacts.

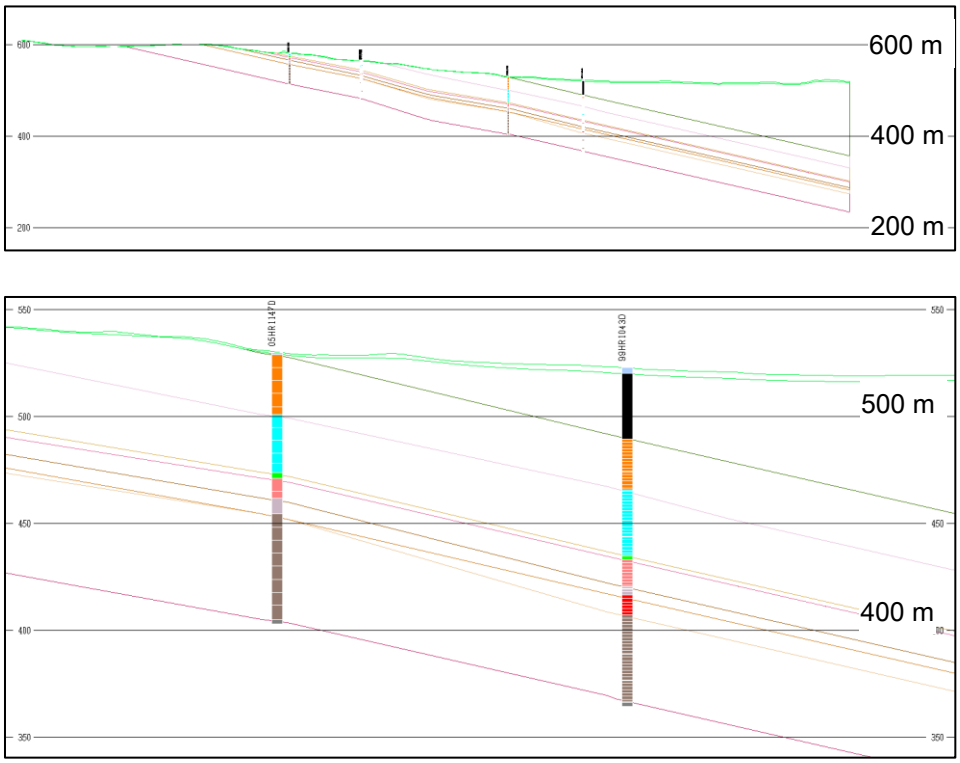

Fig. 29 Manual thickness model - typical cross-section and zoom

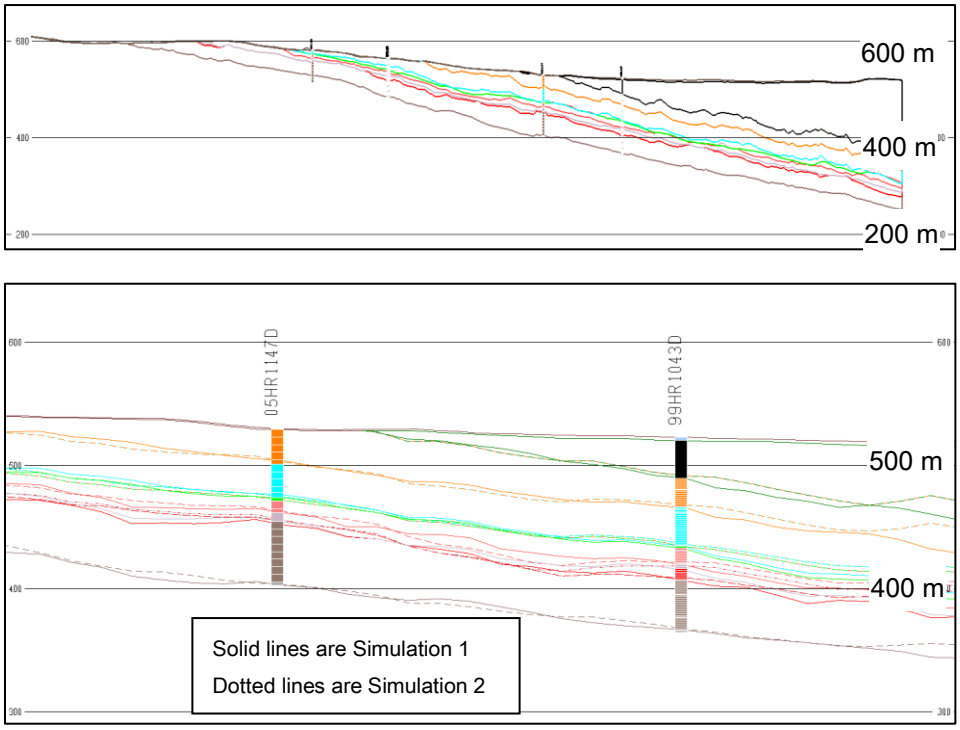

Fig. 30 Thickness simulation results - typical cross-section and zoom

In the second stage, the study zone is separately simulated 10 times for each of the 7 economic units. Each realisation contains 151,580 blocks with simulated values for each of FeH, DTWR, FeC, and SiC. For comparison, at the point-support scale this corresponds to 4,092,660 points per realization. The quality simulation points are on a grid 3x3x3 (27 points spaced out within each block of 100x100x15m). Given that the block height (15m) is greater than most layer thicknesses, there is a mixture of layers in most blocks. However, the layers are ignored during quality simulation: for each layer, block values are determined for each quality using all 27 points. Weighted block averages for each quality are then determined using the layer quantities. The simulations are

subsequently validated as before by histogram comparisons between data and simulated point-support values, and by variogram and cross-variogram validation between data and simulated point-support values.

The histograms of the ore quality data are well-reproduced in the simulations: within a few percent, the simulations have the same range of values, mean, and standard deviation. As an example, a comparison for the LC layer of the grade data histograms to the simulation histograms is shown in Fig. 31 and Fig. 32. The complete set of histograms can be found in Appendix C.

An example of the variograms for both data and simulations are shown in Fig. 33. They are unit-scaled for the purpose of comparison to one another. The complete set of variograms can be found in Appendix D. The simulation variograms are reasonably consistent with the data with higher short-range correlation and a range of approximately 700m. A selected cross-variogram is shown in Fig. 34 for the LC layer. Overall, the simulations reproduce spatial features of the original data.

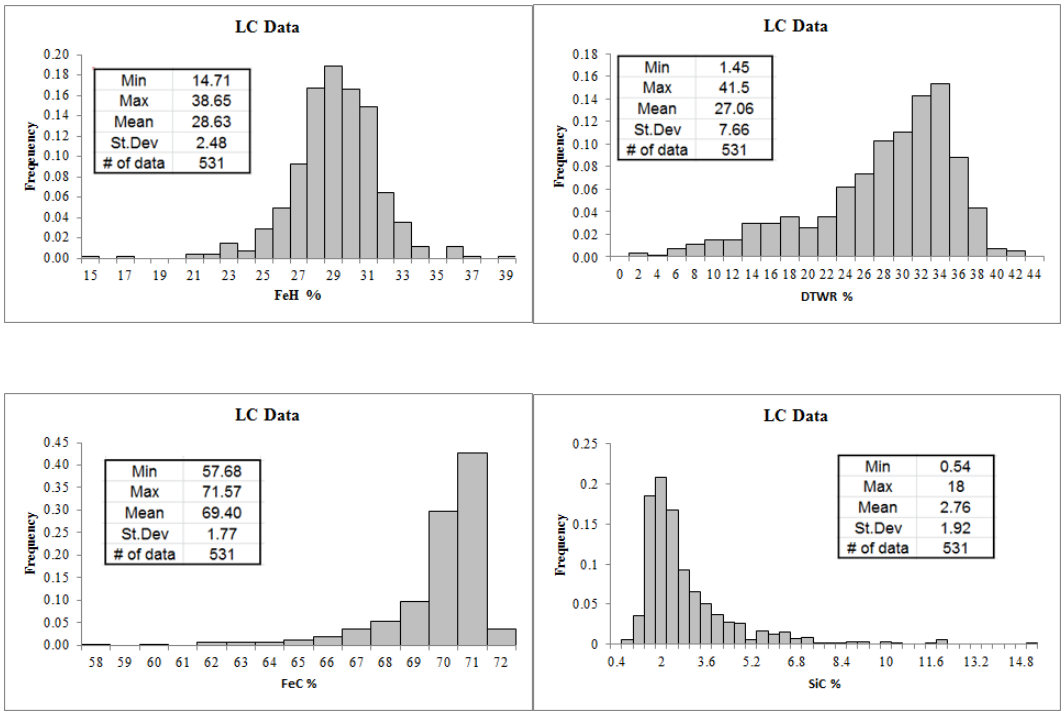

Fig. 31 Data histograms of grades for LC layer

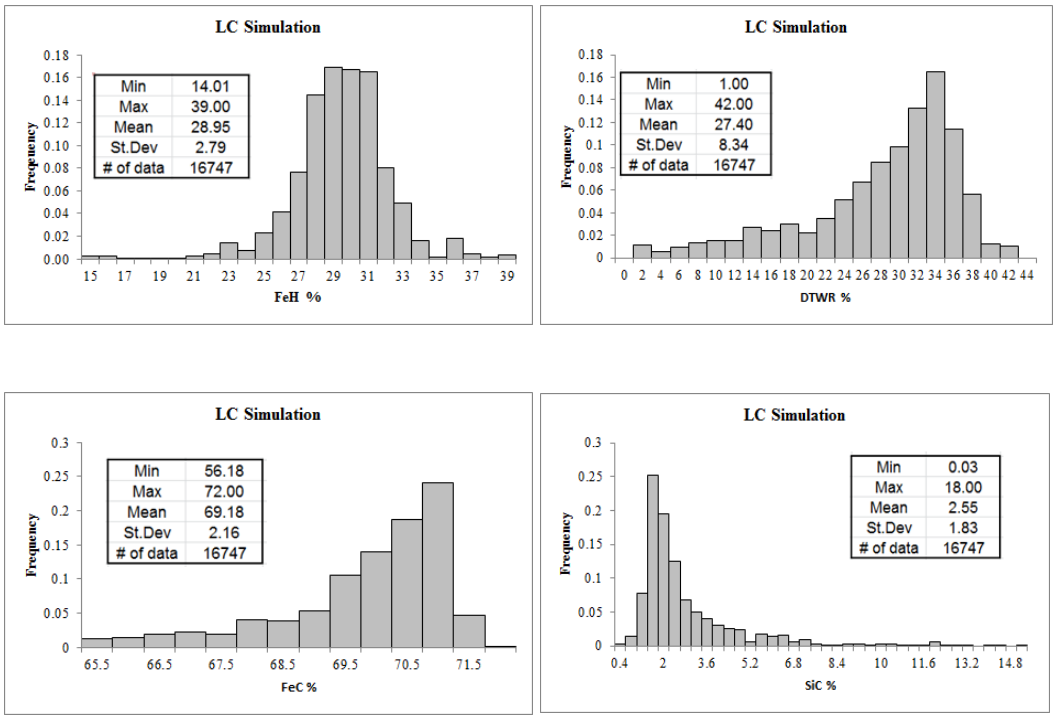

Fig. 32 Simulation 1 histograms of grades for LC layer

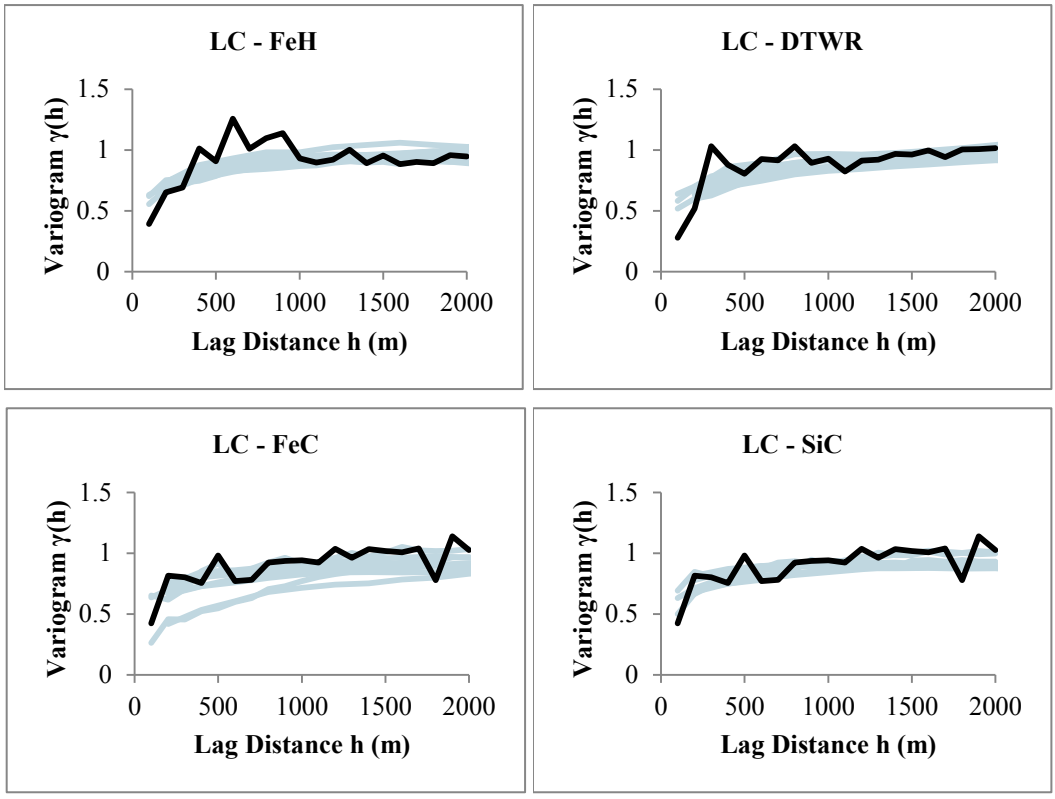

Fig. 33 Simulation variograms of grades for LC layer

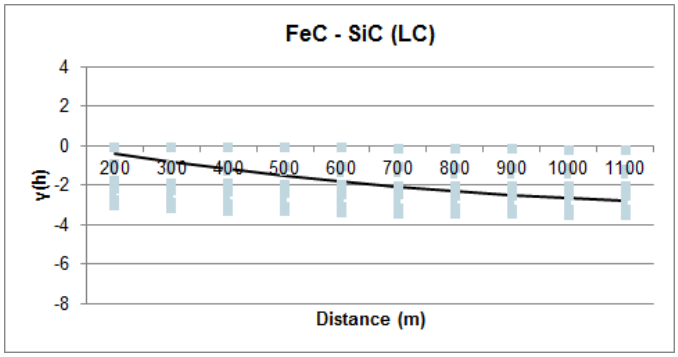

Fig. 34 FeC-SiC cross-variogram for LC

2.4. Mining Schedule: Quantification of Variability

In this section, the effect of geological variability on production and financial aspects of a 25 year mine schedule is quantified. The pit optimization is based on a deterministic geological model constructed using economic criteria to determine the cut-off grade and to what extent

the deposit can be profitably mined. The MineSight® (Mintec 2010) software implementation of the 3D Lerchs-Grossman algorithm was used to determine the economic pit limits based on inputs of mining and processing costs and revenue per block.

For the deterministic schedule (based on the conventional model), an upper cut-off of SiC of 4.0% and a lower cut-off of 21.5% DTWR were applied to the resource model. The intent of these cut-offs is to produce a concentrate with an average SiC of 2.1% and average DTWR of 27.9% (near the desired 27% for which the concentrator was designed). Material that does not meet these cut-offs or that is classified as an inferred resource (i.e. it has a lower level of confidence) is stockpiled, and does not contribute to the cash flows during the 25 year mine plan. The simulations consider inferred resources as ore, however, since the purpose of this study is to quantify the variability and to provide confidence levels on qualities and tonnages.

The mine plan is established annually for the first 10 years of production and in 3 year periods for the remaining 15 years. The plan is based on an annual production target of 22 Mt of concentrate. The mine plan incorporates a ramp up of 60% in Year 1 (13.2 Mt of concentrate) and 85% in Year 2 (18.7 Mt of concentrate) before reaching full capacity. In order to minimize the variations of material hardness that is sent to the

plant, the different rock types are blended during each period of the mine plan. There are typically 4 active ore mining faces planned during the operation to allow for blending.

2.4.1. Deterministic Model

The deterministic model consists of 25 m x 50 m x 15 m blocks. The lithological model was created manually based on sectional interpretations and the qualities interpolated independently for each lithology using inverse distance squared weighting (IDW2). Block averages of each quality were calculated, weighted by the tonnage of each lithology. The annual DTWR in the mine plan fluctuates between a low of 25.8% to a high of 28.9% with an average of 27.1%. The annual run of mine feed to the plant, when in full production, ranges from 80.8 Mt to 114.2 Mt with an average of 93.6 Mt. The ore fluctuates so much here mostly because inferred resources are being considered as processed ore, whereas the schedule was created assuming inferred resources are waste or stockpiled. The annual SiC content in the concentrate fluctuates between 1.6 % and 2.5 % with an average of 2.1 %. For the first 6 years of the mine plan, the average SiC in the concentrate averages 1.7 %. The mine plan was intentionally designed to supply a lower silica concentrate in the initial years. The annual total material moved ranges from 78 Mt in Year 1 to 130 Mt in Year 3 with an average of 113 Mt per year for the 25 year mine plan.

2.4.2. Stochastic Simulations

The results of evaluating the 25 year mine plan with the stochastic simulations are shown in Fig. 35 to Fig. 40. The tonnages and qualities for each period are separately evaluated with each simulation in order to evaluate the variability in each period. All resources within the OB, MS, and LIF layers are considered waste, and all resources within the LC, JUIF, GC, URC, PGC, LRC, and LRGC layers are considered ore. The P10 and P90 bars indicate the range in which there is an 80% probability the true value lies and consist of second lowest and second highest values from the set of ten simulations. The expected value indicates the weighted average across all ten simulations. Note that a traditional, non-risk-based, approach may not provide average assessments of key project indicators in the presence of geological uncertainty (Dimitrakopoulos et al. 2002). The points marked 'Deterministic' show the pit results using the deterministic geological model.

The key elements to look for in analyzing these graphs are: the range covered by the P10 and P90, which indicate the degree of variability; expected values that differ significantly from the predicted deterministic model; and P10-P90 ranges that have a significant portion of their range below the tonnage or DTWR targets, or above the SiC targets.

In general, the variability is higher in the earlier periods, which can be partially explained by Fig. 39, which shows the pit design for the first ten years of production along with the drilling locations. Note that the drilling is the most sparse in this region, which means this region is the most greatly affected by local variability, which can only be estimated due to a lack of drillhole pairs separated by short distances. **Error! Reference source not found.** shows that for Periods 1, 2, and 5, a short-fall in production is likely. This is related to the possible short-falls in scheduled ore (**Error! Reference source not found.**) as well as the likely short-falls in weight recovery (Fig. 37). In fact, the expected average DTWR for the whole 25 year mine plan is 26.3%, which is slightly below the plant design of 27%. This indicates that in general, having a DTWR that meets the target of 27% in some periods is not possible without a trade-off of some periods being less than the target. Fig. 38 shows that Period 8 to 11 and Period 14 and 15 are all likely to have a product silica above the target of 2.1%.

Looking at the ore tonnes (**Error! Reference source not found.**), the expected tonnage is consistent with the deterministic model for periods 2 and 3. However, for periods 1, 4, 5 and 6 to 15, the expected tonnage is less than what is predicted by the deterministic model. This means there will likely be a short-fall of tonnage in those periods. Conversely, in period

3 the expected tonnage is greater than what is predicted by the deterministic model.

Looking at the DTWR (Fig. 37), the expected weight recovery is generally consistent with the deterministic model (in particular, periods 10 and 13). However, for periods 1, 2, 3, 5, 6, 7, 11, 12 a lower DTWR than predicted by the deterministic model is probable. For periods 4, 8, 9, 14, and 15, there is a probability of realizing a higher DTWR than predicted by the deterministic model. Similarly, the expected SiC is generally consistent with the deterministic model (Fig. 38). The expected SiC in periods 4, 6, and 13 is relatively higher than the deterministic model and the expected SiC in periods 8 and 9 is relatively lower than the deterministic model.

For some periods, the deterministic prediction is outside the probable range of tonnage based on the simulations. This can be explained by looking at grade-tonnage curves for those periods. In Fig. 35 and Fig. 36, the grade-tonnage curves for periods 5 and 6 are presented, which are two periods in which the deterministic tonnage in **Error! Reference source not found.** was out, or on the edge, of the predicted range. The grade-tonnage curves drop fairly steeply at a range of cut-off grades slightly below the 18% DTWR cut-off used for ore classification. This indicates that there is a significant amount of material just below 18% DTWR in

some simulations (between 16-18%). This highlights the danger of determining cut-off grades based on

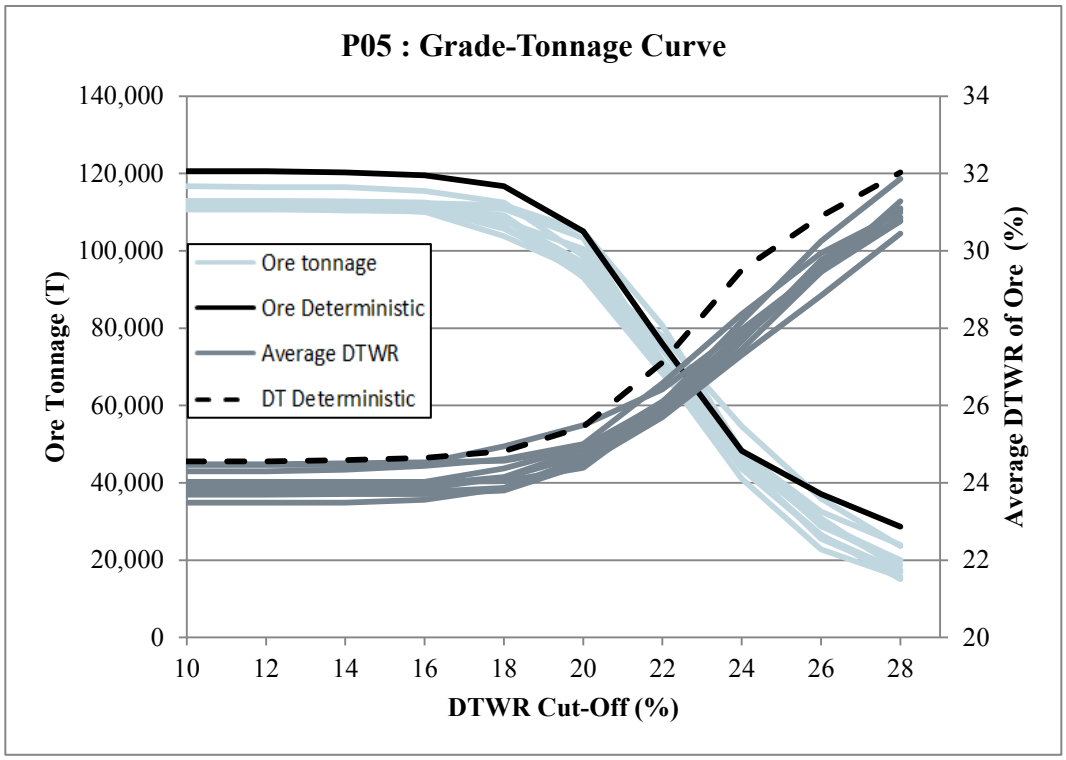

Fig. 35 Grade-tonnage curve for Period 5

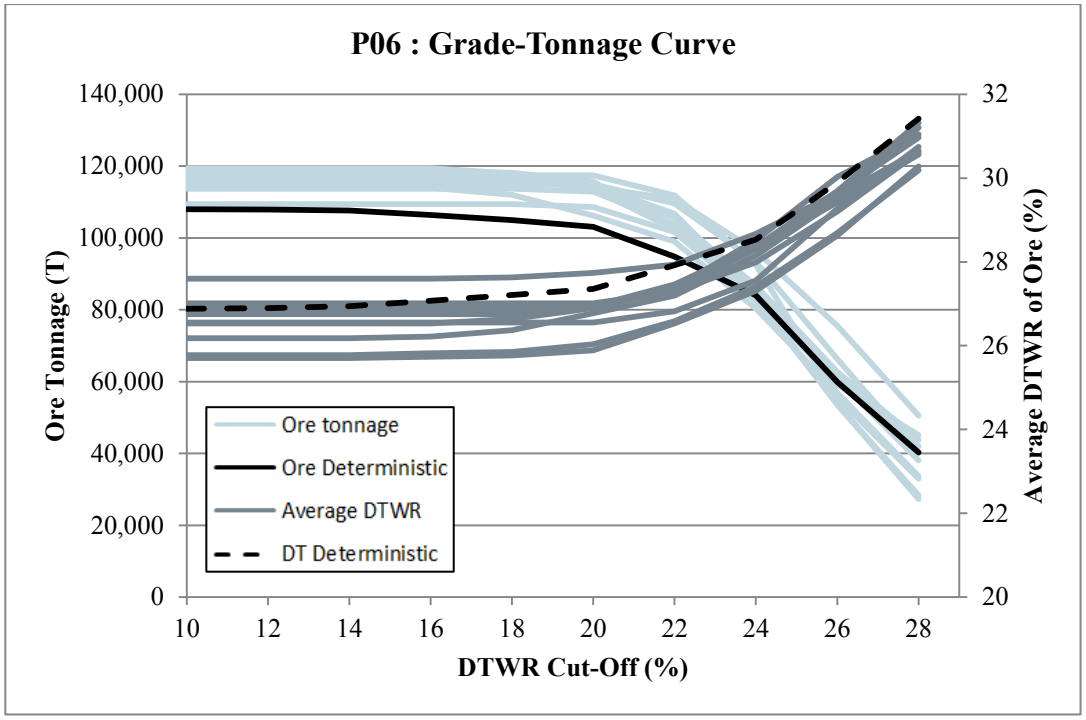

Fig. 36 Grade-tonnage curve for Period 6

deterministic models: production tonnages and ore qualities will not likely be those expected.

In order to evaluate the financial consequences, a detailed financial model that includes operating costs, capital costs, taxes, impact and benefit agreements, and interest on loans was used to evaluate each of the simulation production schedules. Evaluating the production schedule with different geological scenarios results in different revenue streams as well as affecting some elements of the operating cost that are variable with respect to the tonnages of mined, processed, and transported material. The cumulative DCF of the project when considering each of the different simulations, relative to the deterministic model results, is shown in Fig. 40. The expected NPV is 5.8% less than the NPV predicted with the deterministic model. Furthermore, there is an 80% probability that the true NPV realized is between +1.8% and -13.4% of the deterministic value, indicating relatively low chance of a higher NPV, and a strong probability of a lower than expected NPV. However, given other studies such as (Dimitrakopoulos et al. 2002) that have shown possible worst case scenarios with NPVs as low as -45%, the variability in this deposit is relatively low.

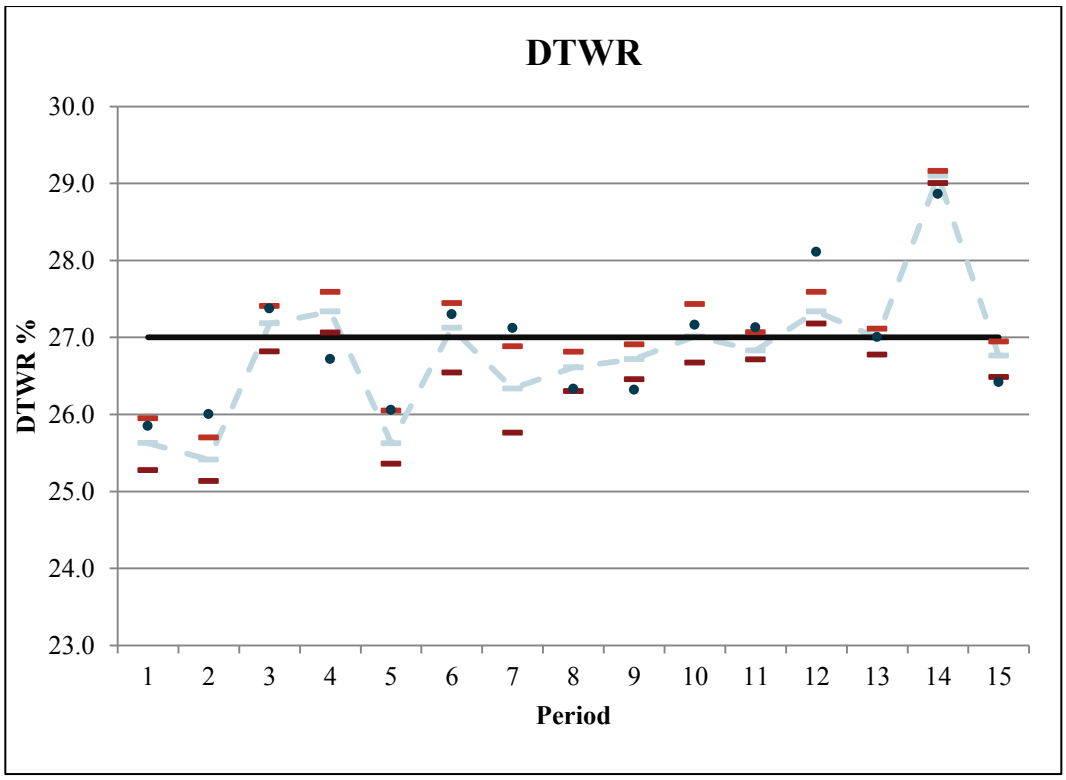

Fig. 37 DTWR variations

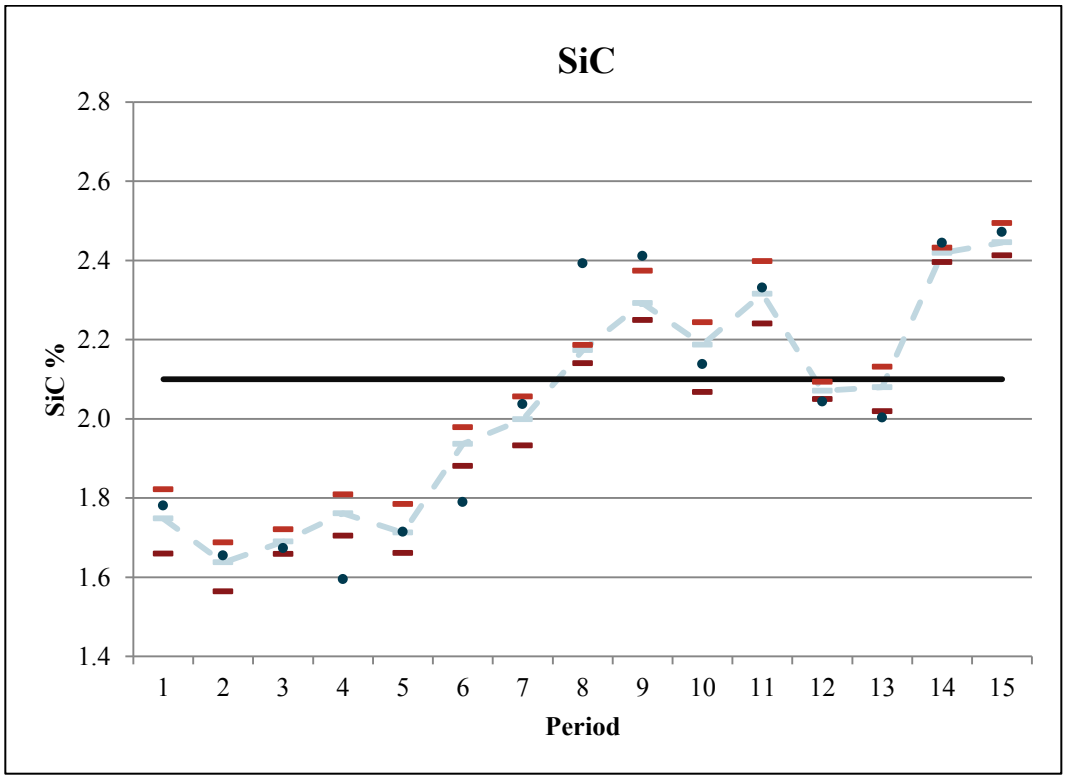

Fig. 38 SiC variations

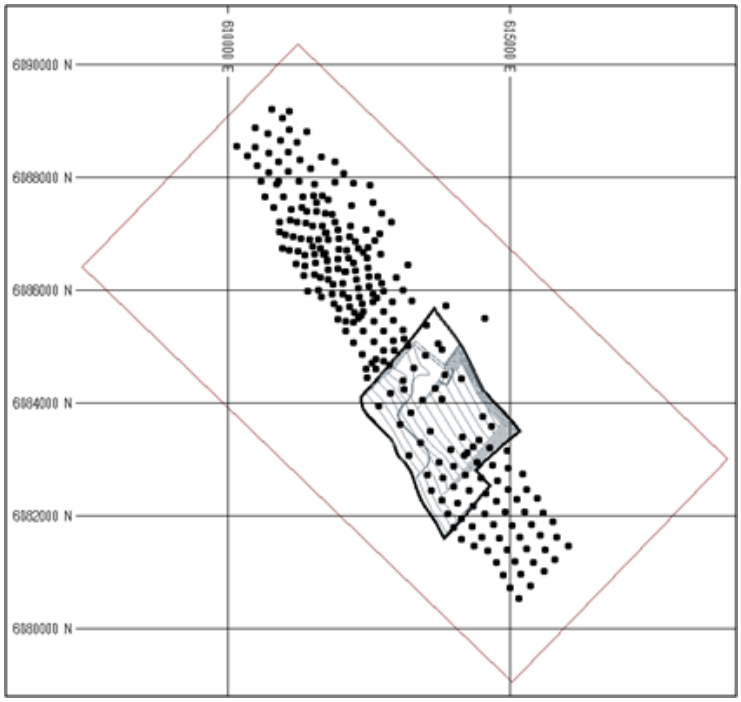

Fig. 39 Drilling locations, pit limit for the first 10 years of the production schedule

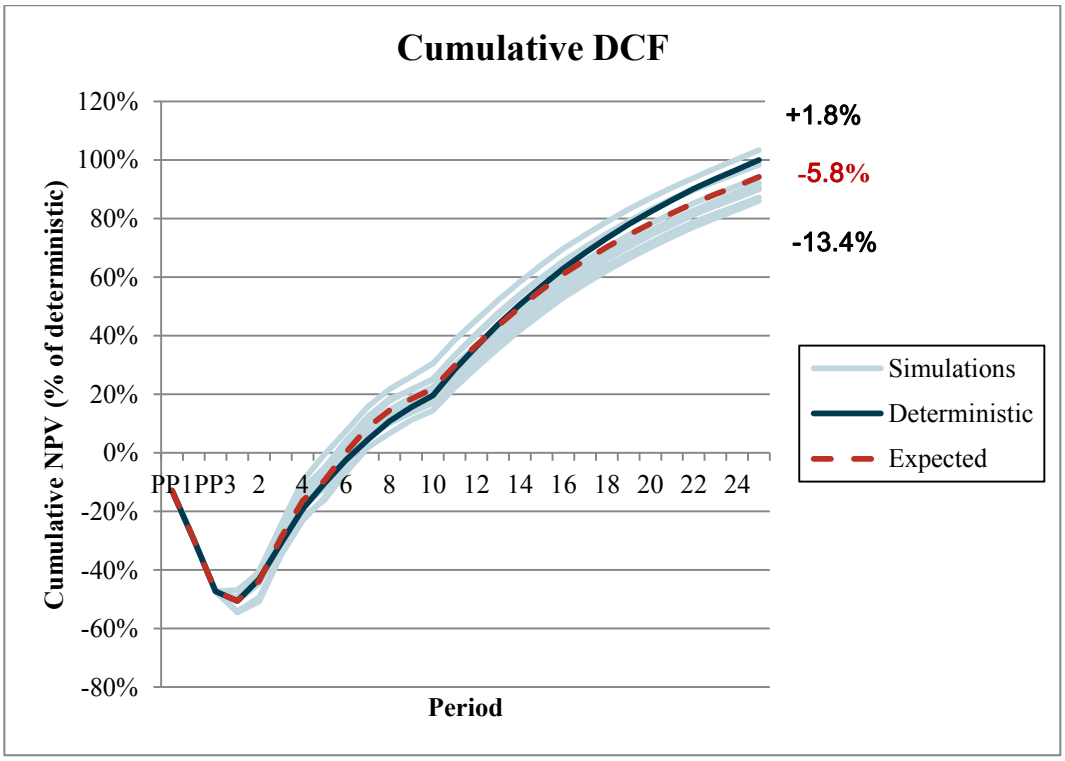

Fig. 40 Cumulative project DCF

2.5. Conclusions

A methodology for stochastically simulating the LabMag iron ore deposit was shown that uses MAF transformation to de-correlate variables of interest within a framework and direct block simulation to independently simulate each MAF factor. This procedure was implemented in two-stages, once for lithology simulation, and once for simulation of ore qualities. The application of the DBMAFSIM algorithm to the simulation of lithology is novel, and yielded good results in terms of the reproduction of data statistics. A set of ten simulations were created in order to quantify the uncertainty in grade and tonnage in an existing mine plan. The variability is relatively low for this deposit in general. In the existing mine plan, the layers have been purposely blended, so even when considering the uncertainty of the location of contact layers, the grades are generally well-blended, which results in low variability. Also, the block size has some effect on this variability: a smaller block size for the simulations could potentially increase the variability. Nonetheless, there are significant variations for some of the first 10 periods, which have an impact on the NPV of the project.

The results from this study indicate that the current mine plan is robust due to the relatively low variability of taconite compared to that of precious metals or hematite. However, significant improvements to the NPV could

be realized by performing a stochastic optimization of the mine plan using the simulations to schedule better quality material in earlier periods, potentially without the need to stockpile ore, while simultaneously managing the risk profile of the grades and tonnages.

Chapter 3

Stochastic Long-Term Production Scheduling of the LabMag Iron Ore Deposit in Labrador, Canada

3.1. Introduction

The LabMag iron ore deposit is part of the Millennium Iron Range, a 210 kilometer belt of taconite in northern Québec and Labrador, Canada. Taconite is a sedimentary rock in which the iron minerals are interlayered with quartz, chert, or carbonate and the iron content is commonly present as finely dispersed magnetite between 20-35% Fe. Although the majority of steel production is supported by iron ore sourced from high-grade hematite deposits (typically around 60% Fe), the long-term growing demand for steel has led to higher raw material prices that allow for comparatively lower grade magnetite deposits (typically 20-35% Fe) to also be developed. LabMag has significant economic potential: it contains 3.7 billion tonnes of measured resources at an average total iron content of 29.8% and a low average silica of 2.1%. However, the capital expenditure needed to build this project is estimated at over 5 billion dollars (SNC-Lavalin 2014), which necessitates careful evaluation of all sources of risk. Resource estimation is one of the main sources of risk in a mining project since knowledge of the orebody is primarily based on

drilling, which is often sparse because it is expensive. If the expected ore tonnages and qualities are not obtained when mining, the project cash flows are directly affected. The expected quantities and qualities of ore and waste are defined by the mine production schedule, which specifies the sequence of extraction and is dependent on the resource estimation. The goal of mine production scheduling is thus to maximize the expected profit (while also meeting all production targets and constraints) by creating an extraction schedule that is robust in the face of geological risk and has the highest chance possible of actually being realized.

Conventional mine planning optimization methods are based on a single deterministic orebody model and can yield misleading results because they do not account for the likely deviation from the model in reality (Ravenscroft 1992, Dowd 1997, Dimitrakopoulos et al. 2002, Godoy and Dimitrakopoulos 2004). In order to consider the geological risk of an orebody, a set of different scenarios can be created that are all equally probable representations of the orebody, and which all reproduce the orebody's spatial variability (Goovaerts 1997). Such geostatistical simulations can be used to quantify the various elements of risk associated with a mining project: operating costs, capital costs, royalties, commodity price, taxation, tonnage, and grade (Dowd 1997, Godoy and Dimitrakopoulos 2011). Previous studies (Albor Consuegra and

Dimitrakopoulos 2009) have shown that a set of 10-15 orebody simulations captures the variability of a deposit since the results converge when more are added. Geological uncertainty can then be managed by directly incorporating stochastic simulations with the mine scheduling framework.

Dimitrakopoulos and Ramazan (2004) introduce a framework that considers grade uncertainty in a mixed integer programming (MIP) formulation that produces a schedule with ore grades within a selected range of probability. The concept of geological risk discounting (GRD) is introduced, which is akin to financial discounting and generates schedules with less geological risk in the earlier periods. Another approach is presented and applied at the Fimiston gold mine in Western Australia that uses a simulated annealing algorithm (Godoy 2002, Godoy and Dimitrakopoulos 2004). This approach perturbs an initial schedule with an optimized net present value (NPV) based on a single orebody model by swapping blocks between different periods in order to reduce geological risk to the schedule. Using this approach, the study achieved a 28% higher expected NPV than a conventional schedule and also had a greater probability of meeting production targets. Variants of this approach were applied to copper deposits where improvements to the NPV of 10% (Albor Consuegra and Dimitrakopoulos 2009) and 26% (Leite and

Dimitrakopoulos 2007) were also seen relative to conventional schedules. In each of these studies, when the optimization was not constrained to the conventional ultimate pit limits, a larger pit limit was found to contain more metal and generate an even higher NPV. A more flexible method for long-term production scheduling is based on stochastic integer programming (SIP) (Birge and Louveaux 1997), a type of mathematical programming and modelling that considers multiple equally probable scenarios and generates the optimal result for a set of defined objectives within the feasible solution space bounded by a set of constraints. SIP for mine scheduling is introduced in Ramazan and Dimitrakopoulos (2004, 2008). Their formulation maximizes the NPV while minimizing deviations from production targets using a different penalty for each target. Leite and Dimitrakopoulos (2014) apply the same formulation at a copper deposit and produce a risk-robust NPV 29% higher than that of a conventional schedule. Benndorf and Dimitrakopoulos (2013) applies a SIP formulation at an iron ore deposit with a formulation that integrates joint multi-element geological uncertainty. Additional considerations are easily incorporated into the modeling framework: two other relevant studies use SIP to optimize the NPV while simultaneously optimizing the cut-off grades (Menabde et al. 2007) and incorporating simulated future grade control data at a gold deposit (Jewbali 2006). Boland et al. (2008) demonstrate

stochastic formulations for mine production scheduling with endogenous uncertainty, in which decisions made in later time periods can depend on observations of the geological properties of the material mined in earlier periods, and most recently they characterize the minimal sufficient constraints for such formulations so that solving them is more efficient (Boland et al. 2014).

In this study, an SIP formulation similar to Benndorf and Dimitrakopoulos (2013) is presented to control the risk profiles of the mine production in terms of four underlying metallurgical properties: the head iron (FeH), Davis Tube (Schulz 1964) weight recovery (DTWR), the product concentrate iron (FeC) and silica (SiC) grades. Additional consideration is given to truck haulage requirements and tailings management. The formulation seeks to minimize haulage costs by considering a truck haulage operating cost that varies with distance of the mined material from the processing plant. The optimization decides dynamically to which of two destinations to send each block: the waste dump or the process plant. Constraints are also included to smooth the annual haul truck fleet requirements in order to avoid purchases that lead to under-utilized equipment. The formulation in this study also seeks to maximize the space available for in-pit tailings disposal. The LabMag tailings (roughly two thirds of the mined ore) can be returned to the mined out pit in order to

reduce the environmental footprint. LabMag is a stratigraphic deposit and its layers come to the surface at a low dip of only six degrees, which makes it amenable to this type of tailings management strategy.

In the following sections, an SIP formulation for long-term production scheduling with equipment and tailings management is presented. The case study at LabMag follows, and the scheduling results are compared to conventionally scheduled results. Finally, the results are discussed and conclusions follow.

3.2. SIP Formulation

The following objective function is defined as the maximisation of the NPV minus various penalty terms that control the geological risk profile, minimize fleet requirements, and promote mining adjacent blocks in the same period in order to generate a practical schedule.

3.2.1. Notation

The constant and variable factors used in the SIP model are defined below:

P Number of periods

N Number of blocks in the orebody model

D Number of destinations

S Number of simulations

Q Number of metallurgical qualities

$V_{i,d,s}$ Value of block i in simulation s going to destination d in time period t

$TH_{d,t}$ Total truck hours in period t for destination d

Small differences in tonnage (and thus truck hours) can be expected due to variations in the lithology and thus the density but are ignored here for simplicity.

C_t^{TH} Operating Cost ($/hour) for trucking, discounted by period t

$b_{i,d,t}$ Binary variable with a value 1 if block i is mined in period t and sent to destination d; and 0 otherwise.

Pen^{conc} The penalty per tonne deviation ($/t concentrate) from the target concentrate production in each period; constant

Pen^{q} The penalty per tonne of quality content ($/t quality q) in each period above or below the associated upper or lower limits respectively; constant

$\overline{dev}_t^{conc}$ Concentrate tonnes in excess of the upper limit

$\underline{dev}_t^{conc}$ Concentrate tonnes less than the lower limit

$\overline{dev}_t^{q}$ Tonnes of metal or mineral q in excess of the upper limit, where q=1,…,Q considered qualities

$\underline{dev}_t^{q}$ Tonnes of metal or mineral q less than the lower limit

$c_t = \frac{1}{(1+\mathrm{r})^{\mathrm{t}-1}}$ A function for discounting profits and costs with the discounting factor r according to the period t when the block is mined

$g_t = \frac{1}{(1+\mathrm{GRD})^{t-1}}$ A function for discounting geological risk with the discounting factor GRD according to the period t when the block is mined

3.2.2. Mining block economic value

The undiscounted value for each block is defined as:

$$V_{i,d,s} = \begin{cases} NR_{i,s} - CONC_{i,s} * \mathrm{PCost} - ROM_{i,s} * \mathrm{OCost} - W_{i,s} * \mathrm{WCost} & , d = 1 \\ -(ROM_{i,s} + W_{i,s}) * \mathrm{WCost} & , d = 0 \end{cases} \quad (8)$$

given that

$$CONC_{i,s} = ROM_{i,s} * eWR_{i,s} \quad (9)$$

where for block *i* and simulation *s*, $NR_{i,s}$ represents the net revenue, $OCost$ and *WCost* the mining cost of ore and waste respectively (excluding truck haulage, which is penalized directly in the objective), *PCost* the processing cost (considers crushing, concentration, filtration, pelletization, transportation, administration, etc.), ROM the run-of-mine tonnage from the iron-bearing lithologies, W the tonnage from waste rock, and *eWR* the effective weight recovery (considers ideal Davis Tube Weight Recovery as well as plant efficiency parameters).

Note that by having trucking costs in the objective function as opposed to the block value, it is possible to consider trucking costs for a block that vary depending on the period that block is scheduled to be mined. In future research, if mobile crushers are considered rather than a fixed plant

location, the haulage cost could also be dependent on the variable distance to the crusher.

3.2.3. Objective function

The objective function of the SIP model is constructed as the maximization of a profit function, defined as the total expected net present value minus penalties for deviations from planned production targets and penalties for not mining the blocks adjacent to a mined block (Benndorf and Dimitrakopoulos 2013).

Maximize Obj =	
$$\sum_{t=1}^{P}\sum_{i=1}^{N}\frac{1}{S}\sum_{d=1}^{D}\sum_{s=1}^{S} c_t V_{i,d,s} b_{i,d,t}$$	(9a)
$$-\sum_{t=1}^{P}\sum_{i=1}^{N}\sum_{d}^{D} b_{i,d,t}\ c_t\ TH_{d,t}\ C_t^{TH}$$	(9b)
$$-g^t\sum_{t=1}^{P}\sum_{s=1}^{S}[Pen^{\text{conc}}\left(\overline{dev}_{st}^{conc}+\underline{dev}_{st}^{conc}\right)+\sum_{q=1}^{Q} Pen^q\left(\overline{dev}_{st}^{q}+\underline{dev}_{st}^{q}\right)$$	(9c)
$$-\sum_{\text{t=1}}^{P}\sum_{i=1}^{N} Pen^{\text{smooth}} dev^{smooth}$$	(9d)

This objective function includes four distinct terms. The term (9a) is the primary term and represents the net present value of all blocks mined in

the optimization. The term (9b) represents the trucking operating cost, which is minimized. The term (9c) acts to penalize deviations from target concentrate tonnes, and the target silica grade and weight recovery (see the next section for more details). The variables for the deviations are determined by the optimization process, based on the corresponding constraints that are set. The term (9d) is a penalty for not mining adjacent blocks. It is desirable to mine blocks in groups in order to generate a practical schedule. There is a trade-off between the penalty terms, and it is the relative size of the penalties that determine this trade-off.

3.2.4. Constraints

Reserve constraints

Reserve constraints ensure a block cannot be mined more than once:

$$\sum_{d=1}^{D}\sum_{t=1}^{P} b_{i,d,t} \leq 1 \qquad \forall\, \mathrm{i},\ \mathrm{i} = 1, \ldots, \mathrm{N} \qquad (10)$$

Slope and sequencing constraints

Each block can only be mined if the blocks above are mined in the same or an earlier period in order to maintain the maximum geotechnical slope angle in all directions. In order to accommodate in-pit tailings disposal as mentioned in the introduction, each block was set to be mined only if the block to the south-west (cross-dip, towards where the deposit daylights at surface) is mined in the same or an earlier period.

For each *i*, where j ϵ { predecessors blocks of block *i* }

$$\sum_{d=1}^{D}(b_{i,d,t} - \sum_{k=1}^{t} b_{j,d,k}) \leq 0 \quad (11)$$

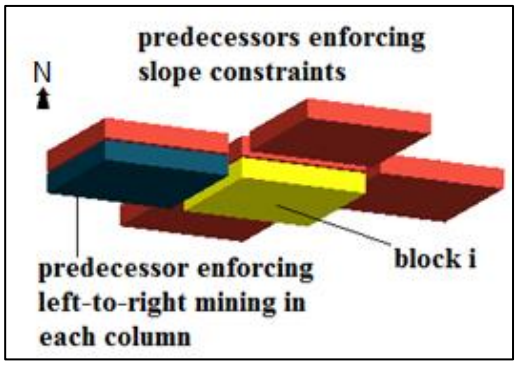

Fig. 41 Predecessor blocks for slope and sequencing constraints

Haulage capacity constraints

The objective function has a term that seeks to minimize truck operating costs by minimizing haul distances. This term competes with the need to meet blending constraints, so it is possible to obtain a schedule that has a given number of trucks in one year that then decreases in the subsequent year. This effectively means a truck is purchased and then left unused, or that an extra truck must be leased. It is more desirable to have the number of trucks only be an increasing function, where more trucks are bought as they are needed, and then fully used in subsequent periods. To allow for small numerical deviations, here the number of trucks required in a given period must be more than the previous period (with leeway of half the available working hours of one truck). That is to say the total number of

truck hours (ore, stockpile, waste) required in a given period cannot be less than the previous period's truck hours minus half of one truck's working hours for a year.

$$\sum_{i=1}^{N}\sum_{d=1}^{D} H_d b_{i,d,t} - \sum_{i=1}^{N}\sum_{d=1}^{D} H_d b_{i,d,(t-1)} \geq -\frac{1}{2} Total\ working\ hours\ available\ for\ one\ truck\ in\ one\ period \quad (12)$$

where t = 2,...,P ; H_d is the total time (hours) required for transportation of a block to destination *d* (the cycle time for one truck is on the order of minutes, but since each block can contain approximately half a million tonnes, many truck cycles are needed).

Processing capacity constraints

The total tonnage of concentrate produced is penalized if in excess or less than the target product tonnage for that period.

For each t = 1,…,p; and each s = 1,…,S

(d=1 for grade/tonnage constraints, since there are no target waste amounts)

$$\text{Upper bound} \quad \sum_{i=1}^{N} CONC_{i,s} b_{i,d,t} - \overline{dev}_{st}^{conc} \leq Conc_t^{target} \quad (13)$$

$$\text{Lower bound} \quad \sum_{i=1}^{N} CONC_{i,s} b_{i,d,t} + \underline{dev}_{st}^{conc} \geq Conc_t^{\text{target}} \quad (14)$$

where $\mathrm{Conc}_{\mathrm{t}}^{target}$ is the target quantity (tonnes) of concentrate that is to be produced in period t.

Quality constraints

For each period, the average grade or value of each metallurgical quality has to be less than or equal to a maximum value and greater than or equal to a minimum value.

For each t = 1,…,P; and q = 1,…,Q

$$\text{Upper bound} \quad \sum_{i=1}^{N} tonnes_{i,s} grade_{i,s,q} b_{i,d,t} - \overline{dev}_{s,t}^{q} \leq \sum_{i=1}^{N} tonnes_{i,s} grade_{q,t}^{max} b_i^{dt} \tag{15}$$

$$\text{Lower bound} \quad \sum_{i=1}^{N} tonnes_{i,s} grade_{i,s,q} b_{i,d,t} + \underline{dev}_{s,t}^{q} \geq \sum_{i=1}^{N} tonnes_{i,s} grade_{q,t}^{min} b_i^{dt} \tag{16}$$

where $tonnes_{i,s}$ is the tonnage of ore or concentrate used to weight each quality; $\mathrm{grade}_{\mathrm{i,s,q}}$ is the value of quality q for block i, simulation s; $grade_{q,t}^{max}$ is the maximum value or grade of quality q allowed in period t (constant); $grade_{q,t}^{min}$ is the minimum concentrate product grade allowed in period t (constant).

Equipment access & mobility constraints

Without specific constraints for smooth mining, the optimization may tend to schedule isolated blocks rather than blocks that are grouped together. Conceptually, the way each mobility constraint operates for a given block i is to sum the binary variables for the surrounding blocks and to penalize the amount of surrounding blocks that are not mined in the same time period as block i. This introduces a cost-element to not mining adjacent blocks, which is balanced with a factor for the relative importance of this constraint to the other goals.

For every time period *t* and block *j* (every 3rd in each direction):

$$\frac{W*O_j*b_{j,t}}{O_j} - \sum_{k=1}^{W} \frac{O_k*b_{k,t}}{O_k} - Y_{j,t} \leq 0 \quad (17)$$

or:

$$W*b_{j,t} - \sum_{k=1}^{W} b_{k,t} - Y_{j,t} \leq 0 \quad (18)$$

Where W is the total number of blocks in the window excluding the central block; k is an index to the W blocks in the window; $Y_{j,t}$ is the smoothing deviation for block *j,* time period *t.*

The $Y_{j,t}$ variables are included in the objective function, which will tend to minimize these values. Combined with these constraints, they will be

forced to exactly the difference in number of surrounding blocks versus the number of surrounding blocks that are mined in the same period (i.e. the deviations). The objective function then penalizes these amounts in order to promote mining the blocks grouped together. Note that this is a simplification of the formulation in (Dimitrakopoulos and Ramazan 2004), where the actual tonnages are used rather than just the number of blocks since some blocks could have only a small tonnage. However, in the case of relatively large blocks of consistent tonnage, as in taconite iron ore deposits, the different in formulations would not have a large impact.

3.3. Application at LabMag iron ore deposit

The formulation in the previous section is applied at the LabMag taconite iron ore deposit in northern Labrador, Canada in order to create a mine production schedule that considers multi-element grade uncertainty as well as equipment and tailings requirements.

3.3.1. Stochastic orebody models at LabMag

Mine production scheduling here considers geological variability by using ten stochastic conditional simulations. Each realization consists of a joint simulation of the seven correlated layer thicknesses as well as the joint simulation of four correlated ore characteristics in each layer. Each model consists of 13,400 blocks (100m x 100m x 15m). Since all ore lithologies

are processed in the plant in the same manner, scheduling considers the average qualities of all layers in each block.

The two primary waste-types for the LabMag deposit are overburden (OB) and Menihek Shale (MS). The OB overlies the entire deposit and is minimal (the underlying rock is commonly exposed at surface). The MS layer is present on the north-east side of the deposit, overlying the iron layers and dipping parallel to them at approximately 6 degrees (see Fig. 42).

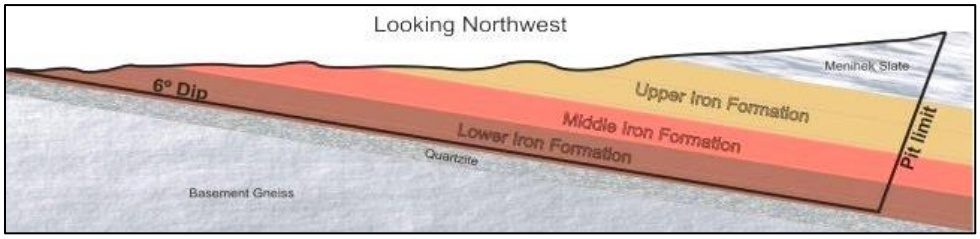

Fig. 42 Typical cross-section

3.3.2. Implementation

The SIP model described above was implemented in Visual C++ using the ILOG CPLEX API. The initial attempts to solve the full orebody model for all 10 periods proved to be unsolvable in a reasonable amount of time (the optimization had made little progress after several days, running on a 64-bit Dell Precision M6500 Intel I7 quad-core @ 1.73 GHz and 16 GB of RAM). The initial 13,400 blocks considered are the blocks contained within the ultimate pit derived using the nested Lerchs-Grossman algorithm.

Since only the first ten years are scheduled within the optimization and the LabMag ultimate pit contains more than twenty-five years of ore at the planned capacity, the precise pit limit need not be discussed further here. To reduce the number of blocks, a new pit was designed that takes as many blocks as possible but avoided the MS waste layer. Since the optimization targets the first 10 years and tries to minimize trucking hours as well as unnecessary waste, it was evident that the optimization would avoid the MS region of the deposit anyway. This brought the number of blocks down to 8,411. The optimization is broken down into four sub-optimizations (see Fig. 43) each set to stop once there was less than 1% gap between the solution and the optimal solution.

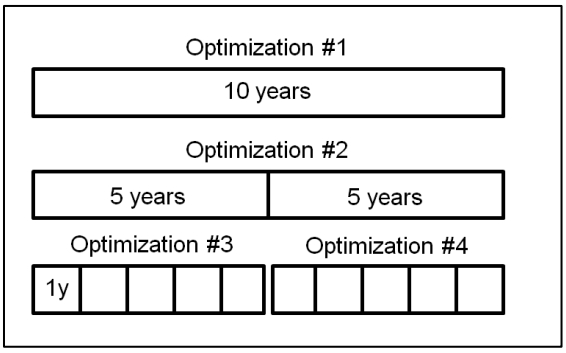

Fig. 43 Schematic representation of four-stage schedule optimization

Table 8 Annual concentrate production targets

Year	1	2	3-10
Production level	60%	85%	100%
Target concentrate	13.2	18.7	22.0

Table 9 Grade targets and penalties

Optimization		#1	#2	#3	#4
DTWR	Max %	29			
	Min %	23			
SiC	Max %	2.5	2.2	2.2	2.2
	Min %	1.8	2.2	2.2	2.2
Concentrate tonnage	Excess Penalty $/t	800M			
	Shortage Penalty $/t	1000M			
SiC	Penalty on % above max	100M			
	Penalty on % below min	100M			
DTWR	Penalty on % above max	1M			
	Penalty on % below min	1M			
Smoothing	Penalty per block	1000			

Table 8 shows the annual targets for the concentrate production, with a ramp-up of the process plant. Table 9 shows the DTWR and SiC targets that are used in the optimization along with the various penalties. The process plant is designed for 27% DTWR, but an range around this target that the plant can still handle is permitted to allow the optimization to select the most economic material when also considering haul cycle times and the other constraints. The silica range is selected to be within the plant tolerance levels. The average silica of the single period (10 year) optimization is 2.2%, so this became the new target for subsequent optimizations because a consistent silica blend is desired across all periods. The DTWR range is kept the same to allow for scheduling higher DTWR material whenever possible. Scheduling higher DTWR has a trade-

off with haul distance however, because most of the higher grade DTWR material is located in the north end of the deposit, which is further from the crusher.

Deviations from the targets are penalized in the objective function, and it is the relative magnitude and not the exact values of the penalties that control how they are balanced in the objective function. The highest weight penalty is given to the concentrate tonnage, with a slightly higher penalty for shortages than excess tonnage. Due to the discrete nature of the blocks being scheduled, an even tonnage equal to the target is unlikely, and this promotes scheduled tonnages slightly higher than the target rather than slightly lower. The value is determined by increasing it until the expected scheduled concentrate tonnages meet the targets. The other quality penalties are then set relative to the concentrate tonnage deviations penalty. The second highest weighting is given to silica deviations to enforce a consistent blend. The third and fourth highest weightings are given to DTWR deviations and non-smooth mining. The penalty for non-smooth mining is determined last. As discussed in Benndorf and Dimitrakopoulos (2013), high penalties for tonnage and quality deviations relative to non-smooth mining penalties tend to yield schedules with more dispersion of the scheduled blocks. The non-smooth mining penalty here are determined by setting it to zero initially, and then

slowly increasing it until the number of scattered blocks in each period are few enough that a feasible schedule could be manually designed without too much difficulty.

3.4. Results

The results of the optimization are shown in Fig. 44 and provide the optimal period in which to mine each block, and whether to send the block for processing or to the waste dump. An interesting result is that the only blocks sent to the waste dump are located at the surface of the deposit and contain mostly OB, and/or MS waste, which means that all scheduled material within the 7 iron-bearing units is sent to the plant. Had ore blocks with a low DTWR been sent to the dump, this would have promoted the concept of stockpiling ore with a low weight recovery. However, this is not the case. Given the cost of mining and low DTWR economic break-even cut-off, the only reason to stockpile ore would be to restrict the silica levels. In the optimized schedule, the silica levels are managed without the need for such a restriction.

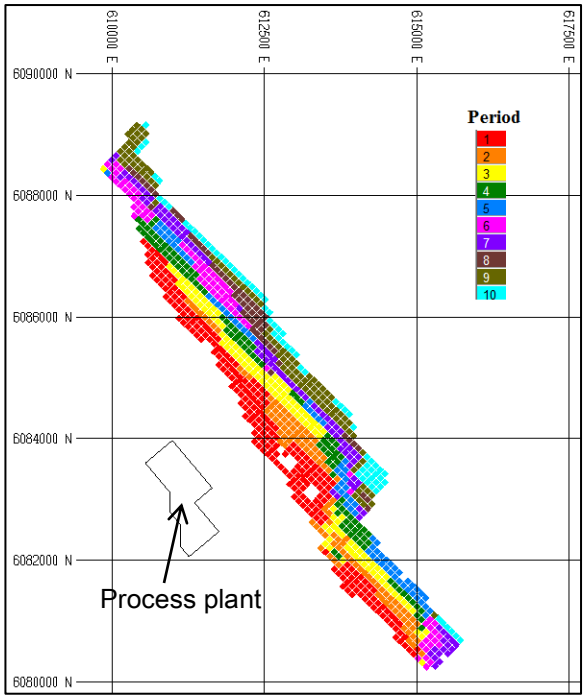

Fig. 44 Blocks colored by period in the stochastic optimization schedule

A practical mining schedule (Fig. 45) was designed based on the block-scale optimization. The optimization considers the first 10 years, and an additional 15 years were scheduled manually to allow for full comparison against a previous deterministic schedule. The pit designs use a 15 m bench height, 45 degree slope angle for the pit sides and hanging wall, and the pit bottom follows the natural inclination of the orebody at approximately 6 degrees (10.5%). Although this slope is not optimal for the haul trucks, various truck manufacturers were consulted and they agreed that it is manageable. Catch berms of 9.5 m with a face angle of 70 degrees were included for additional safety considerations. Since the orebody daylights at surface, the ultimate pit does not require the design

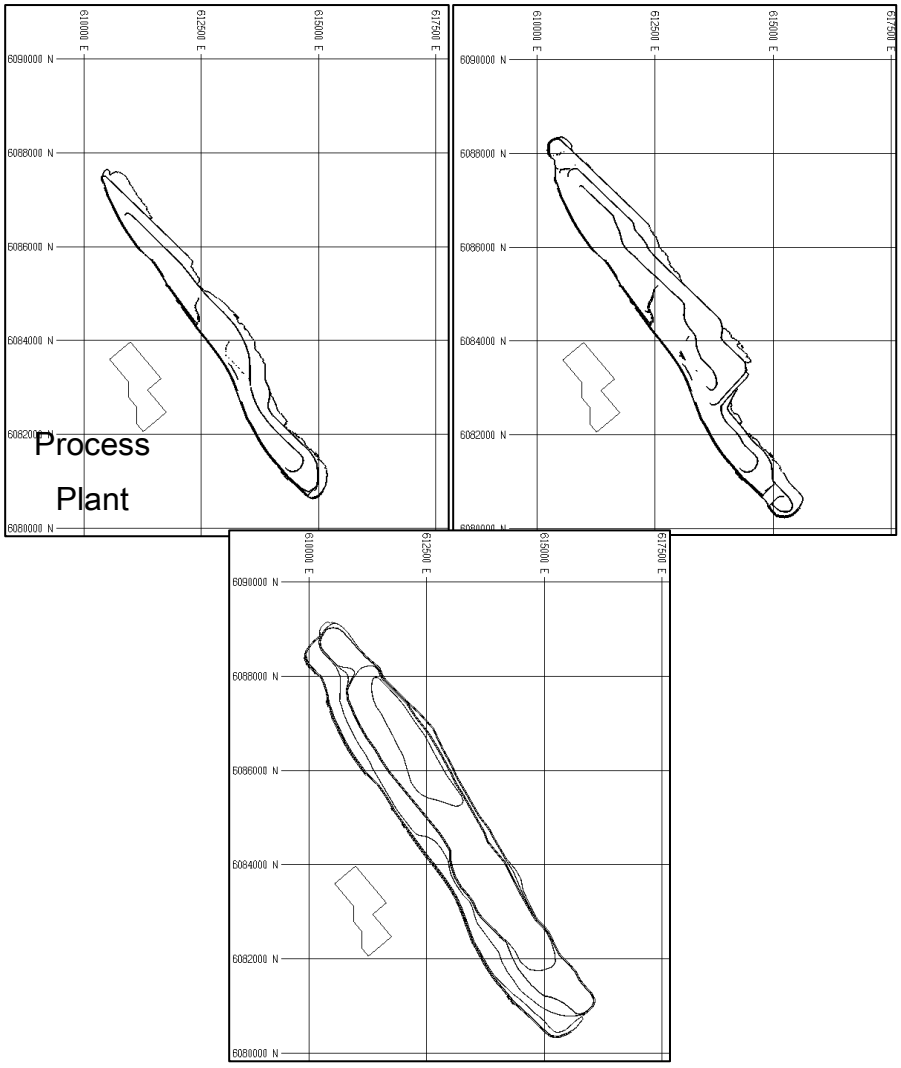

Fig. 45 End of period mine designs based on the stochastic optimization schedule (Year 5, 10, 25)

of a permanent access ramp to the pit bottom. The benches will be mined flat and the pit access will be developed along the floor as the pit wall advances towards the East.

A previous conventional design is shown in Fig. 46. For this schedule, the pit is divided into 8 slots that are roughly 1,000 m wide at surface. There is

an opening slot, 4 slots on the North side and 3 slots on the South side. The slots are mined from West to East (to the full-width extent of the defined resources) and developed down to the final pit floor. Once a slot is completely mined out additional coarse tailings can be placed in the pit.

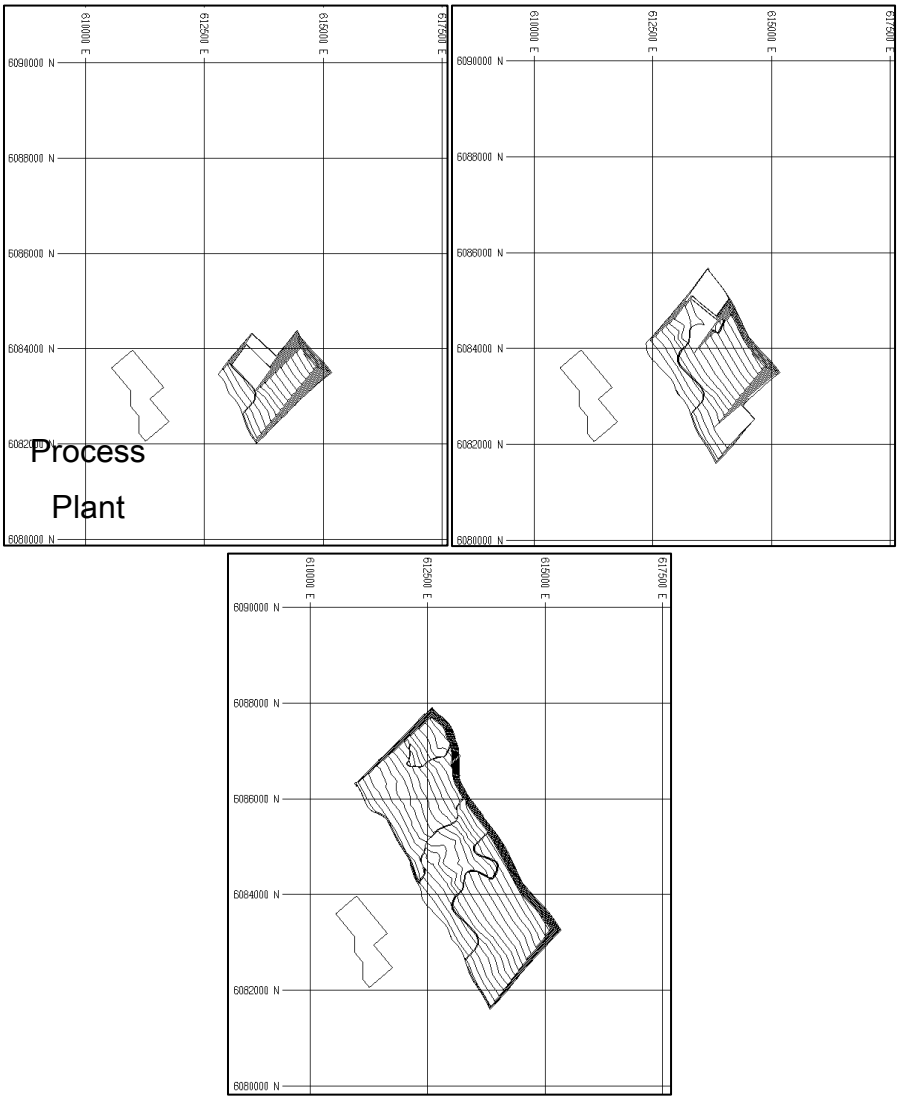

Fig. 46 End of period mine designs based on the deterministic schedule (Year 5, 10, 15)

The evolution of the pit in the stochastic optimization schedule (Fig. 45) is along the full length of the deposit, progressively deepening perpendicular to the strike. This means that compared to the deterministic schedule, shorter haul times are required in earlier periods and less trucks since the trucks can travel at near top-speed (30-35 km/h on a straight-away), whereas on an incline of 8% with 2-3% rolling resistance, they are limited to 15 km/h or less. Another advantage of mining along the length of the deposit is that the grades vary primarily along the strike: higher DTWR material is found to the north, but with higher SiC as well. Having open faces along the full length of the deposit allows for more flexibility during operations to achieve the necessary blend.

Fig. 47 shows that the truck productivity of the optimized schedule is at its maximum in the earlier periods, and steadily declines with each period as the pit is deepened and the cycle times increase. For the deterministic schedule, the productivity moves up and down as each full-width slot is mined. The optimized schedule ensures higher productivity in earlier periods and thus lower corresponding operating costs.

In Fig. 48 to Fig. 53, the previous results from the conventionally derived schedule based on a deterministic geological model are contrasted with the results from the stochastic optimization schedule. Besides showing the

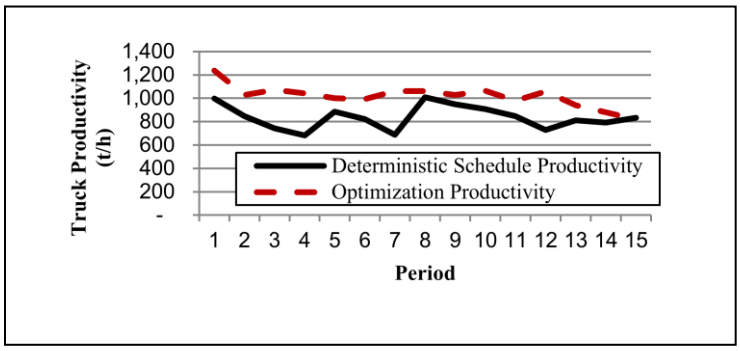

Fig. 47 Truck productivity for the conventional and optimized schedules

tonnages and qualities of each schedule, the risk profiles of each are also shown. The red bars shown correspond to the P10 and P90 values, which show an 80% confidence interval within which to expect the true value. The dotted blue lines show the expected value, which is the mean of the values from each simulation. The dotted black lines represent the evaluation of each push-back using the deterministic model. Any differences between the confidence levels derived using the simulations and the values derived using the deterministic model demonstrate where relying on the deterministic model can be misleading.

3.4.1. Risk management in the stochastic optimization schedule

The analysis in this section pertains exclusively to the lower charts in Fig. 48 to Fig. 53, which show the results from the optimized schedule. Fig. 48 shows that the predicted annual ROM ore tonnes (with ramp-up of 60% and 85% target product tonnage in years 1-2 respectively) will be achieved with little risk. Although the ROM varies up to 10 million tonnes year-to-

year, with peaks in years 5 and 7 in particular, this is not problematic in and of itself: achieving the target concentrate tonnages is the primary scheduling goal, which depends on the DTWR and FeC as well as the ROM tonnage. Another concern could be that these fluctuations indicate fluctuations in fleet requirements, but the fleet requirements depend not only on the ROM tonnes, but the haul distance and the waste tonnages as well. The deterministic model systematically over-estimates the quantity of concentrate tonnes. The is due to differences in the head iron (FeH) in the simulations compared to the FeH in the deterministic model. The densities of each lithology are dependent (and calculated using regressions) on the FeH in each layer as determined in a previous study on density (Milord 2012). The fact that the deterministic model predicts slightly higher ROM tonnages per period indicates that the averaged FeH values of the deterministic model result in overestimation of the tonnages.

Fig. 49 shows that the predicted annual concentrate tonnes will meet the target of 22 mtpy in all years with a high degree of probability. Although the ROM tonnes fluctuate annually, this is balanced by the DTWR (i.e. a year with less ROM has a greater average weight recovery) and/or by a greater FeC. Even though there may be variability in the individual qualities for a given period, their combined interplay results in low variability in concentrate tonnes. This non-intuitive result highlights the

necessity of the SIP formulation for managing the variability of all four qualities. Furthermore, when evaluating the stochastic schedule with the deterministic model, we see 1-2 million tonnes more per year than the mean of the simulations. In general, the deterministic model over-estimates the DTWR by 1-2%, which has a significant impact on the expected concentrate tonnage.

The annual waste tonnages are shown in Fig. 50. The optimization was performed on a pit that purposely excluded the MS, so little MS was expected. There is some very small amount of MS due to variations in the surfaces between the various simulations. The waste in the schedule consists mostly of OB only and is low in all years. The overlying OB is very thin, so fluctuations of the amounts of OB within each simulation were relatively small and so the risk profiles for the waste here are relatively low. The very low amount of waste mining was intended, and is a crucial component to minimizing costs in the first 10 years.

The annual DTWR values (Fig. 51) vary by only 0.4% on average. An interesting result was that the DTWR was not higher in earlier periods as expected. This was expected because a greater weight recovery means less ore must be mined to produce the same tonnage of concentrate, which means lower costs. This result can be explained by the benefit of a higher DTWR compared to a higher cost of mining at depth. The

optimization seeks the greatest profit, so lower DTWR ore can be mined as long as the benefit of mining nearer to the surface offsets the benefit of any potential material with a higher DTWR. However, this may be an artificial result: processing costs and plant efficiencies are variable with respect to feed material, yet they are assumed fixed in this study. With the inclusion of more detailed variable processing costs and efficiencies, it is likely that higher DTWR material would be scheduled in earlier periods before the process plant is fully commissioned and operating consistently.

Fig. 52 shows that the FeC varies very little year to year, although its slight variation does have an impact on the concentrate tonnes. The annual SiC values (Fig. 53) are all less than the maximum specified silica of 2.5%, and is relatively constant around a mean of 2.2%.

3.4.2. Schedule comparison

The stochastic optimization schedule is now compared to the conventionally derived deterministic schedule to demonstrate the benefit of stochastic modeling.

The reduction in the risk of tonnage deviation is seen immediately in comparing the two schedules in Fig. 48 to Fig. 50. The 80% confidence range in the stochastic schedule for ROM ore, concentrate tonnes, and waste tonnes is significantly less than that of the pre-existing deterministic schedule. In addition to a reduced range of tonnage variation, the

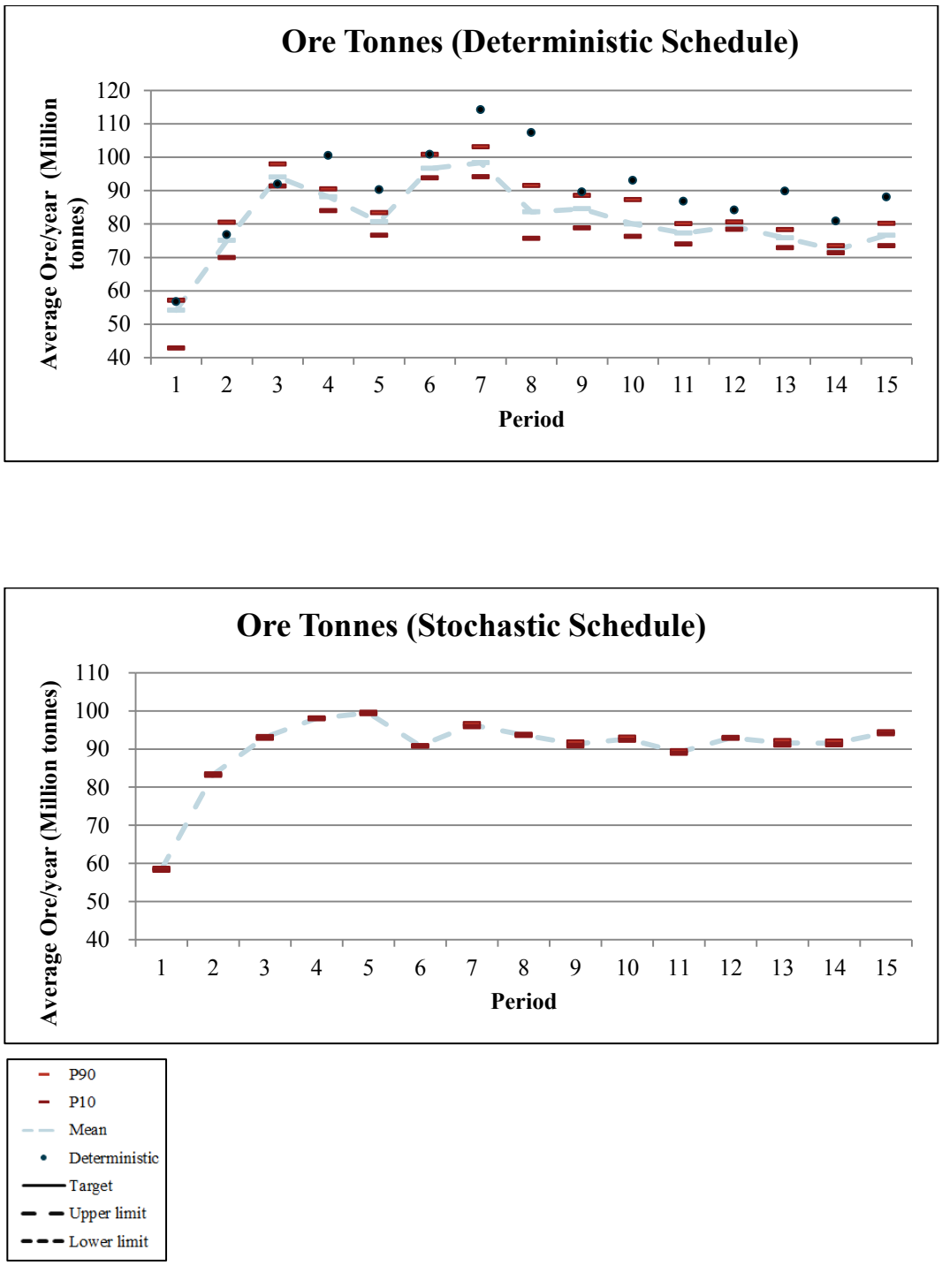

Fig. 48 ROM ore tonnes in deterministic schedule (above) and stochastic schedule (below)

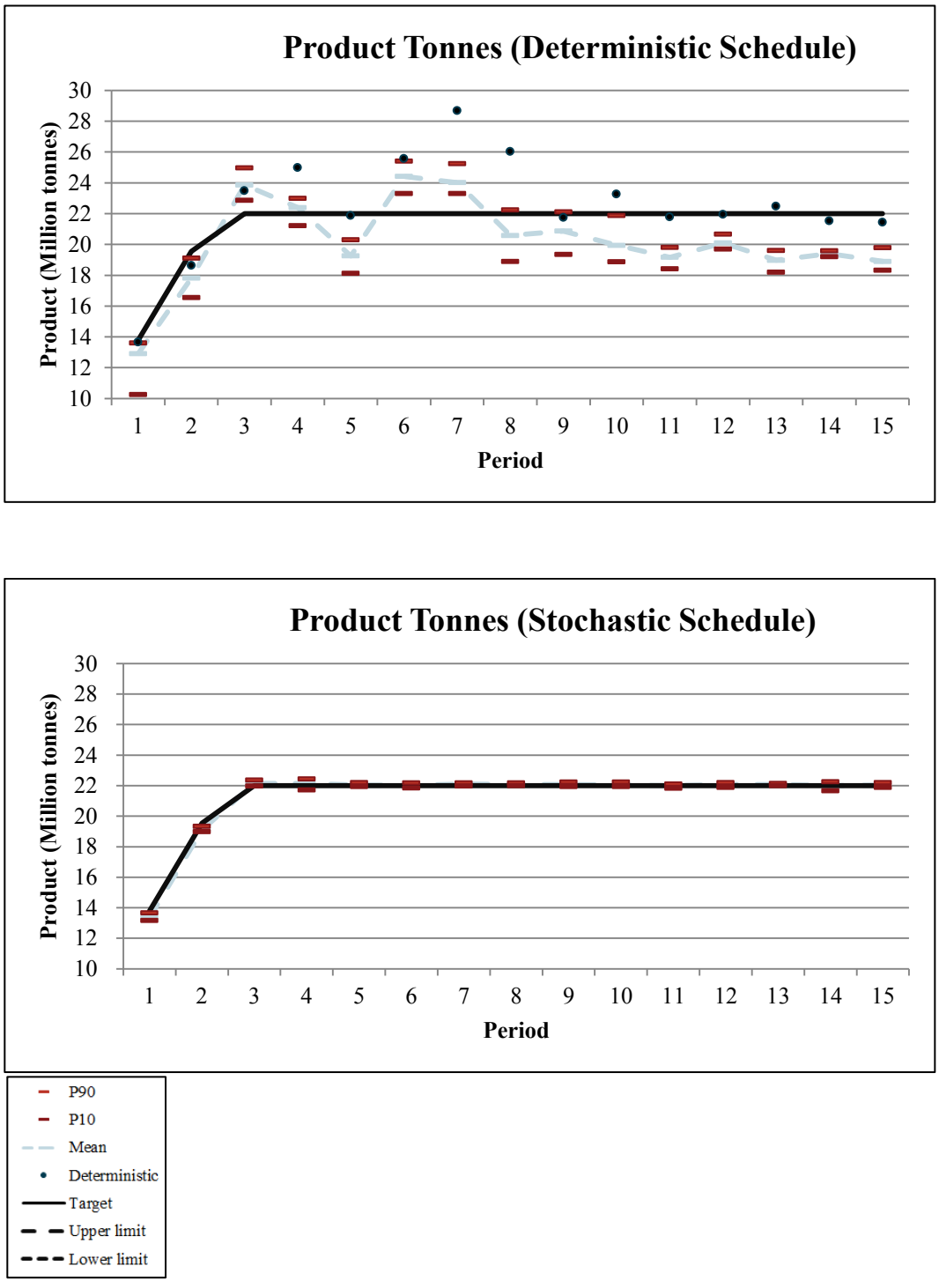

Fig. 49 Product tonnes in deterministic schedule (above) and stochastic schedule (below)

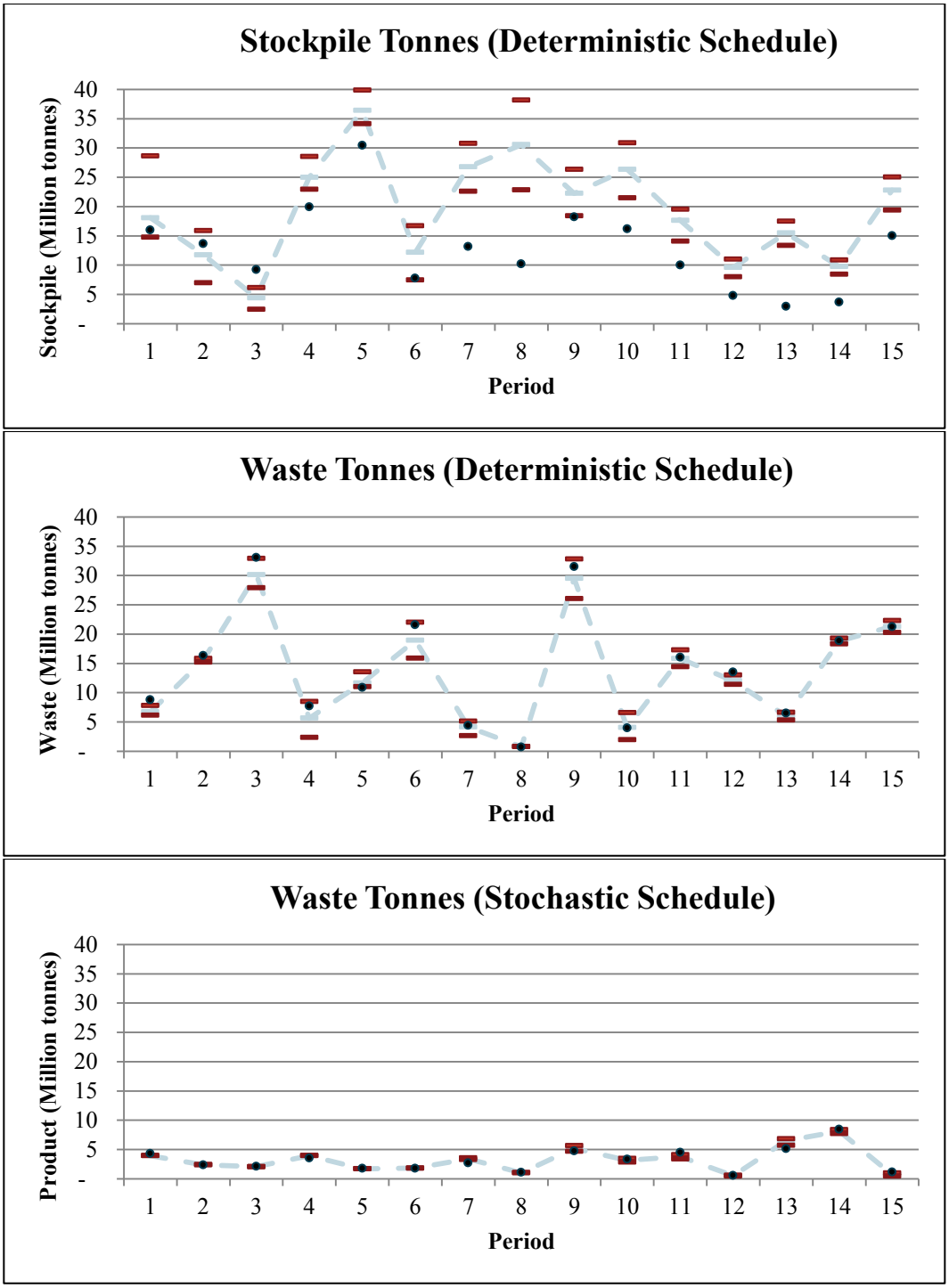

Fig. 50 Stockpile and waste tonnes in the deterministic schedule (above 2) and waste tonnes in the stochastic schedule (below)

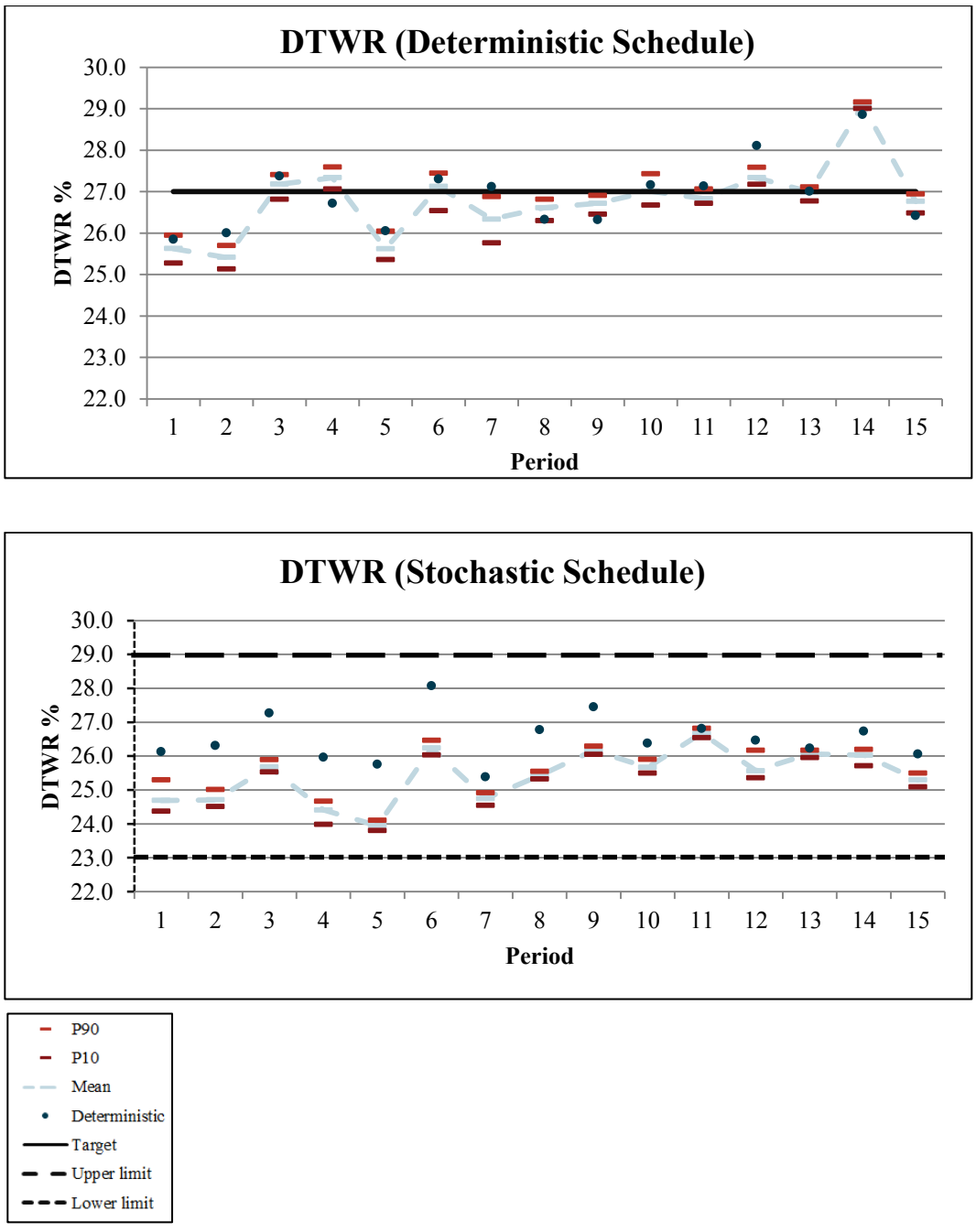

Fig. 51 DTWR of ore in deterministic schedule (above) and stochastic schedule (below)

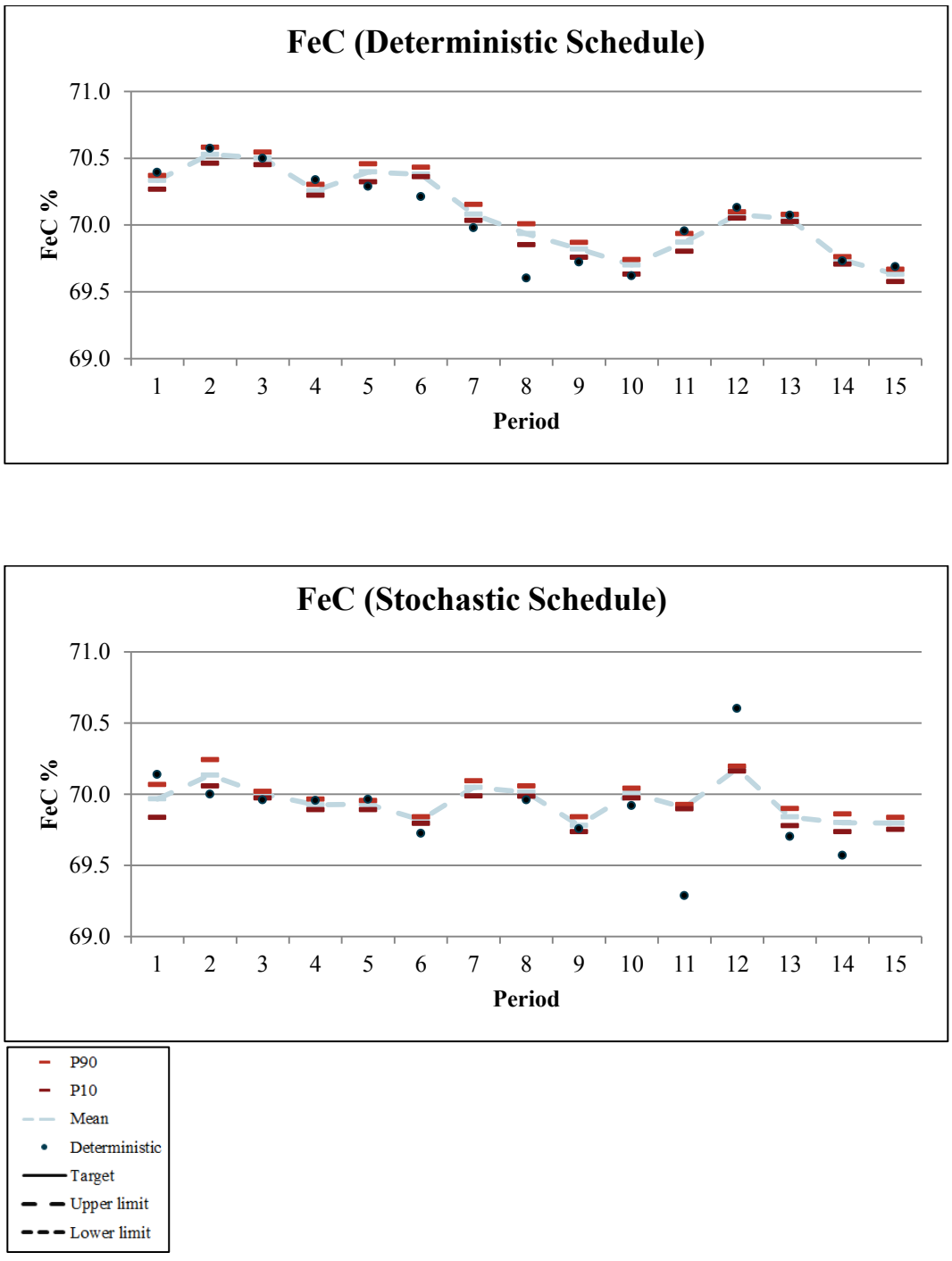

Fig. 52 FeC of ore in deterministic schedule (above) and stochastic schedule (below)

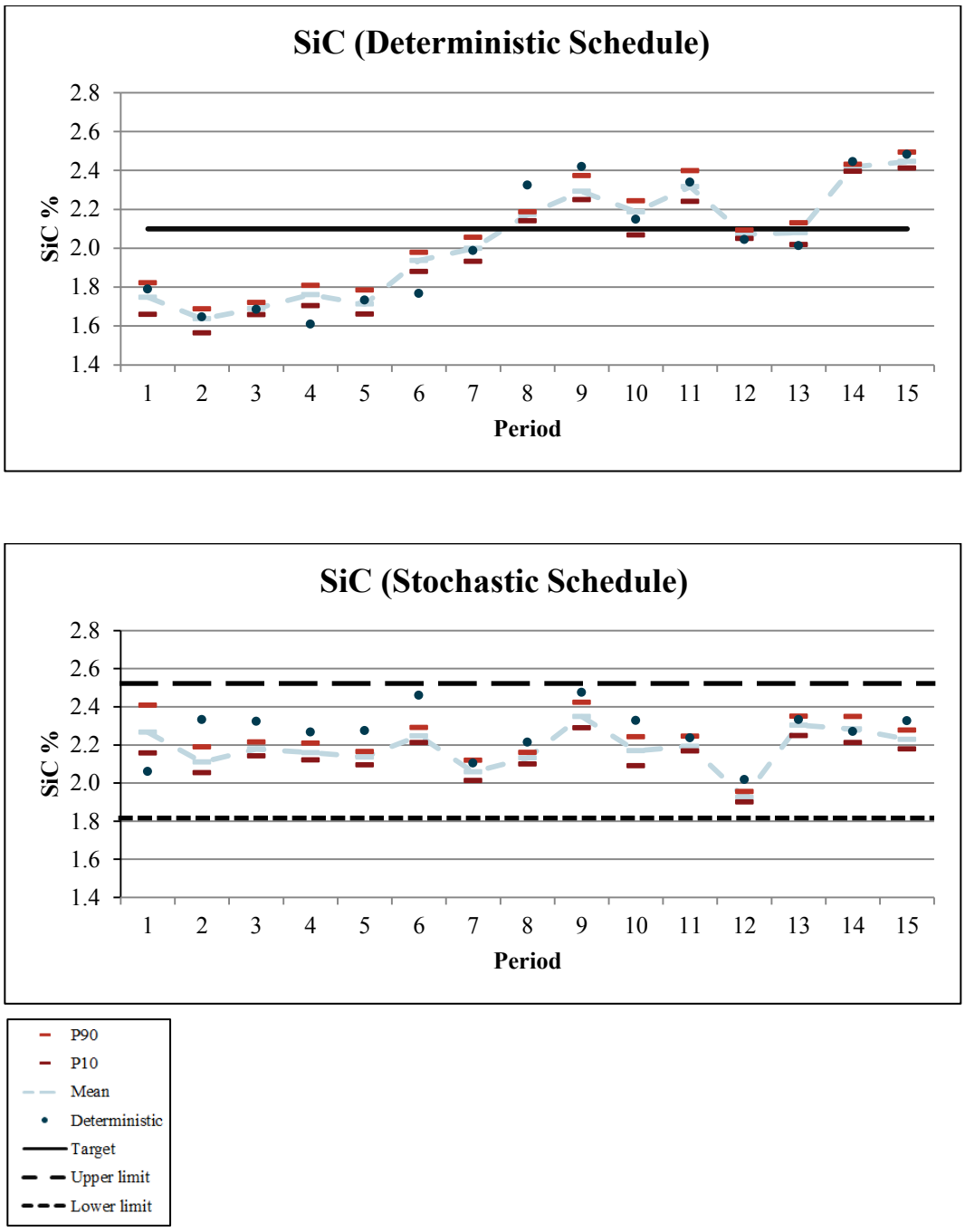

Fig. 53 SiC of ore in deterministic schedule (above) and stochastic schedule (below)

expected product tonnage is centered precisely around the target values. This is not the case for the deterministic schedule, which potentially has both shortfalls and excesses of product tonnes. Although more tonnes need to be mined in the stochastic schedule in order to meet the product targets, it is important to note this is due to the trade-off with haulage costs: the net profit is in fact larger because the location of the material mined is nearer to both the surface and to the process plant.

Compared to the stochastic optimization schedule, Fig. 50 shows that the deterministic schedule mines a significant amount of MS waste as well as additional ore that is stockpiled instead of being sent to the plant. These two materials account for a large difference in equipment requirements, which translates to higher costs than those for the stochastic schedule.

Less variation is expected in the DTWR of the optimized schedule compared to that of the deterministic schedule, although not for all periods. As previously explained, this relates to the interplay of DTWR, FeC, and FeH in determining the concentrate tonnes. Although the deterministic schedule had a target of 27% DTWR, this target was often not met. The stochastic schedule did not have a target DTWR, only hard upper and lower bounds, which are met for all periods.

The silica (SiC) range for each year in the stochastic schedule can be seen to fall within the specified upper and lower limits of 2.5% and 1.8%

respectively, hovering around the target of 2.2% and demonstrating the ability of the stochastic modeling to reduce risk of not meeting targets. Some values are slightly higher than the target, and this occurs because the weighting of the silica constraints (Eq. 9 and 10) are lower than the weighting of the concentrate tonnage constraints (Eq. 7 and 8). This also explains why there is no significant reduction in the range of variability of SiC from the range in the deterministic schedule. Note that the deterministic schedule had no hard upper and lower limits: it just had a target of 2.1% silica. However, the deterministic schedule silica varies considerably from this target, with much lower values in earlier periods, and much higher values in later periods.

Fig. 54 shows the previous truck and cable shovel fleet along with the required equipment based on the schedule in this study. Equipment calculations take into account a variety of factors including mechanical availability, utilization, job efficiency, operating delays, payload, spot times, dump times, load times, and cycle times. The new maximum number of trucks required over the 10 year period is 20 trucks, as opposed to the previous 35 trucks. Less trucks are needed because the haul cycle times are shorter, so the trucks are more productive. In addition, there is less waste mining (almost no mining of the waste MS layer), which also contributes to the reduced number of equipment. The necessary cable

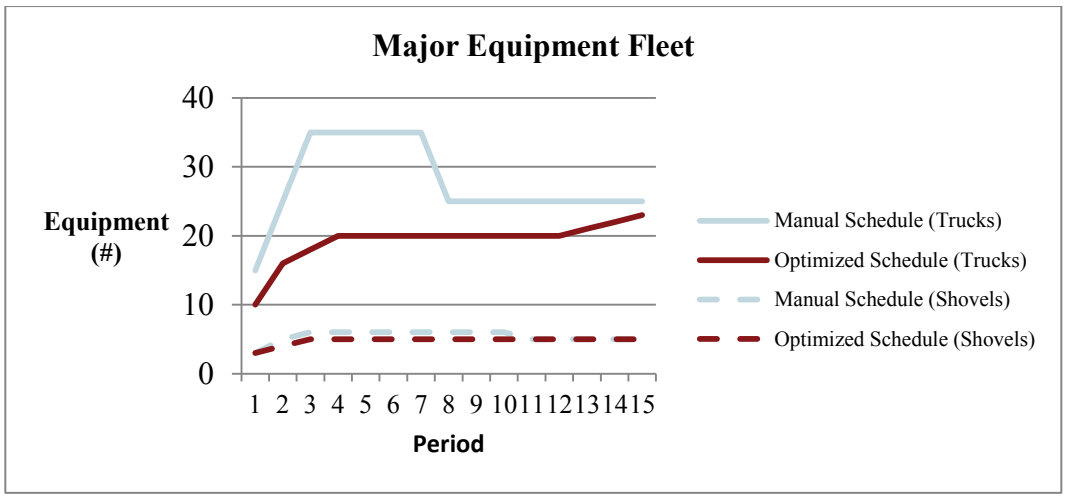

Fig. 54 Major equipment fleet comparison between that of the current optimization study and that of a conventional production schedule

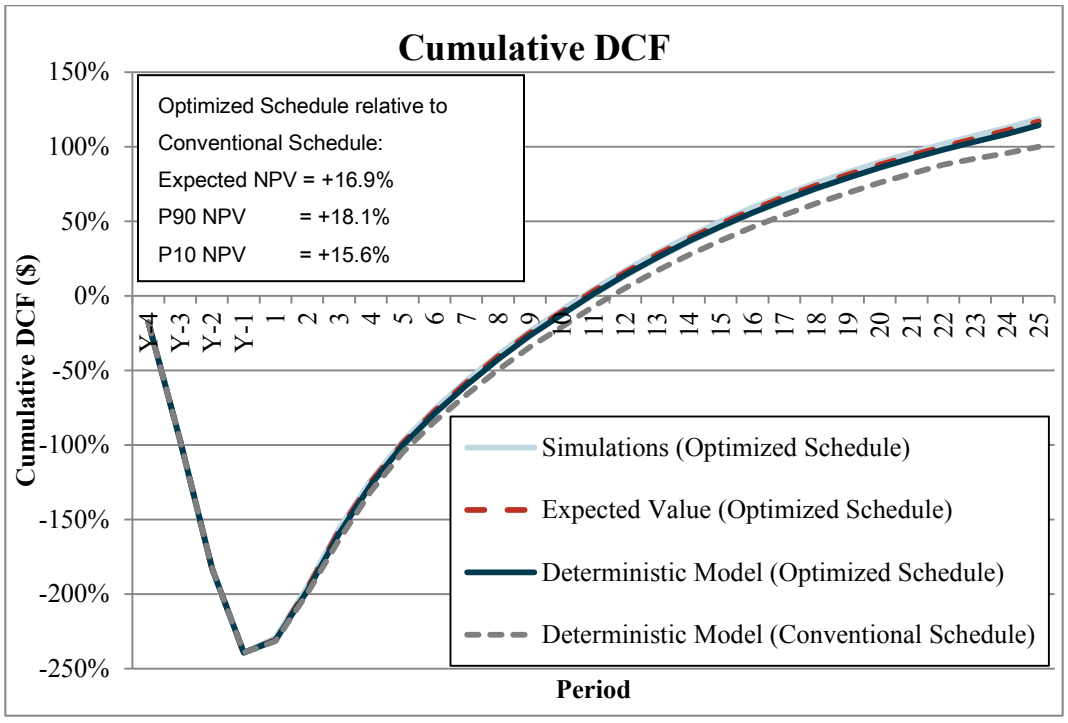

Fig. 55 Cumulative DCF of optimized schedule relative to that of a conventional schedule

shovels was reduced by one, which is significant because each cable shovel costs almost four times as much as one truck. Fig. 54 shows a comparison between the fleet requirements of the two schedules for haul trucks and the primary cable shovels. The change in fleet requirements reduces the capital cost requirements by 23.7% and a corresponding reduction in the operating costs by 26.2%.

The impact of these cost reductions and the reduction of geological variability can be seen together in a comparison of discounted cash flows for both schedules (Fig. 55). Compared to the deterministic schedule, the optimized schedule has an expected NPV that is +16.9%. The 80% confidence range is 2.5%, ranging from a P10 value for the NPV of +15.6 to a P90 value of +18.1% of the deterministic schedule.

3.5. Conclusions

A feasible mining schedule was derived for the LabMag iron ore deposit using a SIP formulation that minimizes the risk of deviation of concentrate tonnages and product silica grades from their targets. The optimized schedule also yielded an expected NPV 16.9% higher than that of a conventional schedule and has a higher chance of being realized due to the reduced risk in concentrate tonnages. These benefits are obtained because stochastic scheduling uses multiple simulations to assess the risk of different block groupings, which is ignored by conventional scheduling

based on a single estimated orebody model. The SIP framework used here also allows for easily balancing multiple goals simultaneously, which is otherwise a challenging task. An even higher NPV could potentially be achieved if the optimization used a block selectivity closer to that of the equipment selectivity, as there would be greater flexibility in the combinations of blocks for scheduling purposes.

The presented scheduled formulation accounts for haulage distances by minimizing trucking costs while also ensuring a smooth truck fleet with no sudden jumps or drops in requirements. In comparison to the first ten years of the previous life-of-mine schedule, the proposed schedule reduces the required number of trucks by 15 (previous total of 35 trucks) to 20 total trucks and the required number of shovels by 1 to 5 shovels total. This has a corresponding impact of 23.7% reduction in capital costs, and 26.2% reduction in operating costs over the first 10 years. The proposed schedule mines the orebody in a progressively deepening fashion, maintaining a larger working area at any given time, rather than mining a slot that reaches the full depth of the deposit. This also permits the eventual disposal of dry tailings and waste inside the pit in order to reduce the environmental footprint.

Chapter 4

Conclusions and Recommendations

4.1. Conclusions

This thesis addresses mine planning of the LabMag deposit, controlled by New Millennium Iron, in northern Labrador, Canada. LabMag has a mine life of over 39 years at the proposed rate of production of 22 million tonnes of concentrate per year. According to the feasibility study on LabMag, the required capital expenditure is estimated at over 5 billion dollars and the average annual operating cost is estimated at approximately 1 billion dollars (SNC-Lavalin 2014). With so much at stake, it is crucial that the highest degree of profitability be sought and that decision-makers have the best information available and an understanding of all risks involved in the development of this project. One of the key risks in a mining project is geological uncertainty because the understanding of the geology, spatial distribution, and variability of the ore qualities can only be inferred from limited data. This thesis thus addresses the optimization of LabMag's long-term mine production schedule while considering geological uncertainty.

A critical review of the technical literature documented that mine plans that do not consider geological uncertainty have significant risk of not meeting production targets, and that optimized mine production schedules based

on single orebody estimates can in fact be severely sub-optimal. Methods for stochastic geological simulation were presented in the technical literature that result in a set of equally probable geological scenarios, which capture the related uncertainty. Methods for stochastically optimizing mine production scheduling were presented that incorporate the scenarios in order to manage risk while seeking an optimal extraction sequence. A mathematical modeling framework known as stochastic integer programming (SIP) was discussed and shown to be a viable method of stochastic production scheduling.

With the motivation to consider geological risk, the LabMag deposit was stochastically simulated and the variability in an existing mine production schedule was quantified. LabMag has seven economic iron-bearing layers whose thicknesses are correlated and there are four primary metallurgical properties of interest (head iron, Davis Tube weight recovery, Davis Tube concentrate iron and silica), which are also strongly correlated. Preserving these correlations is important for creating simulations that correspond to the input data. A methodology for stochastically simulating the LabMag iron ore deposit was shown that is able to preserve the correlations that exist between the ore qualities as well as the correlations between lithology thicknesses. The joint simulation was accomplished using an algorithm (DBMAFSIM) that consists of a MAF transformation to de-

correlate the variables of interest, and direct block simulation to independently simulate each MAF factor. This procedure was implemented in two-stages: once for lithology simulation, and once for simulation of ore qualities. The application of the DBMAFSIM algorithm to the simulation of lithology is novel, and yielded good results in terms of the reproduction of data statistics. A set of ten simulations were created to represent the LabMag deposit.

The simulations were then used to quantify the uncertainty in grade and tonnage in an existing mine design and production schedule. It was shown that actual production tonnages and qualities could significantly vary from what was forecast using a single orebody model. These deviations also affect the discounted cash flows of the project. The expected NPV was shown to be 5.8% less than the NPV predicted with the deterministic model. Furthermore, there is an 80% probability that the true NPV realized is between +1.8% and -13.4% of the deterministic value, indicating relatively low chance of a higher NPV, and a strong probability of a lower than expected NPV.

A subsequent stochastic optimization of the production schedule used an SIP framework that was developed specifically for LabMag. The SIP framework maximizes the expected value of the discounted cash flows by managing the geological risk. It reduces risk in the earlier years, which

have the greatest effect on NPV, by minimizing the risk of deviation of target concentrate tonnages and product silica grades from their targets. The formulation also accounts for haulage distances by minimizing trucking costs while also ensuring a smooth truck fleet with no sudden jumps or drops in requirements. In comparison to the first ten years of the previous life-of-mine schedule, the proposed schedule reduces the required number of trucks by 15 (previous total of 35 trucks) to 20 total trucks and the required number of shovels by 1 to 5 shovels total. This has a corresponding impact of 23.7% reduction in capital costs, and 26.2% reduction in operating costs over the first 10 years. The proposed schedule mines the orebody in a progressively deepening fashion, maintaining a larger working area at any given time, rather than mining a slot that reaches the full depth of the deposit. This also permits the eventual disposal of dry tailings and waste inside the pit in order to reduce the environmental footprint. The application of the SIP framework yielded an NPV 16.9% higher than that of the traditional schedule. This is an important result, because taconite iron orebodies have relatively low variability (compared to higher grade hematite iron, copper, or gold orebodies.

4.2. Recommendations

The block size for the geological simulations in this study was 100 m x 100 m x 15 m in order to compare with a conventional schedule using the same level of selectivity. This block size is appropriate for an estimated model but for simulations, a smaller block size could be potentially important for capturing variability at the scale of equipment selectivity. Ideally, more drilling would be performed to increase the number of drillhole pairs at shorter distances from one another, which would better inform the short-range variability of the variogram models used for simulation.

Due to the large problem size, it was not possible to obtain an optimal result for the SIP formulation in a reasonable amount of time. The optimization was broken down into four sub-optimizations set to stop once there was less than 1% gap between each solution and the optimal solution. A stronger problem formulation could allow for solving the initial problem in one pass, finding a truly optimal result in a reasonable amount of time. An alternate approach to take could be to use one of a number of heuristic methods developed in recent years (Lamghari and Dimitrakopoulos 2012, 2014). Heuristics may not find the optimal result, but could find a near-optimal result for the problem without the need for breaking the problem down into sub-problems.

Beyond optimizing just the production schedule, global optimization strategies could be applied to holistically optimize multiple aspects of the mining project. This could include managing the tonnage and qualities of waste as well as ore, integrating social elements, and including processing considerations. For example, rather than hauling all mined material to a fixed plant location, it could be economically beneficial to consider semi-mobile crushers located within the pit. In this case, the trucks would only need to travel as far as the closest crusher, which could further reduce the number of trucks required. There are costs and time-delays associated with moving a crusher, but these could be modeled and added to the formulation in order to let the optimization determine the ideal crusher locations in each period. Another consideration for global optimization would be the inclusion of variable processing costs and plant efficiencies that depend on the quality of the ore being processed.

References

Albor Consuegra, F., and R. Dimitrakopoulos. "Algorithmic approach to pushback design based on stochastic programming: method, application and comparisons." *Mining Technology* 19, no. 2 (2010): 88-101.

Albor Consuegra, F., and R. Dimitrakopoulos. "Stochastic mine design optimization based on simulated annealing: Pit limits, production schedules, multiple orebody scenarios and sensitivity analysis." *IMM Transactions, Mining Technology* 118, no. 2 (2009): 80-91.

Arpat, G., and Caers J. "Conditional simulation with patterns." *Mathematical Geology* 39 (2007): 177-203.

Asad, M.W.A., and R. Dimitrakopoulos. "Implementing a parametric maximum flow algorithm for optimal open pit mine design under uncertain supply and demand." *Journal of the Operational Research Society* 64 (2013): 185-197.

Benndorf, J., and R. Dimitrakopoulos. "New efficient methods for conditional simulation of large orebodies." *Orebody Modelling and Strategic Mine Planning, The Australasian Institute of Mining and Metallurgy, Spectrum Series 14.* 2007. 61-67.

Benndorf, J., and R. Dimitrakopoulos. "Stochastic long-term production scheduling of iron ore deposits: integrating joint multi-element geological uncertainty." *Journal of Mining Science* 49, no. 1 (2013): 68-81.

Bertrand, J., et al. *NI 43-101 technical report on a prefeasibility study completed on the Hopes Advance Bay iron deposits Ungava Bay Region, Quebec, Canada NTS 24M/08, 24N05.* Toronto: Micon International Limited, 2012.

Birge, J.R., and F. Louveaux. *Introduction to Stochastic Programming.* New York: Springer series in operations research, 1997.

Boilard, A., et al. *NI 43-101 technical report on the preliminary economic assessment for 50 MTPY Otelnuk Lake iron ore project, Quebec, Canada.* Montreal: Met-Chem Canada Inc. and Watts, Griffis, and McOuat Limited, 2011.

Boland, N., I. Dumitrescu, and G. Froyland. "A multistage stochastic programming approach to open pit mine production scheduling with uncertain geology." *Optimizaton Online.* 2008. http://www.optimization-online.org/DB_FILE/2008/10/2123.pdf (accessed April 10, 2014).

Boland, N., I. Dumitrescu, G. Froyland, and T. Kalinowski. "Minimum cardinality non-anticipativity constraint sets for multistage stochastic programming with endogenous observation of uncertainty." *University of New South Wales, School of Mathematics and Statistics.* 2014. http://web.maths.unsw.edu.au/~froyland/Non-anticip_Gen_Matroid_v6.pdf (accessed April 10, 2014).

Boucher, A., and R. Dimitrakopoulos. "Block simulation of multiple correlated variables." *Mathematical Geosciences* 41, no. 2 (2009): 215-237.

Boucher, A., and R. Dimitrakopoulos. "Multivariate block-support simulation of the Yandi iron ore deposit, Western Australia." *Mathematical Geosciences* 44, no. 4 (2012): 449-467.

Caccetta, L., and S.P. Hill. "An application of branch and cut to open pit mine scheduling." *Journal of Global Optimization* 27 (2003): pp. 349–365.

Chatterjee, S., R. Dimitrakopoulos, and H. Mustapha. "Dimensional reduction of pattern-based simulation using wavelet analysis." *Mathematical Geosciences* 44 (2012): 343-374.

Chiles, J. P., and P. Delfiner. *Geostatistics. Modelling spatial uncertainty.* New York: Wiley Series in Probability and Statistics: Wiley Inter-Science, 1999.

David, M. *Geostatistical ore reserve estimation.* Amsterdam: Elsevier, 1977.

—. *Handbook of applied advanced geostatistical ore reserve estimation.* Amsterdam: Elsevier, 1988.

Desbarats, A. J., and R. Dimitrakopoulos. "Geostatisical simulation of regionalized pore-size distributions using min/max autocorrelation factors." *Mathematical Geology* 32, no. 8 (2000): 919-942.

Dimitrakopoulos, R., and A. Jewbali. "Joint stochastic optimisation of short and long term mine production planning: method and application in a large operating gold mine." *Mining Technology* 122 (2013): 110-123.

Dimitrakopoulos, R., and M. B. Fonseca. "Assessing risk in grade-tonnage curves in a complex copper deposit, northern Brazil, based on an efficient joint simulation of multiple correlated variables." *Application of Computers and Operations Research in the Minerals Industries.* South African Institute of Mining and Metallurgy, 2003.

Dimitrakopoulos, R., and S. Ramazan. "Stochastic integer programming for optimizing long term production schedules of open pit mines: methods, application and value of stochastic solutions." *Mining Technology: Transactions of the Institute.* 2008. 155-167.

—. "Uncertainty based production scheduling in open pit mining." *SME Transactions.* Society for Mining, Metallurgy, and Exploration, 2004. 106-112.

Dimitrakopoulos, R., and X. Luo. "Generalized sequential Gaussian simulation on group size v and screen-effect approximations for large field simulations." *Mathematical Geology* 36 (2004): 567-591.

Dimitrakopoulos, R., C. Farrelly, and M. C. Godoy. "Moving forward from traditional optimisation: grade uncertainty and risk effects in open pit mine design." *Transactions of the IMM, Section A Mining Industry.* 2002. A82-A89.

Dimitrakopoulos, R., H. Mustapha, and E. Gloaguen. "High-order statistics of spatial random fields: Exploring spatial cumulants for modelling complex, non-Gaussian and non-linear phenomena." *Mathematical Geosciences* 42, no. 1 (2010): 65-97.

Dimitrakopoulos, R., L. Martinez, and S. Ramazan. "A maximum upside / minimum downside approach to the traditional optimization of open pit mine design." *Journal of Mining Science* 43, no. 1 (2007): 73-82.

Dowd, P. A. "Risk assessment in reserve estimation and open pit planning." *Transactions of the Institute of Mining and Metallurgy, Section A: Mining Industry.* 1994. A148-A154.

—. "Risk in minerals projects: analysis, perception and management." *Transactions of the IMM, Section A Mining Industry.* 1997. A9-18.

Eggins, R. "Modelling thickness in a stratiform deposit using joint simulation techniques." M.Phil. Thesis, University of Queensland, Brisbane, Queensland, Australia, 2006.

Escudero, L.F. "Production planning via scenario modelling." *Annals of Operations Research.* 1993. 311-335.

Geostat Systems International Inc. "Update of the resource model of the LabMag iron ore deposit." Geostat Systems International Inc., Blainville, 2007.

Godoy, M. "The effective management of geological risk in long-term production scheduling of open pit mines." PhD Thesis, University of Queensland, Brisbane, Queensland, Australia, 2002.

Godoy, M., and R. Dimitrakopoulos. "A risk quantification framework for strategic risk management in mine design: method and application at a gold mine." *Journal of Mining Science* 84, no. 2 (2011): 235-246.

Godoy, M., and R. Dimitrakopoulos. "Managing risk and waste mining in long-term production scheduling." *SME Transactions* 316 (2004): pp. 43-50.

Goodfellow, R., and R. Dimitrakopoulos. "Global optimization of open pit mining complexes with uncertainty." *Applied Soft Computing*, 2014: Submitted.

Goovaerts, P. *Geostatistics for natural resources evaluation.* New York: Oxford University Press, 1997.

Grandillo, A., P Live, P Deering, M. Kociumbas, and R. Risto. *Technical report on the feasibility study of the Rose deposit and resource estimate for the Mills Lake deposit of the Kamistiatusset (Kami) iron ore property, Labrador.* Montreal: BBA Inc., Stantec, and Watts, Griffis, and McOuat Limited, 2012.

Guardiano, F., and R. M. Srivastava. *Multivariate geostatistics: beyond bivariate moments.* Vol. 1, in *Geostatistics Troia 1992*, edited by A. Soares, 133-144. Dordrecht: Kluwer, 1993.

Hoerger, S., L. Hoffman, and F. Seymour. "Mine planning at Newmont's Nevada operations." *Mining Engineering*, October 1999: 26-30.

Honarkhah, M., and J. Caers. "Stochastic simulation of patterns using distance-based pattern modelling." *Mathematical Geosciences* 42 (2010): 487-517.

Huang, T., D. Lu, X. Li, and L. Wang. "GPU-based SNESIM implementation for multiple-point statistical simulation." *Computers & Geosciences* 54 (2013): 75-87.

IBM. *IBM ILOG CPLEX V12.1 user's manual for CPLEX.* IBM Corp., 2009.

Jewbali, A. *Modelling geological uncertainty for stochastic short-term production scheduling in open pit metal mines.* PhD Thesis, Queensland: School of Engineering , University of Queensland, 2006.

Journel, A. "Roadblocks to the evaluation of ore reserves — The Simulation overpass and putting more geology into numerical modelsof deposits." *Orebody modelling and strategic mine planning: Uncertainty and risk management models, AusIMM*

Spectrum Series 14, 2nd edition. Melbourne, Australia: The Australasian Institute of Mining and Metallurgy, 2007. 29-32.

Journel, A., and Ch. J. Huijbregts. *Mining geostatistics.* New York: Academic Press, 1978.

Kakela, P. "Iron ore companies consolidated." *The International Resource Journal*, June 6, 2014.

King, H. F., D. W. McMahon, G. J. Bujtor, and A. K. Scott. "Geology in the understanding of ore reserve estimation: an Australian viewpoint in ore reserve estimation." Edited by D. E. Ranta. *Applied Mining Geology* 3 (1986): 55-68.

Kirkpatrick, S., C.D. Gelatt, and M.P. Vecchi. "Optimization by simulated annealing." *Science* 220 (1983): 671-680.

Kuchta, M., A. Newman, and E. Topal. "Production scheduling at LKAB's Kiruna mine using mixed-integer programming." *Mining Engineering*, April 2003: 35-40.

Lamghari, A., and R. Dimitrakopoulos. "A diversified Tabu search approach for the open-pit mine production scheduling problem with metal uncertainty." *European Journal of Operational Research* 222, no. 3 (2012): pp. 642 – 652.

Lamghari, A., and R. Dimitrakopoulos. "A hybrid method based on linear programming and variable neighborhood descent for scheduling production in open-pit mines." *Journal of Global Optimization*, 2014.

Leite, A., and R. Dimitrakopoulos. "A stochastic optimisation model for open pit mine planning: application and risk analysis at a copper deposit." *Mining Technology* 116, no. 3 (2007): 109-116.

Leite, A., and R. Dimitrakopoulos. "Production scheduling under metal uncertainty: application of stochastic mathematical programming at an open pit copper mine and comparison to conventional scheduling." *Journal of Mining Science and Technology* 24 (2014): (in press).

Menabde, M., G. Froyland, P. Stone, and G. Yeates. "Mining schedule optimization for conditionally simulated orebodies." In *Orebody Modelling and Strategic Mine Planning: Uncertainty and risk management models*, 379-384. AusIMM Spectrum Series 14, 2nd ed., 2007.

Menabde, M., P. Stone, B. Law, and B. Baird. "Blasor - A generalized strategic mine planning optimization tool." *SME Annual Meeting.* Denver: Society of Mining Engineers, 2007. Preprint 07-053.

Metropolis, N., A.W. Rosenbluth, M.N. Rosenbluth, A.H. Teller, and E. Teller. "Equations of state calculations by fast computing machines." *Journal of Chemical Physics* 21 (1953): 1087-1092.

Milord, I. "Densité relative de LabMag et KéMag." Table jamésienne de concertation minière, Chibougamau, 2012.

Mintec. "MineSight and mineral evaluation and planning." Reference Manual, Mintec, Tucson, 2010.

Montiel, L., and R. Dimitrakopoulos. "Optimizing mining complexes with multiple processing and transportation alternatives: An uncertainty-based approach." *European Journal of Operational Research* , 2014: Submitted.

Mustapha, H., and R. Dimitrakopoulos. "High-order stochastic simulations for complex non-Gaussian and non-linear geological patterns." *Mathematical Geosciences* 42 (2010): 65-99.

Mustapha, H., and R. Dimitrakopoulos. "HOSIM: a high-order stochastic simulation algorithm for generating three-dimensional complex geological patterns." *Computers & Geosciences* 37 (2011): 1242-1253.

Mustapha, H., and R. Dimitrakopoulos. "New approach for geological pattern recognition using high order spatial cumulants." *Computers & Geosciences* 32, no. 3 (2009): 313-334.

Mustapha, H., R. Dimitrakopoulos, and S. Chatterjee. "Geologic heterogeneity representation using high-order spatial cumulants for

subsurface flow and transport simulations." *Water Resources Research*, 2011: 1-16.

Mustapha, H., S. Chatterjee, and R. Dimitrakopoulos. "CDFSIM: Efficient stochastic simulation through decomposition of cumulative distribution functions of transformed spatial patterns." *Mathematical Geosciences* 46 (2014): 95–123.

Newman, A., and M. Kuchta. "Using aggregation to optimize long-term production planning at an underground mine." *European Journal of Operational Research* 176 (2007): 1205-1218.

Osterholt, V., and R. Dimitrakopoulos. "Simulation of orebody geology with multiple-point geostatistics: Application at Yandi Channel iron ore deposit." *Orebody modelling and strategic mine planning: Uncertainty and risk management models, AusIMM Spectrum Series 14, 2nd edition.* 2007. 51-60.

Ramazan, S., and R. Dimitrakopoulos. "Production scheduling with uncertain supply: A new solution to the open pit mining problem." *Optimization and Engineering* 14 (2013): 361-380.

Ramazan, S., and R. Dimitrakopoulos. "Stochastic optimization of long term production scheduling for open pit mines with a new integer programming formulation." In *Orebody Modelling and Strategic Mine Planning*, 385-391. Melbourne: Spectrum Series vol. 14, 2nd ed., 2007.

Ramazan, S., and R. Dimitrakpoulos. "Traditional and new MIP models for production scheduling with in-situ grade variability." *International Journal of Surface Mining* 18, no. 2 (2004): 85-98.

Ravenscroft, P. J. "Risk analysis for mine scheduling by conditional simulation." *Transactions of the Institute of Mining and Metallurgy, Section A (Mining Technology).* 1992. 104-108.

Sabour, S.A., and R Dimitrakopoulos. "Incorporating geological and market uncertainty and operational flexibility into open pit mine design." *Journal of Mining Science* 47, no. 2 (2011): 191-201.

Schulz, N.F. "Determination of the magnetic separation characteristics with the Davis Magnetic Tube." *SME-AIME Transactions* 229 (1964): 211-216.

Sinclair, A. J., and G. H. Blackwell. *Applied mineral inventory estimation.* Cambridge: Cambridge University Press, 2002.

SNC-Lavalin. "Technical report on the feasibility study of the LabMag iron ore deposit, Labrador, Canada." Montréal, 2014.

Stone, P., G. Froyland, M. Menabde, B. Law, R. Pasyar, and P. Monkhouse. "Blasor - blended iron-ore mine planning optimization at Yandi." *Orebody Modelling and Strategic Mine Planning, AusIMM Spectrum Series 14, 2nd ed.* Perth: Australian Institute of Mining and Metallurgy, 2004. 285-288.

Straubhaar, J., P. Renard, G. Mariethoz, R. Froidevaux, and O. Besson. "An improved parallel multiple-point algoirthm using a list approach." *Mathematical Geosciences* 43 (2011): 305-328.

Strebelle, S. "Conditional simulation of complex geological structures using multiple-point geostatistics." *Mathematical Geology* 34, no. 1 (2002): 1-21.

Strebelle, S., and C. Cavelius. "Solving speed and memory issues in multiple-point statistics simulation program SNESIM." *Mathematical Geosciences* 46 (2014): 171-186.

Switzer, P., and A. A. Green. "Min/Max autocorrelation factors for multivariate spatial imagery." Technical Report No. 6, Department of Statistics, Stanford University, 1984, 14.

Tahmasebi, P., A. Hezarkhani, and M. Sahimi. "Multiple-point geostatistical modeling based on the cross-correlation functions." *Computers & Geosciences* 16 (2012): 779–797.

Tahmasebi, P., M. Sahimi, and J. Caers. "MS-CCSIM: Accelerating pattern-based geostatistical simulation." *Computers & Geosciences* 67 (2014): 75-88.

Tran, T.T. "Improving variogram reproduction on dense simulation grids." *Computers & Geosciences* 20, no. 7-8 (1994): 1161-1168.

Vallée, M. "Mineral resource + engineering, economic and legal feasibility = ore reserve." *CIM Bulletin* 93, no. 1038 (2000): 53-61.

Vargas-Guzman, J. A., and R. Dimitrakopoulos. "Conditional simulation of random fields by successive residual." *Mathematical Geology*, 2002: 507-611.

Whittle, G. "Global asset optimization." *Orebody Modelling and Strategic Mine Planning Spectrum Series*, 2010: 331-336.

Whittle, J. "The global optimizer works, what next?" *The Australasian Institute of Mining and Metallurgy, Spectrum Series.* 2010. 3-5.

Wu, J., T. Zhang, and A. Journel. "Fast FILTERSIM simulation with score-based distance." *Mathematical Geosciences* 40, no. 7 (2008): 773-788.

Zhang, T., P Switzer, and A. G. Journel. " Filter-based classification of training image patterns for spatial simulation." *Mathematical Geology* 38, no. 1 (2006): 63-80.

Zuckerberg, M., P. Stone, R. Pasyar, and E. Mader. "Joint ore extraction and in-pit dumping optimization." *SME Annual Meeting.* Denver, CO: Society of Mining, Metallurgy & Exploration, 2007. 1-3.

Appendix A – Layer Thickness Histograms: Data vs Simulation

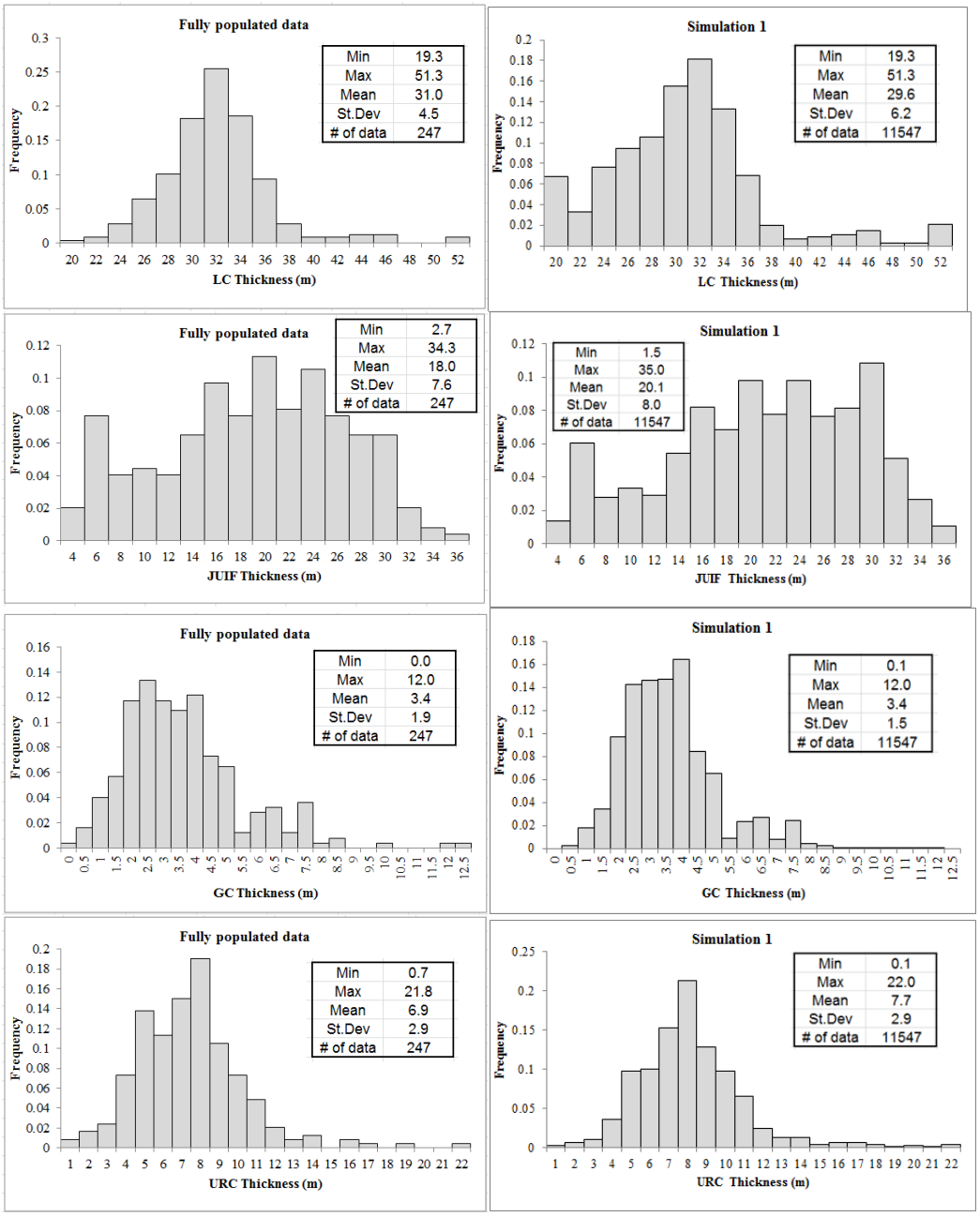

Left: Source data, Right: Simulation 1 results

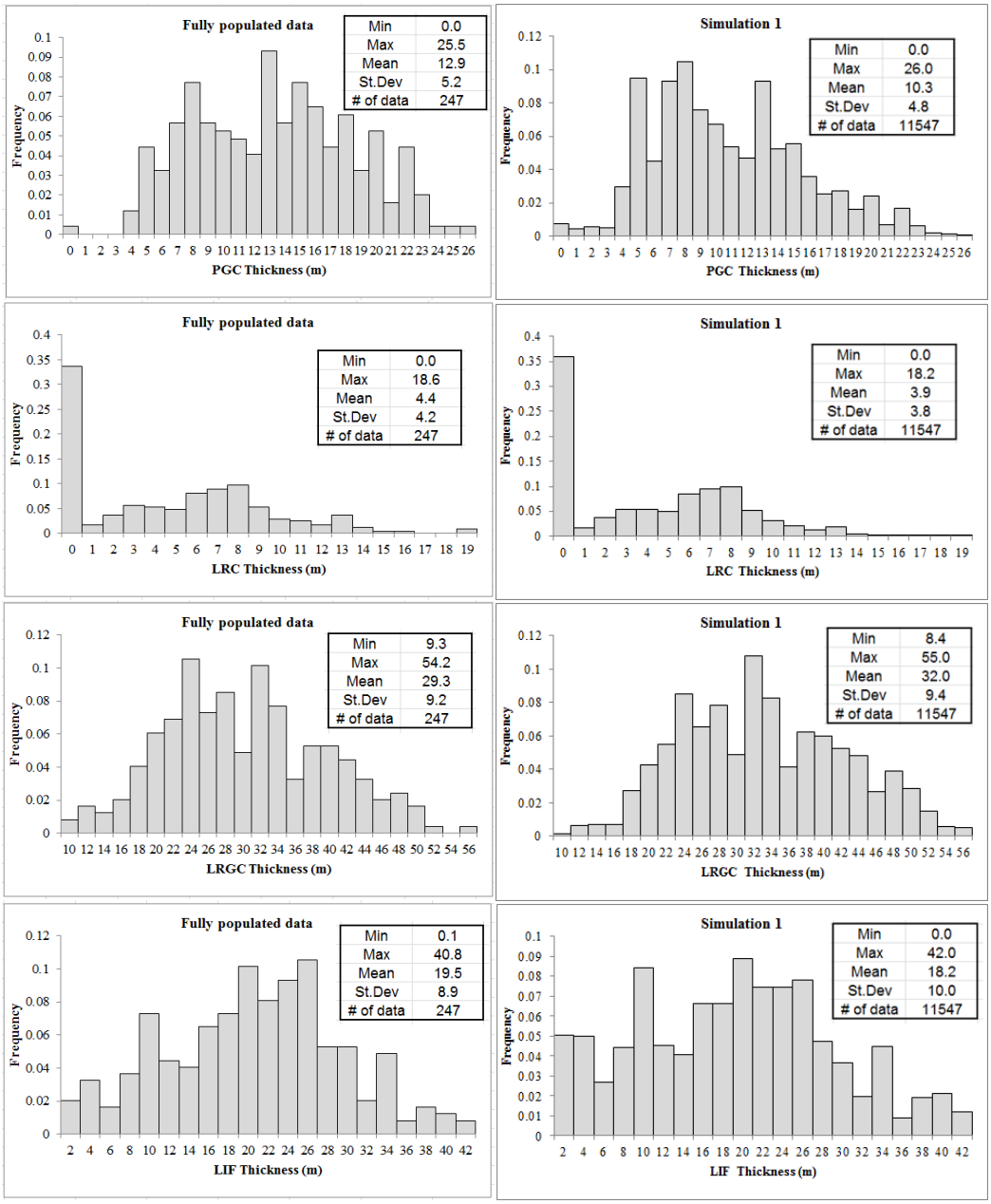

Left: Fully populated data, Right: Simulation 1 results

Appendix B – Layer Thickness Simulation Variogram Reproduction

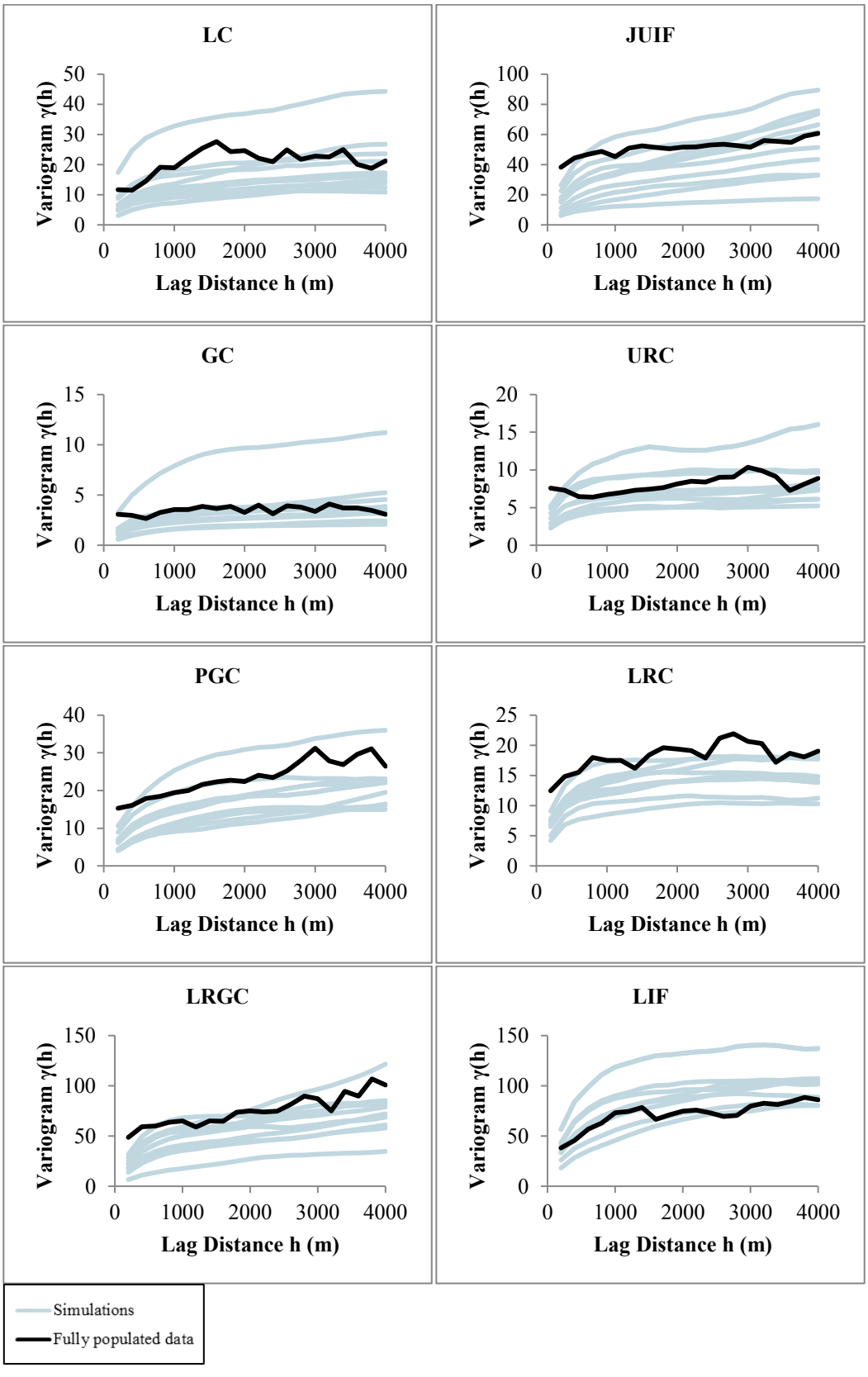

Appendix C – Ore Quality Data and Simulation Histograms

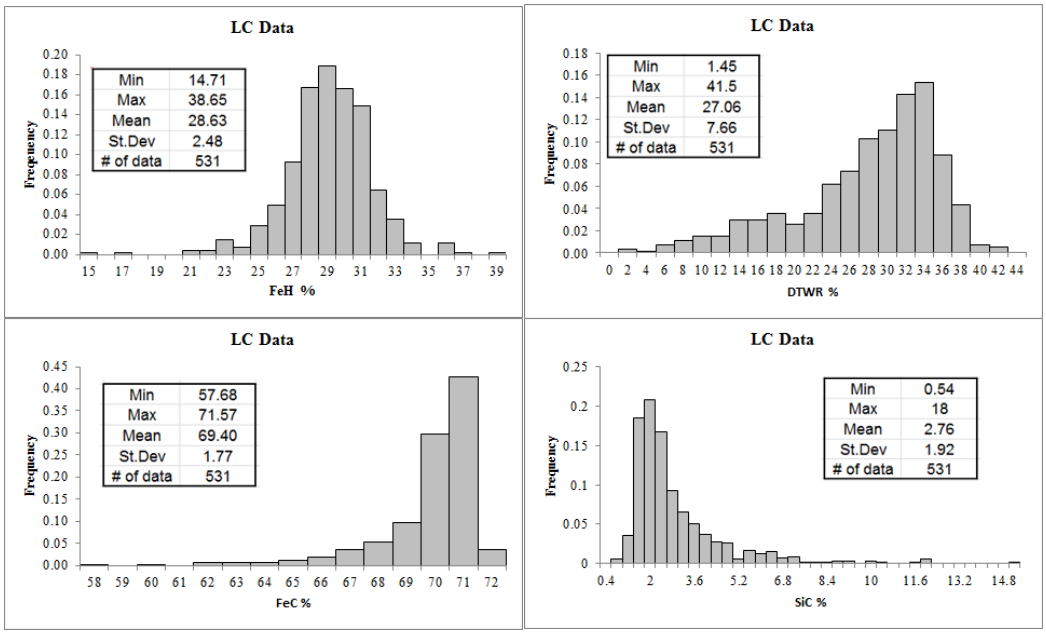

Data histograms of grades for LC layer

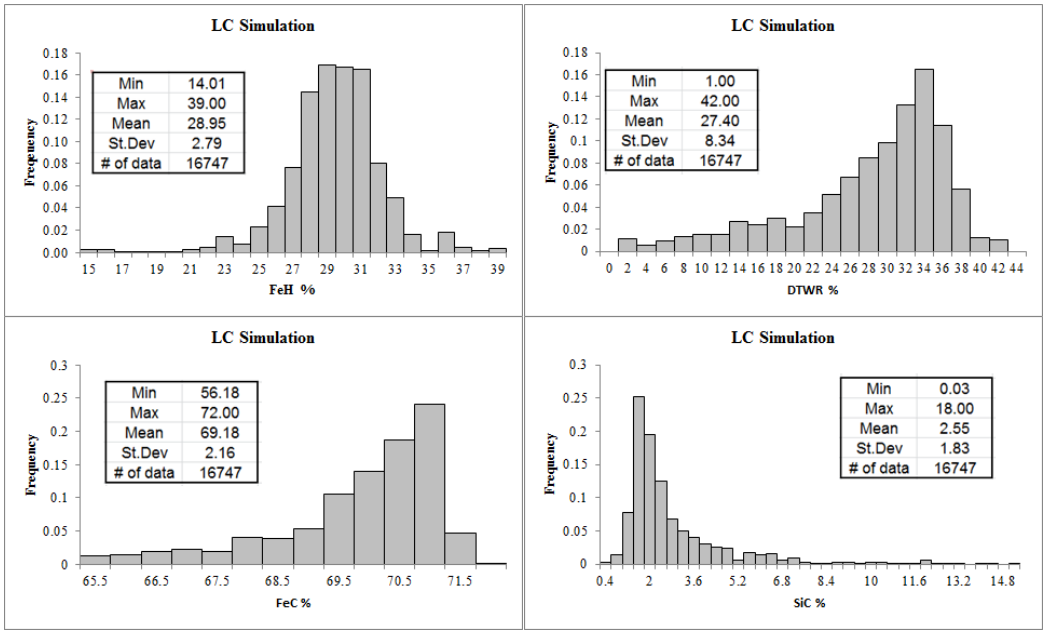

Simulation 1 histograms of grades for LC layer

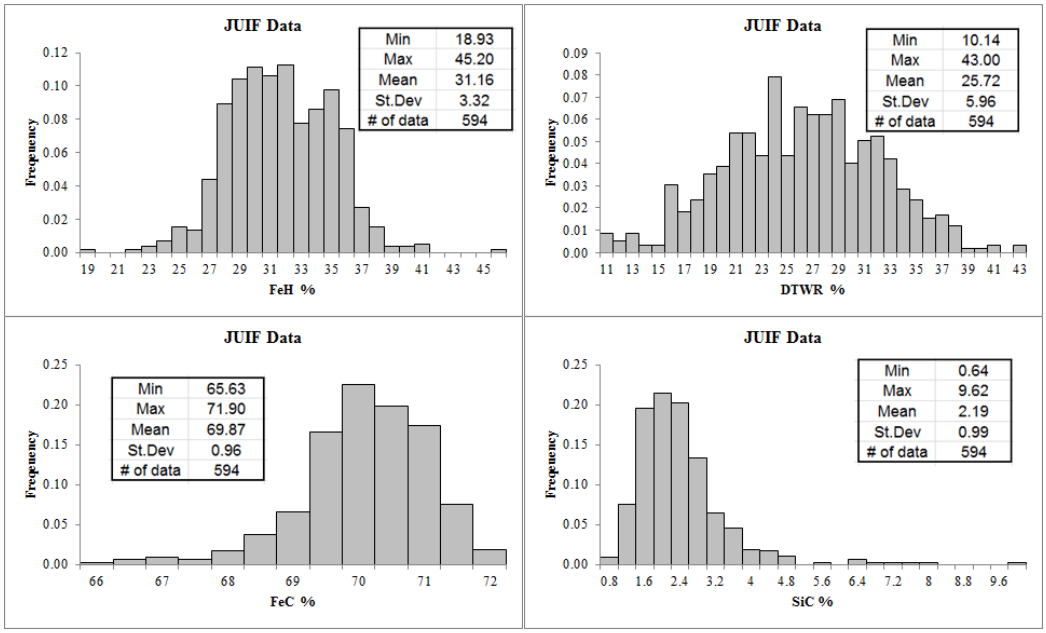

Data histograms of grades for JUIF layer

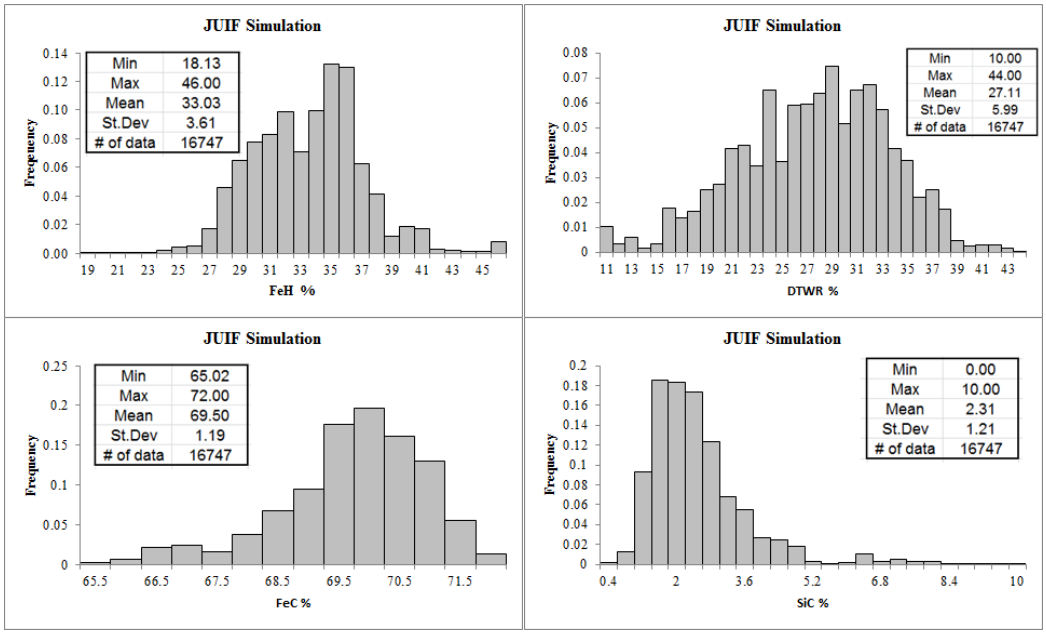

Simulation 1 histograms of grades for JUIF layer

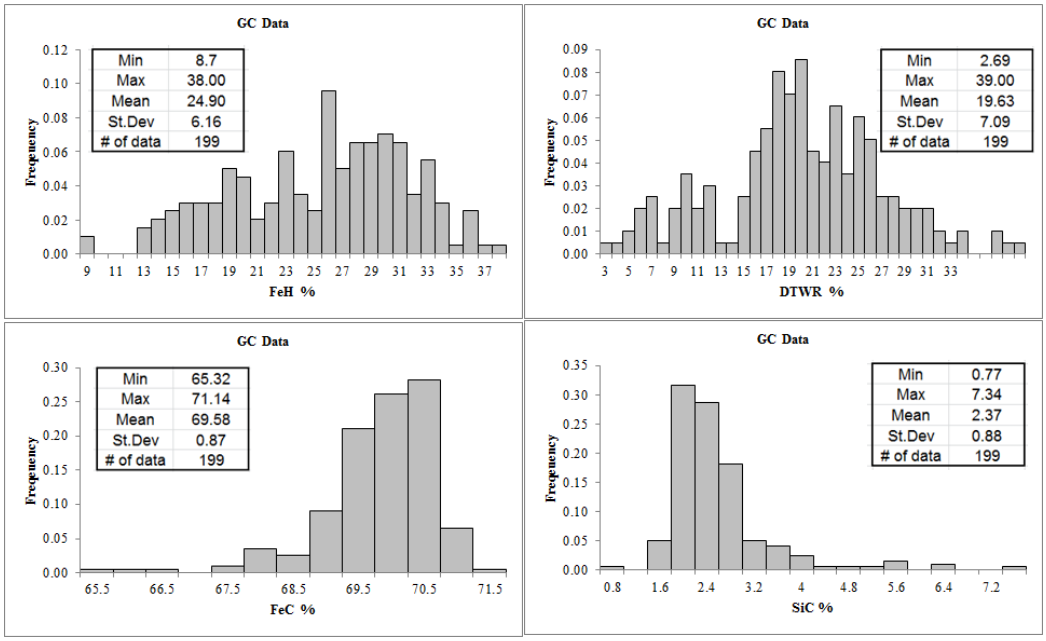

Data histograms of grades for GC layer

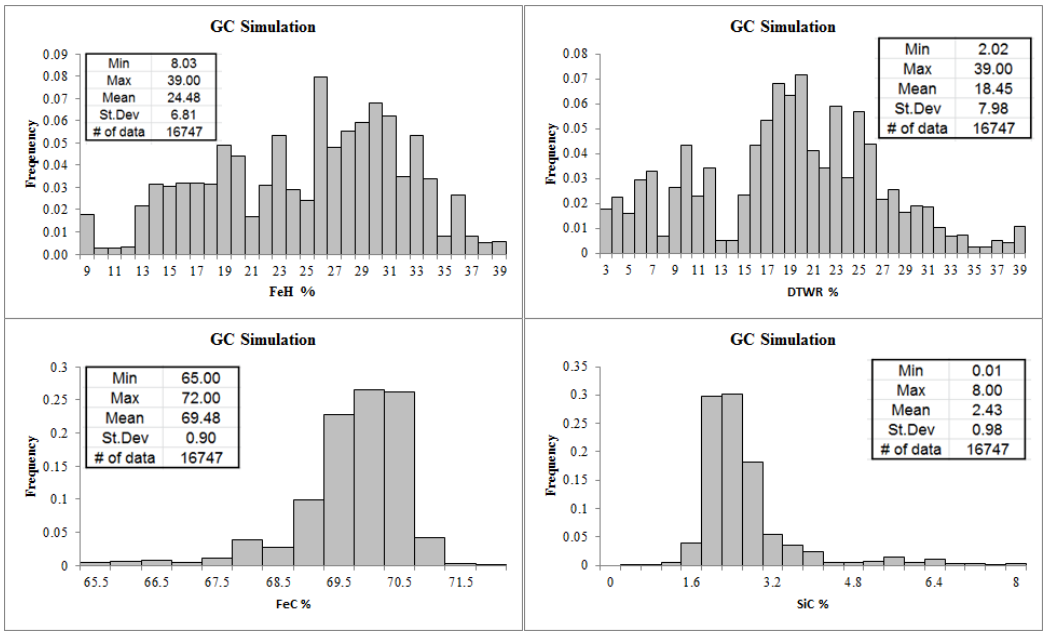

Simulation 1 histograms of grades for GC layer

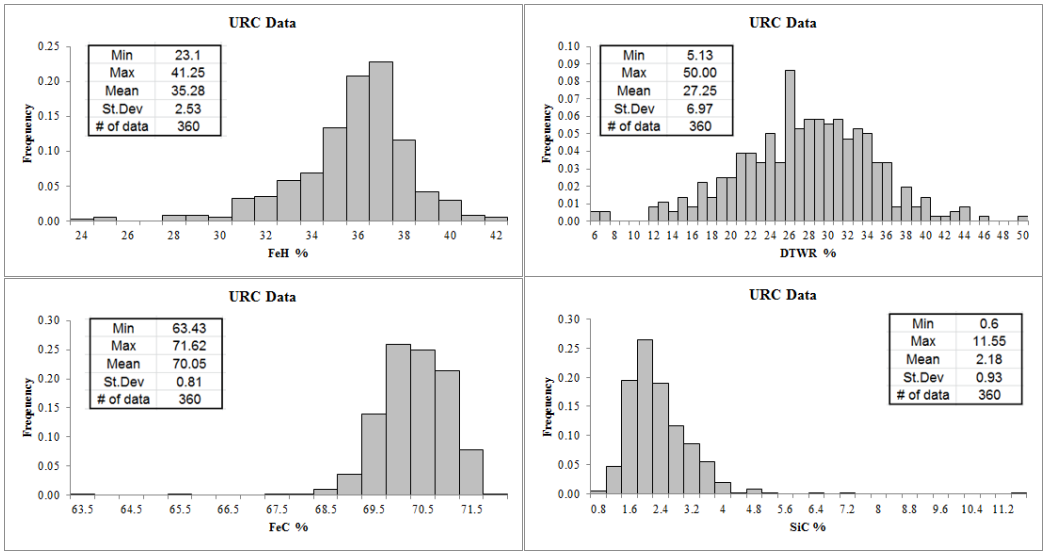

Data histograms of grades for URC layer

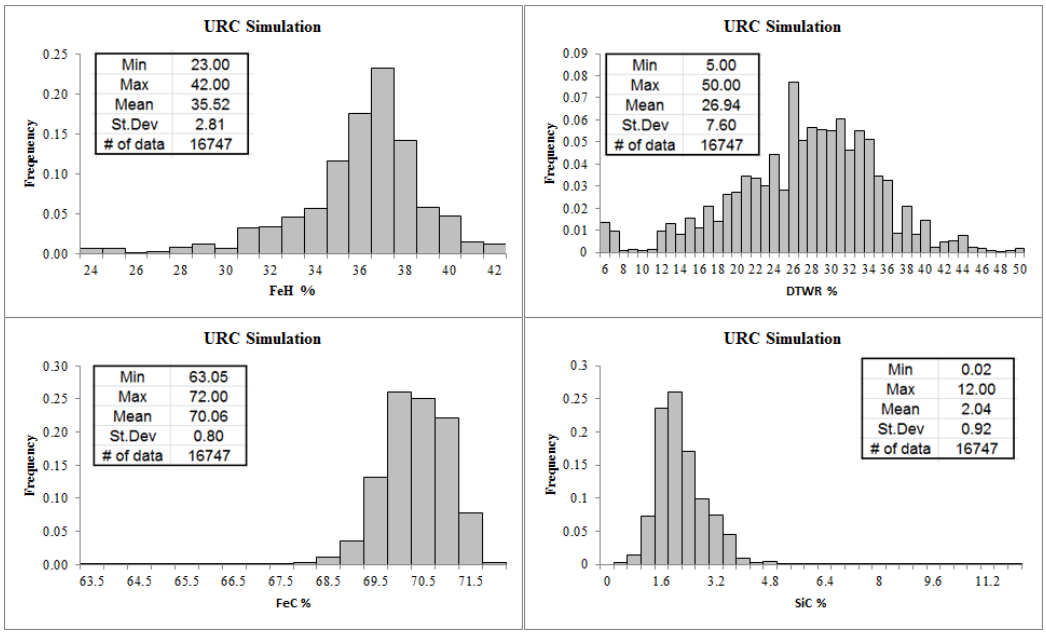

Simulation 1 histograms of grades for URC layer

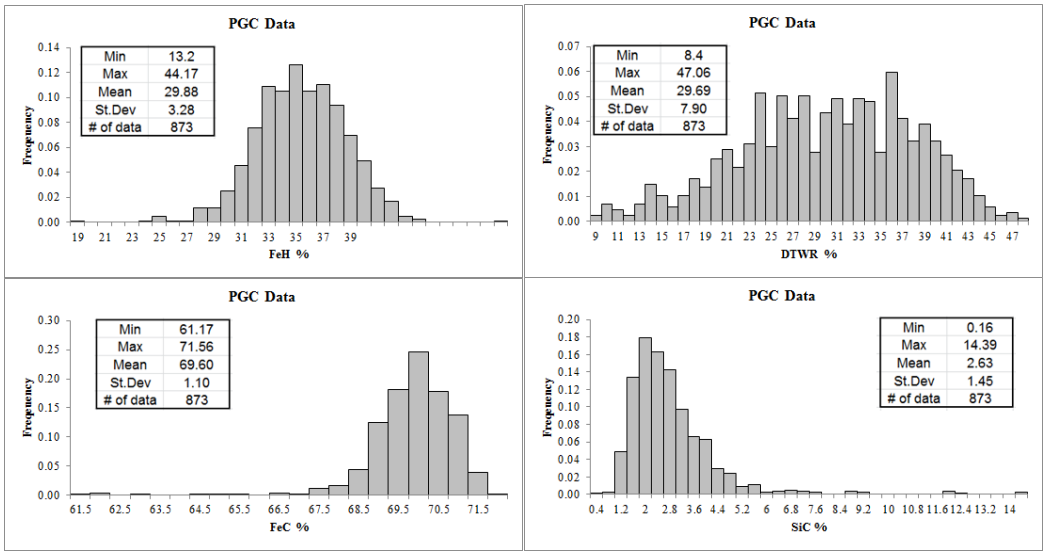

Data histograms of grades for PGC layer

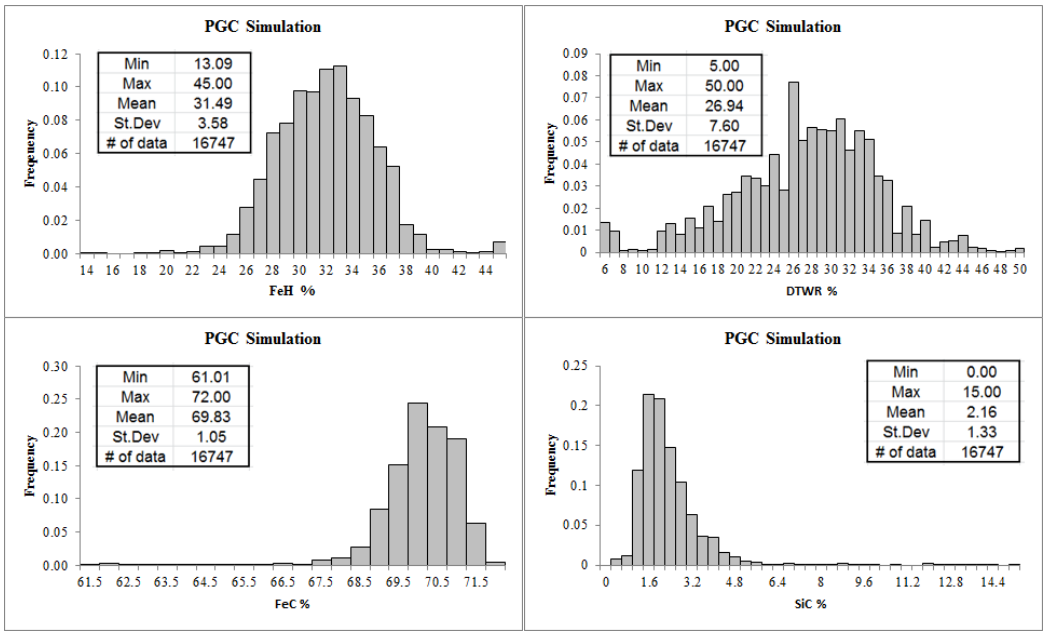

Simulation 1 histograms of grades for PGC layer

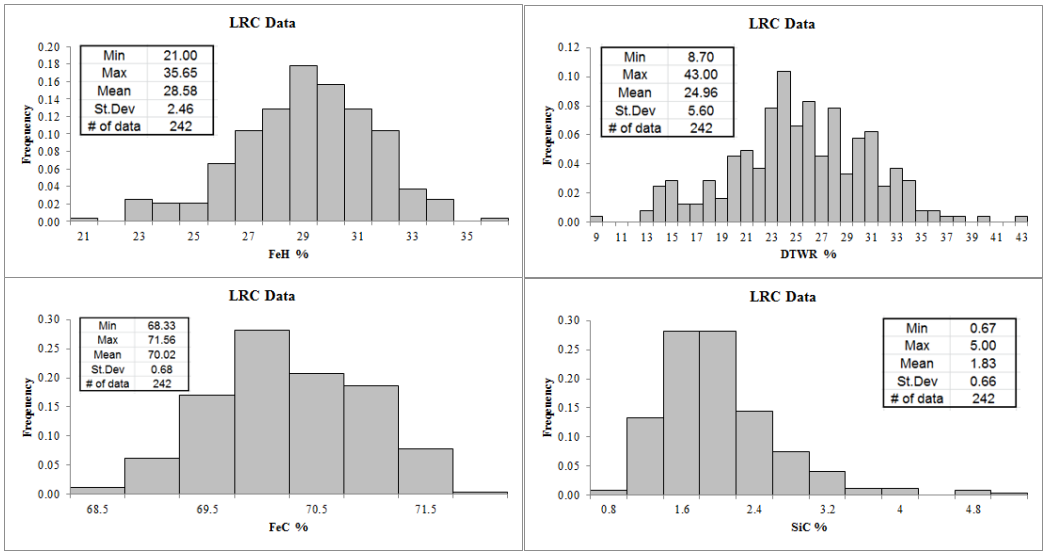

Data histograms of grades for LRC layer

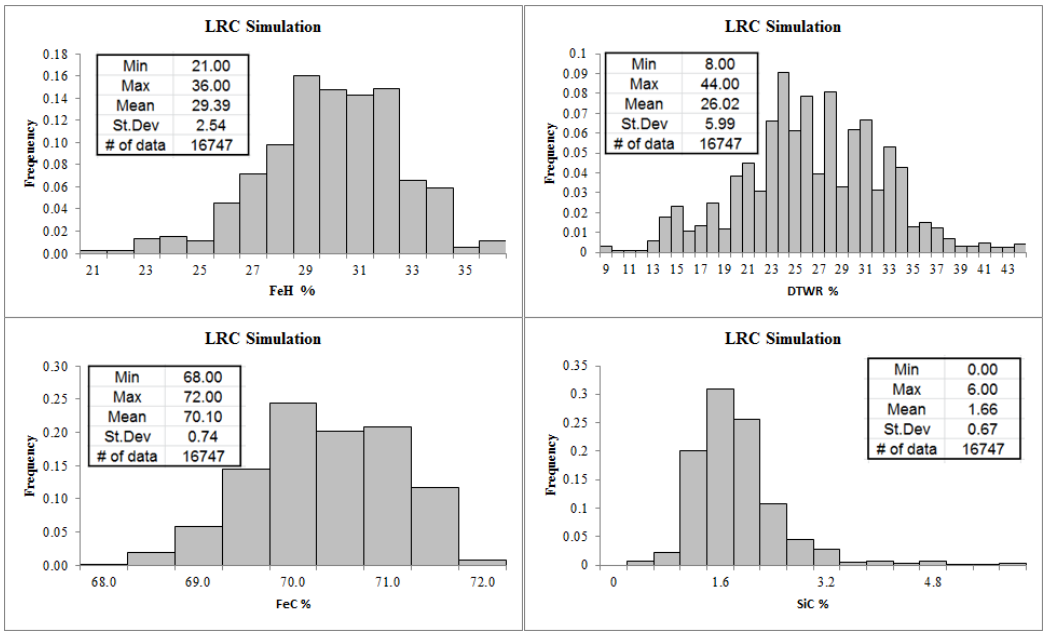

Simulation 1 histograms of grades for LRC layer

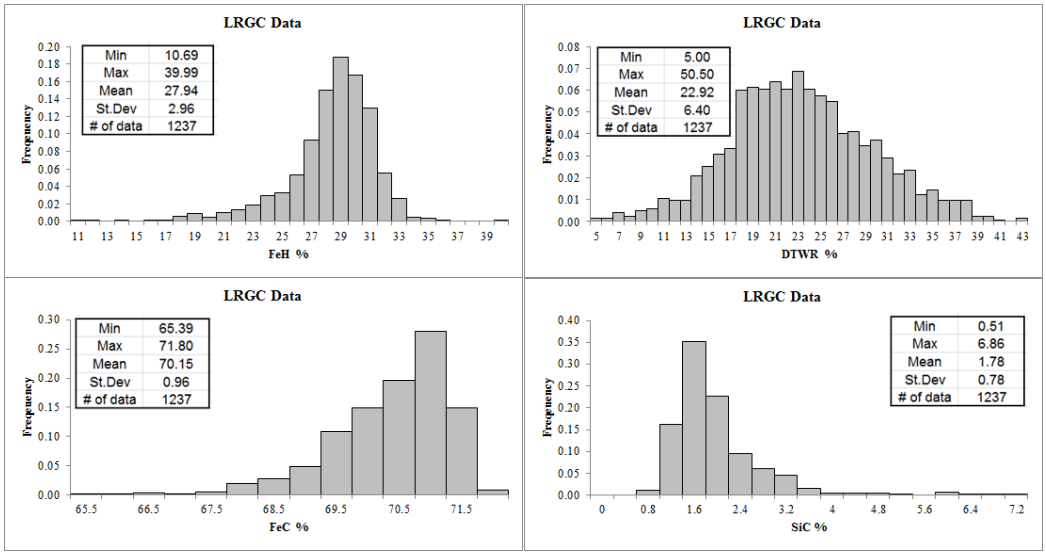

Data histograms of grades for LRGC layer

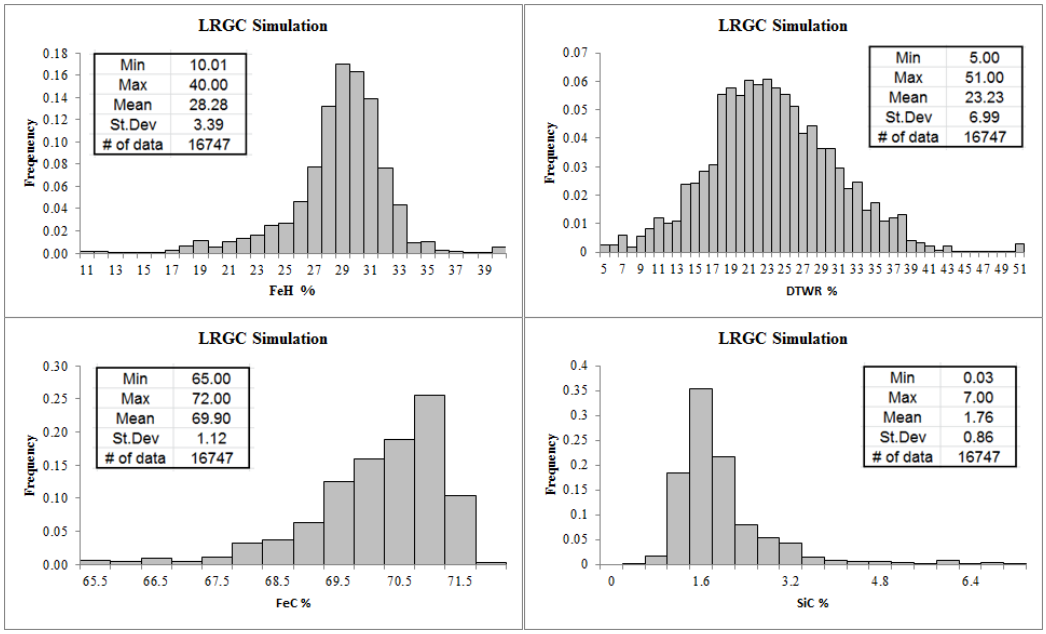

Simulation 1 histograms of grades for LRGC layer

Appendix D – Ore Quality Simulation Variogram Reproduction

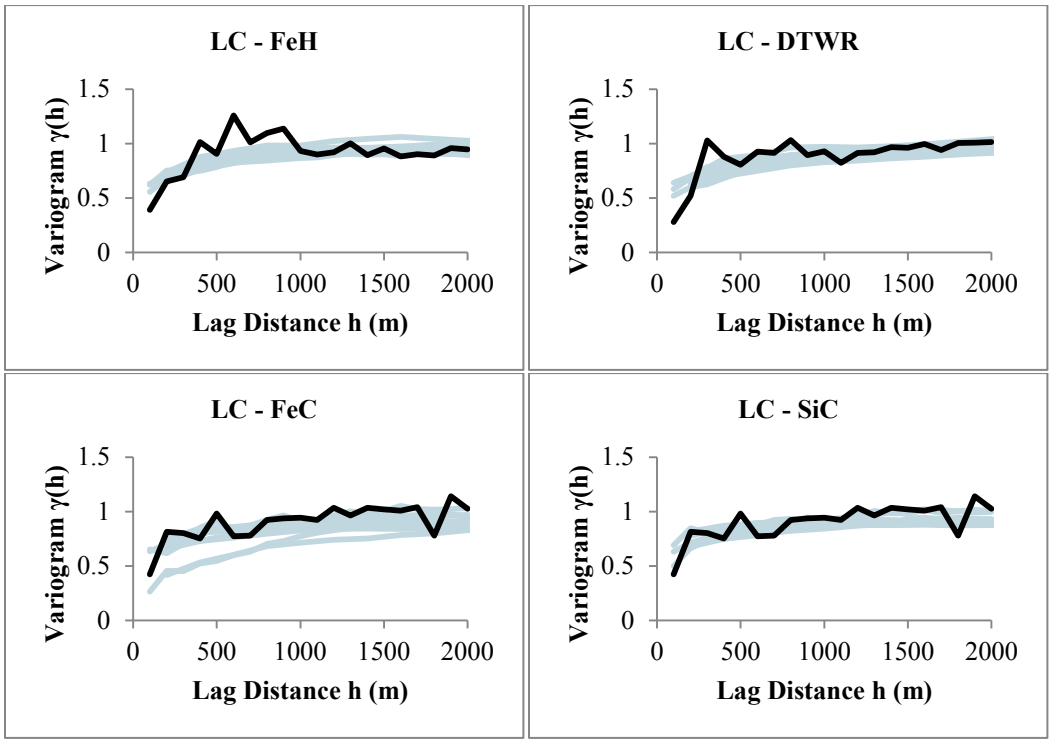

Ore quality simulation variograms of grades for LC layer

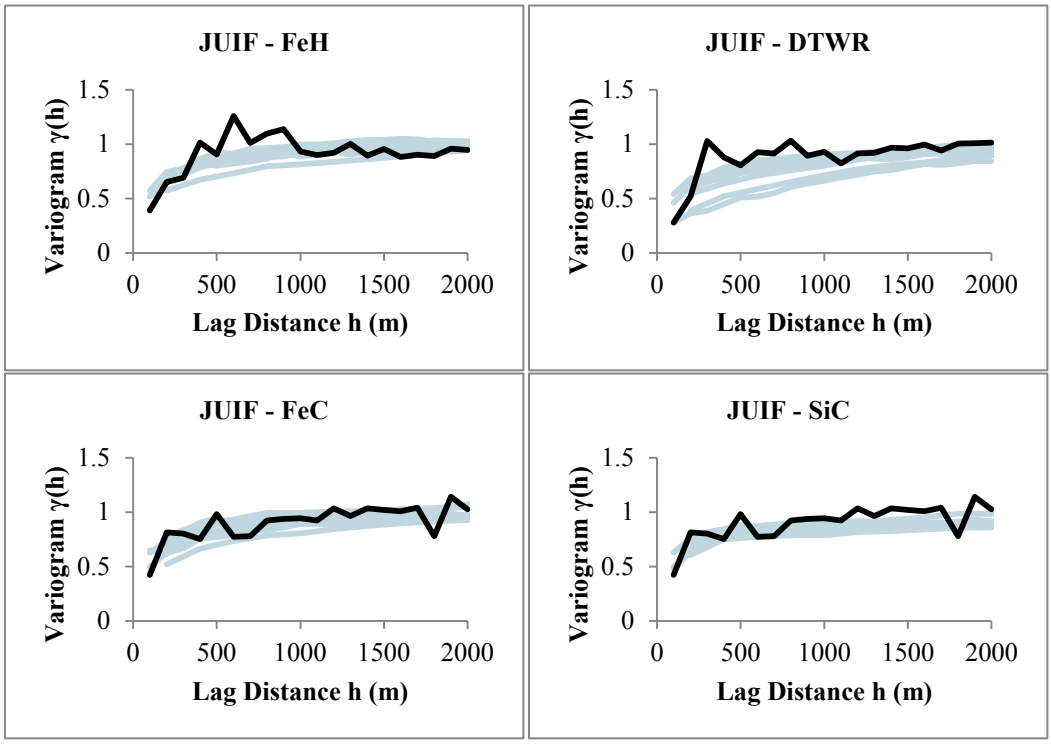

Ore quality simulation variograms of grades for JUIF layer

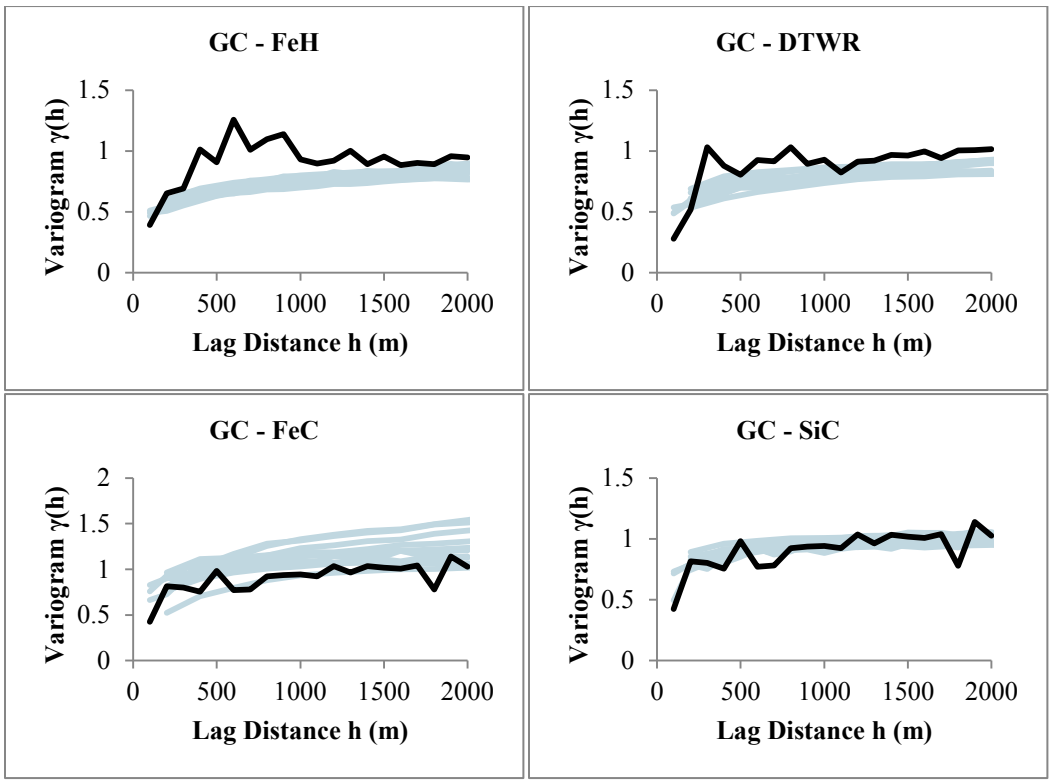

Ore quality simulation variograms of grades for GC layer

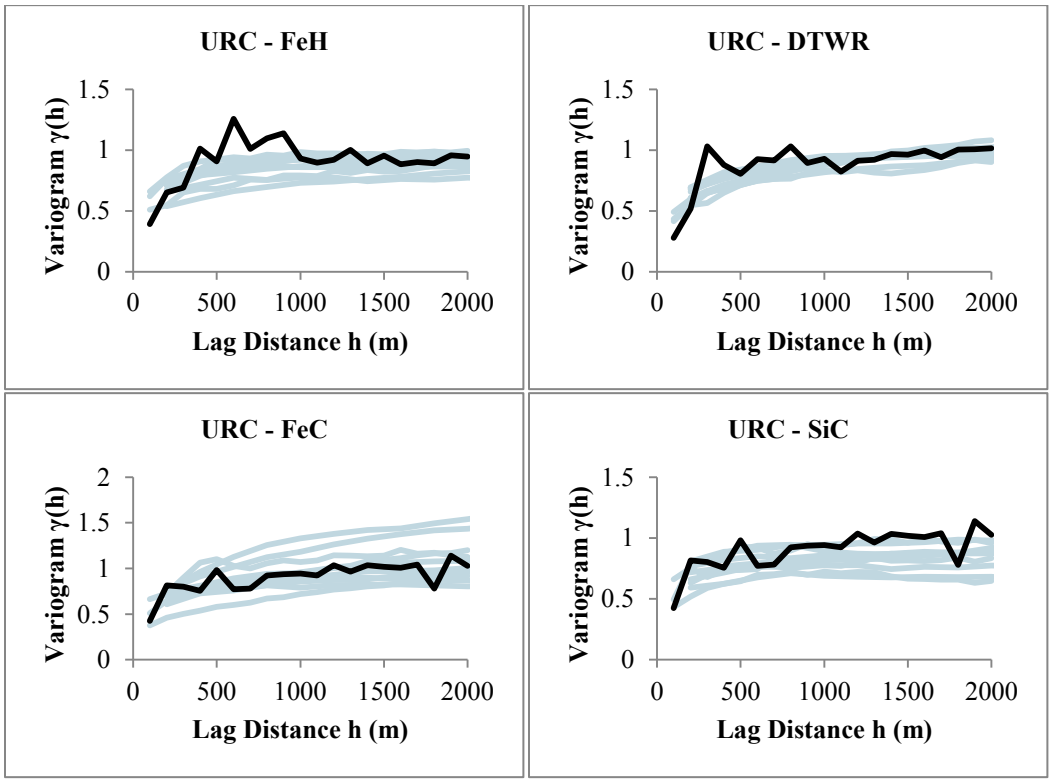

Ore quality simulation variograms of grades for URC layer

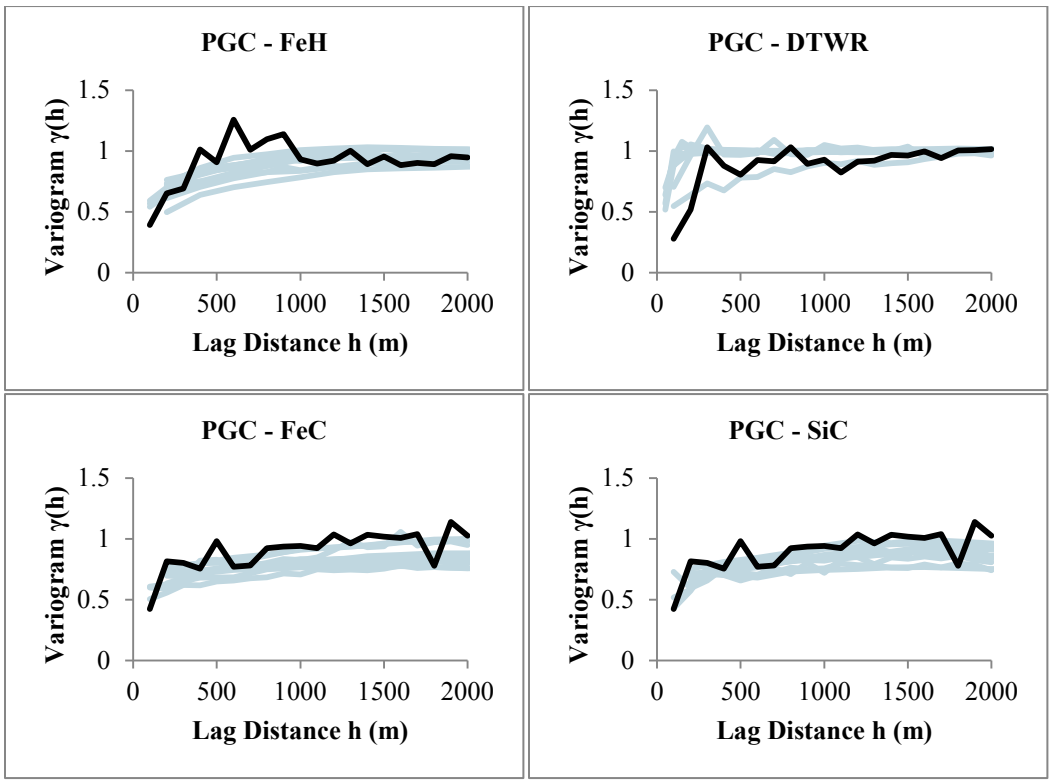

Ore quality simulation variograms of grades for PGC layer

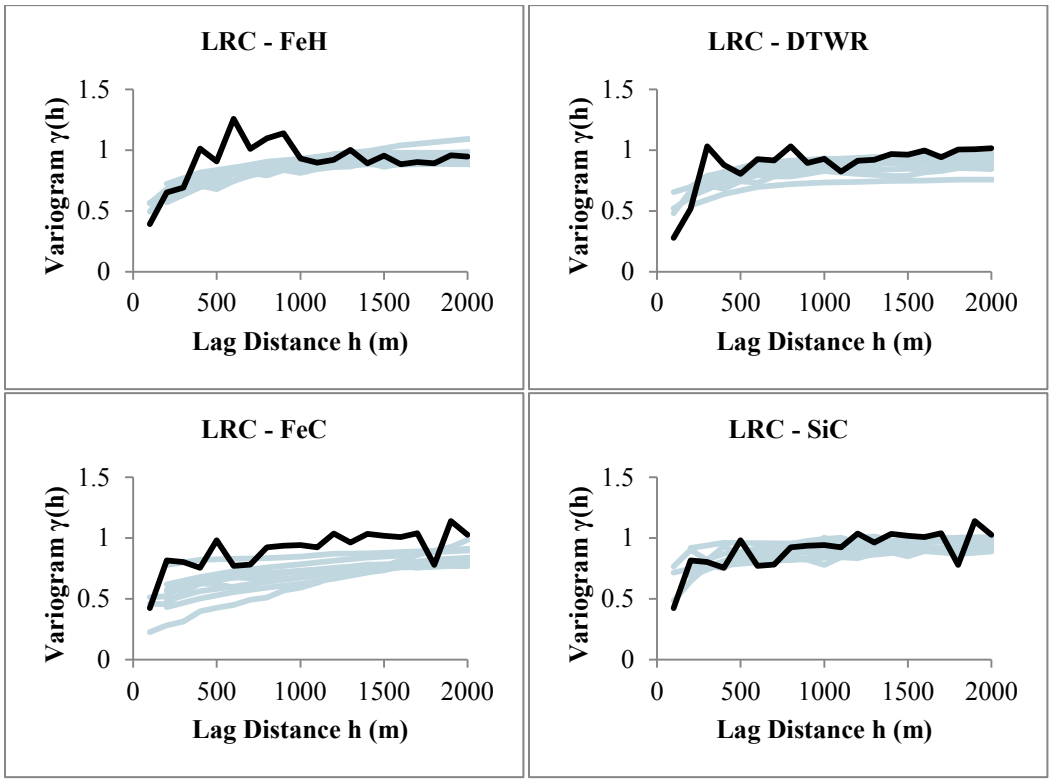

Ore quality simulation variograms of grades for LRC layer

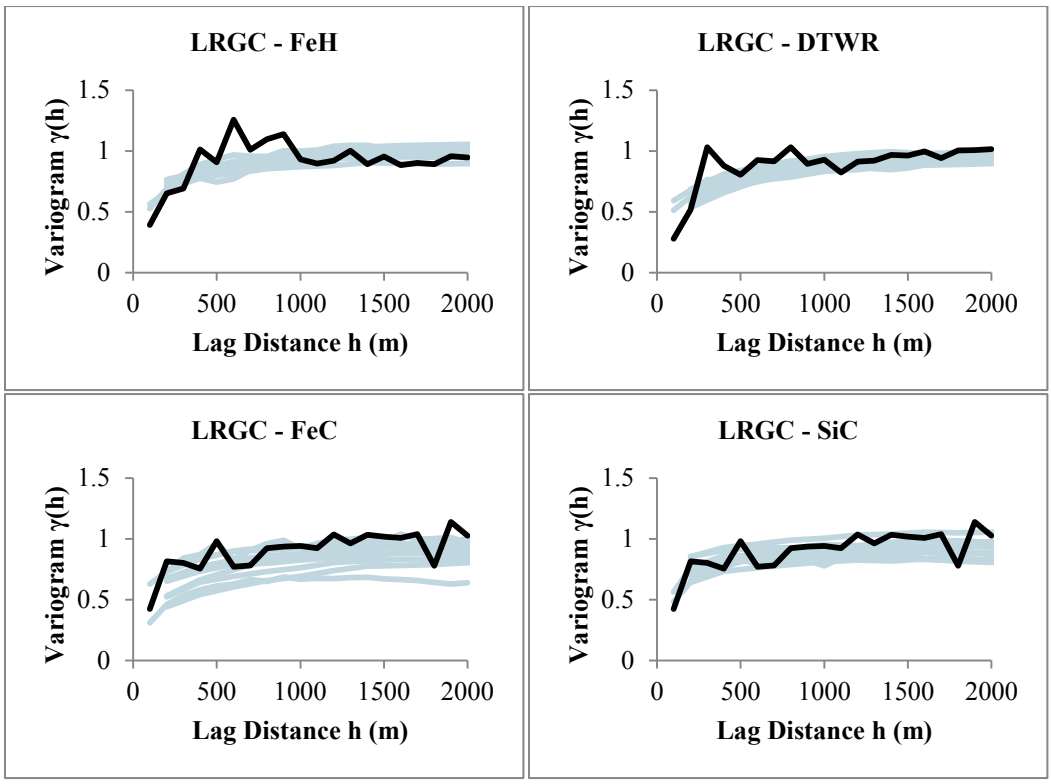

Ore quality simulation variograms of grades for LRGC layer